ADVERSARY PATH ANALYSIS OF A PHYSICAL PROTECTION SYSTEM DESIGN USING A STOCHASTIC APPROACH

A Thesis

by

YANUAR ADY SETIAWAN

Submitted to the Office of Graduate and Professional Studies of
Texas A&M University
in partial fulfillment of the requirements for the degree of

MASTER OF SCIENCE

Chair of Committee,	Sunil Chirayath
Committee Members,	Craig Marianno
	Sergiy Butenko
Head of Department,	Yassin Hassan

May 2018

Major Subject: Nuclear Engineering

ABSTRACT

The Estimate of Adversary Sequence Interruption (EASI) model is a single path analysis model to calculate the Probability of Interruption (P_I) of a Physical Protection System (PPS) in a facility. However, the P_I value estimated by the EASI model does not have uncertainty value which is important to represent the confidence level of the PPS's performance. A stochastic (Monte Carlo) approach to analyze the effectiveness of a PPS, specifically estimating the P_I value and uncertainty in the P_I estimation, is implemented into the EASI model approach in a software code developed as part of this study. The software code is tested by analyzing a hypothetical facility by estimating P_I values considering the characteristics [Probability of Detection (P_D) and delay time (t_d)] of the protection elements in the PPS, uncertainties in the P_D and t_D values, and various adversary strategies including collusion with an insider. Sensitivity analysis of P_I value with regards to P_D and t_d values is performed for the Most Vulnerable Path (MVP) of the facility by considering the Critical Detection Point (CDP) of the facility's Adversary Sequence Diagram (ASD).

Sensitivity analysis of P_I value estimation shows that the relationship between P_D and P_I is linear however the relationship between t_d and P_I is non-linear. The implementation of stochastic (Monte Carlo) approach successfully produces P_I value distribution from which the mean and standard deviation values are estimated. The P_I value is the lowest in the simulations where the insider's act is included, whether the insider acts on the detection or delay function or both simultaneously. The lowest mean value of P_I distribution is for the rushing strategy, among the other adversary strategies analyzed. This is due to an unbalanced PPS design of the hypothetical

facility analyzed. Frequency analysis of P_I value also shows that simulations of rushing strategy have a higher frequency of lower P_I value (below 0.8) compared to the other strategies.

In conclusion, the implementation of the stochastic (Mote Carlo) method is valuable in modeling the P_D values in the EASI model, and in the estimation of P_I value distribution and the uncertainty associated, especially in modeling the adversary path including the collusion of an insider for multi-path analysis. Frequency analysis performed on the P_I values is valuable in modifying the PPS design instead of just using the mean value of the P_I distribution and its standard deviation in the multi-path analysis.

DEDICATION

This thesis is dedicated to my father, my mother, my two sisters, and especially to the God of creation. They are the reasons I am still moving forward in this life even though I am fragile and full of weaknesses. There are no words that can fully express my gratitude for their love, pray, and encouragement in my life.

ACKNOWLEDGEMENTS

I would like to thank my committee chair, Dr. Sunil Chirayath, who has accepted me in NSSPI from my very first day at Texas A&M University. He provides me assistance, guidance, and support for me to learn as much as I can through many opportunities. Thank you for being patient in helping me learn in my study and research in nuclear engineering. And thank you for all valuable feedbacks and comments in my writing. I also want to thank my committee members, Dr. Marianno and Dr. Butenko, for their time, feedback, and involvement in the completion of my master's degree. I also thank Dr. Kitcher who gave me feedback in the early phase of this research.

I also want to thank my NSSPI friends at AI 2nd floor since my first year: Athena, Linda, Henry, Drew, Hawila, Paul, Jackson, Patrick, Rob; and those whom I hung out or traveled with: Barbara, Katie, Ernesto, Rainbow, Logan, Robert and all the NSSPI 2017 students. I appreciate our time and experience together. I would like to thank Gayle Rodgers who has been supporting my administration business during my time at NSSPI, and Kelley Ragusa as the administrator of NSSEP from which I learn things for my class and research. And last but not least in NSSPI, Dr. Gariazzo who has been a good friend, colleague, and supporter. Thanks also go to my friends and colleagues and the department faculty and staff for making my time at Texas A&M University a great experience.

I want to thank my roommate, Farid Putra Bakti, and all the Indonesian students in College Station for the warm welcome, friendship, and memorable moments in these two years. I am also sending my gratitude to all my friends and colleague in Indonesia or abroad, for their continuous prayers, encouragement, friendship, and love. At last, no word or poem can express my ultimate gratitude to be born and raised by my family in Christ. Jesus blesses us all. Amen.

CONTRIBUTORS AND FUNDING SOURCES

Contributors

All the work for the thesis was completed by the student, under the primary advisement of Dr. Sunil Chirayath of the Department of Nuclear Engineering. Feedback from Dr. Marianno and Dr. Kitcher of the Department of Nuclear Engineering and Dr. Butenko from the Department of Industrial and Systems Engineering was valuable for the completion of the thesis. Advises from Dr. Kitcher of the Center for Nuclear Security Science and Policy Initiatives (NSSPI) were also essential for the thesis.

Funding Sources

Graduate study was fully sponsored by the government of Republic of Indonesia, through the Indonesian Endowment Fund for Education (LPDP) institution under the authority of Ministry of Finance.

NOMENCLATURE

PPS	Physical Protection System
P_D	Probability of Detection
t_d	Delay Time
P_I	Probability of Interruption
P_N	Probability of Neutralization
P_E	PPS overall effectiveness
EASI	Estimate of Adversary Sequence Diagram
P_{ND}	Probability of Non-Detection
P_{NDet}	Probability of No Detection
P_{FDet}	Probability of First Detection
C_F	Correction Factor
RFT	Response Force Time
P_C	Probability of Alarm Communication
$P_{(R\|A)}$	Probability of Response Force Arrival
ASD	Adversary Sequence Diagram
CDP	Critical Detection Point
NARI	Nusantara Atomic Research Institute
SNL	Sandia National Laboratories
MVP	Most Vulnerable Path
TR	Time Remaining

TABLE OF CONTENTS

Page

LIST OF FIGURES

Page

LIST OF TABLES

Page

1. INTRODUCTION AND LITERATURE REVIEW

Radiological and Nuclear (RN) materials present in a nuclear facility are attractive targets for some adversaries. The intent of the adversary here is either to steal the RN materials or to sabotage the facility itself, which can cause severe unwanted consequences. Vivid examples of adversaries' malicious acts involving RN materials can be found in the Incident and Trafficking Database (ITDB) established in 1995 by the International Atomic Energy Agency (IAEA). The ITDB information system provides data on incidents of illicit trafficking, unauthorized activities, and events involving RN material outside of regulatory control. To prevent such malicious acts of the adversaries, an appropriately designed and evaluated Physical Protection System (PPS) should be installed at a nuclear facility. The IAEA has adopted a convention [1] on PPS since 1980 and has published several guidance documents on physical protection for nuclear facilities [2]. After the 9/11 terrorist event in 2001, the international community and the IAEA has made substantial efforts that focused on the improvement of security of nuclear facilities.

1.1. Physical Protection System (PPS)

Physical Protection System (PPS) is a security system which integrates equipment, procedures, and people to protect assets or facilities against theft, sabotage or another kind malevolent adversary attack [3]. A robust PPS should have deterrence, detection, delay and response components to defeat the success of the adversary [4]. An adversary might be a criminal, protester, or terrorist group [5]. The adversary threat can vary based on three attributes, which are its motivation, intention, and capability. An adversary threat spectrum is generally prepared for a

given nuclear facility depending on these three attributes of the adversaries who are likely to attack the facility. The threat spectrum analysis leads to the creation of a Design Basis Threat (DBT) document, a base on which a PPS design is made upon for a nuclear facility [6]. The insider threat is another aspect that needs to be considered while designing a PPS. This is because of insiders have knowledge, access, and authority, which could be misused for malicious acts including assistance to an outside adversary.

The primary functions of a PPS are (a) provide barriers to stop the adversary intrusion, (b) detect the adversary intrusion, (c) delay the adversary action (after the intrusion has occurred and detected), and (d) respond to neutralize the adversary. Integration of various types of protection elements into the PPS provides those mentioned functions. The detection protection element of a PPS (for example, a motion sensor on a fence) is characterized quantitatively by its Probability of Detection (P_D). The detection process consists of three parts, which are intrusion sensing with the probability of producing a signal (P_s), the probability of signal transmission as an alarm (P_t), and the probability of accurate alarm assessment (P_a). These probability values are used to determine P_D using the relationship expressed in Equation 1.1.

$$P_D = P_s \times P_t \times P_a \tag{1.1}$$

The delay protection element (for example, a locked door) of a PPS provides the ability to slow down the adversary intrusion progress towards the target, which in turn provides time for the response force, after a genuine alarm, to interrupt the adversary before he or she reaches the target. The capability of a delay protection element is characterized by the delay time (t_d) it provides.

The last element of the PPS is the response force, made up of trained security personnel and the necessary equipment, such as weapons, body protection, transportation, communication, etc. The purpose of the response force is to intercept and neutralize the intruding adversary. The Probability of Interruption (P_I) is defined as the probability that the response force can interrupt (intercept) the adversary after a genuine intrusion detection alarm. The capability of response force is characterized by the Probability of Neutralization (P_N), which is defined as the probability that the response force can neutralize the adversary. The product of P_I and P_N represents the overall effectiveness (P_E) of the PPS as shown in Equation 1.2.

$$P_E = P_I \times P_N \tag{1.2}$$

1.2. Estimate of Adversary Sequence Interruption (EASI)

Estimate of Adversary Sequence Interruption (EASI) model is used to determine the overall Probability of Interruption (P_I) value of a PPS [3]. The EASI model is based on the assumption that the response force must be notified of the adversary's attempt of theft or sabotage while there is still sufficient time to interrupt and neutralize the adversary [7]. It is developed as a single path analysis tool, in which the adversary path in the facility has been defined by the user along with the detection, delay, and response force capability information for every protection layer as shown in Figure 1. The EASI model has three calculation sections in general. The first one is the detection function calculation section. The second one is the delay function calculation section. The third one is the response function calculation section, in which the results from two other sections are combined and used to calculate the total P_I value.

	Probability of Interruption:				0.88
Estimate of Adversary Sequence Interruption (EASI)	Probability of Alarm Communication		**System Response** Time **(in seconds)** Mean		Standard Deviation
	0.97		270		81

Task	Description	P(Detection)	Location	Delays (in seconds): Mean:	Standard Deviation
1	**Penetrates the Fence (Entrance)**	0.8	B	10	3.0
2	**Runs through Limited Access Area**	0.02	M	90	27.0
3	**Penetrates Vehicle Door P9**	0.5	E	30	9.0
4	**Runs through Protected Area**	0.02	M	90	27.0
5	**Penetrates door P5**	0.99	E	54	16.2
6	**Runs through Plant Controlled Building**	0.02	M	20	6.0
7	**Penetrate door P6**	0.99	E	127	38.1
8	**Runs to the target**	0.02	M	15	4.5
9	**Sabotage**	1	B	51	15.3

Figure 1. Example of a single path analysis of EASI model

In the detection function calculation section, EASI model uses the P_D values of each protection layer along the adversary path. The P_D values are used to calculate three other probability values; the Probability of Non-Detection (P_{ND}), the Probability of No Detection (P_{NDet}), and the Probability of First Detection (P_{FDet}). P_{ND} is the probability that the adversary is not detected in a protection layer of interest. P_{NDet} is the probability that there is no detection from the first protection layer until a protection layer of interest. P_{FDet} is the probability that the adversary's intrusion is detected for the first time at the corresponding protection layer of interest. P_{ND}, P_{NDet}, and P_{FDet} can be expressed as shown in Equations 1.3, 1.4, and 1.5 respectively.

$$P_{ND_i} = 1 - P_{D_i} \tag{1.3}$$

$$P_{NDet_i} = \prod_1^i P_{ND_i} \tag{1.4}$$

$$P_{FDet_i} = P_{D_i} \times P_{NDet_{i-1}} \tag{1.5}$$

In the delay function calculation section, there are several delay-related values calculated for every protection layer along the adversary path. The first value is the cumulative delay time, which is the summation of the t_d values from protection layer of interest until the last protection layer along the adversary path, as expressed by Equation 1.6. The cumulative delay time variance of each protection layer along the adversary path is also calculated from the standard deviation (σ_{td}) of the t_d value, as expressed by Equation 1.7.

Detection location information indicates a Correction Factor (C_F) which is used to calculate other delay-related values, as shown in Equation 1.8. 'B' represents detection right at the beginning of current protection element, 'M' represents the detection mid-way between current protection element to the next, and 'E' represents detection very late almost at the next protection element so that no delay time credit can be given at the current protection element. C_F is used to calculate the real amount of time along the path that needs to be spent by the adversary to go to the next protection layer after being detected in a protection layer of interest, expressed by Equation 1.9. This real amount of time in the path is called true delay time value, which also has an associated true variance value as expressed in Equation 1.10. Finally, EASI model calculates the true cumulative delay time and true cumulative variance of each protection layer along the adversary path by using Equations 1.11 and 1.12 respectively. In Equations 1.6 through 1.12, 'n' represents the total number of protection element layer of the PPS while 'i' is the protection layer of interest.

$$cumulative\ t_{d_i} = \sum_{i=i}^{n} t_{d_i} \tag{1.6}$$

$$cumulative\ \sigma^2{}_{t_{d_i}} = \sum_{i=i}^{n} (\sigma_{t_{d_i}})^2 \tag{1.7}$$

$$C_F \begin{cases} 1 & for\ 'B' \\ 0.5 & for\ 'M' \\ 0 & for\ 'E' \end{cases} \tag{1.8}$$

$$true\ \ t_{d_i} = \ C_F \times t_{d_i} \tag{1.9}$$

$$true\ \sigma^2{}_{t_{d_i}} = (C_F \times \sigma_{t_{d_i}})^2 \tag{1.10}$$

$$true\ cumulative\ t_{d_i} = true\ \ t_{d_i} + \sum_{i=i+1}^{n} t_{d_i} \tag{1.11}$$

$$true\ cumulative\ \sigma^2{}_{t_{d_i}} = true\ \sigma^2{}_{t_{d_i}} + \sum_{i=i+1}^{n} (\sigma_{t_{d_i}})^2 \tag{1.12}$$

In the response function calculation section, true cumulative delay time and true cumulative delay variance values are used to calculate the z-value for each protection layer using Equation 1.13. Response Force Time (RFT) in Equation 1.13 is the cumulative time which is the sum of alarm transmission time, alarm assessment time, alarm communication time to the response force, the response force preparation time, the response force travel time, and the response force muster and deployment time. σ_{RFT} is the standard deviation of the RFT. The Probability of Alarm Communication (P_C) represents the probability that the assessed alarm was communicated correctly by the alarm assessor to the response force and is assumed to be a constant for all the detection elements in the PPS.

$$z_i = \frac{x - \mu}{\sigma} = \frac{true\ cumulative\ t_{d_i} - RFT}{\sqrt{true\ cumulative\ \sigma^2{}_{t_{d_i}} + \sigma_{RFT}^2}} \tag{1.13}$$

Given the response force team is alerted by the detection of the adversary's intrusion at any protection layer, based on the remaining cumulative delay time at that protection element to the target, the Probability of Response Force Arrival ($P_{(R|A)}$) before the adversary reach the target has to be calculated. $P_{(R|A)}$ is calculated as the integration of the probability density function from -∞

to the z-value (Equation 1.13) of the protection layer of interest using the RFT normal distribution. This calculation can be done by using the Norm.S.Dist function in Microsoft Excel to integrate the probability density function from -∞ to the z-value. Figure 2a shows the location of a z-value in which the true cumulative delay time is more than the RFT, which means that the adversary is detected in earlier protection layer. Figure 2b shows the location of a z-value in which the true cumulative delay time is less than the RFT, which means that the adversary is detected in later protection layer almost at the end of the adversary's mission. Specific Probability of Interruption (P_I) value for each protection layer is calculated by using Equation 1.14.

$$Specific\ P_{I_i} = P_{FDet_i} \times P_C \times P_{(R|A)_i} \tag{1.14}$$

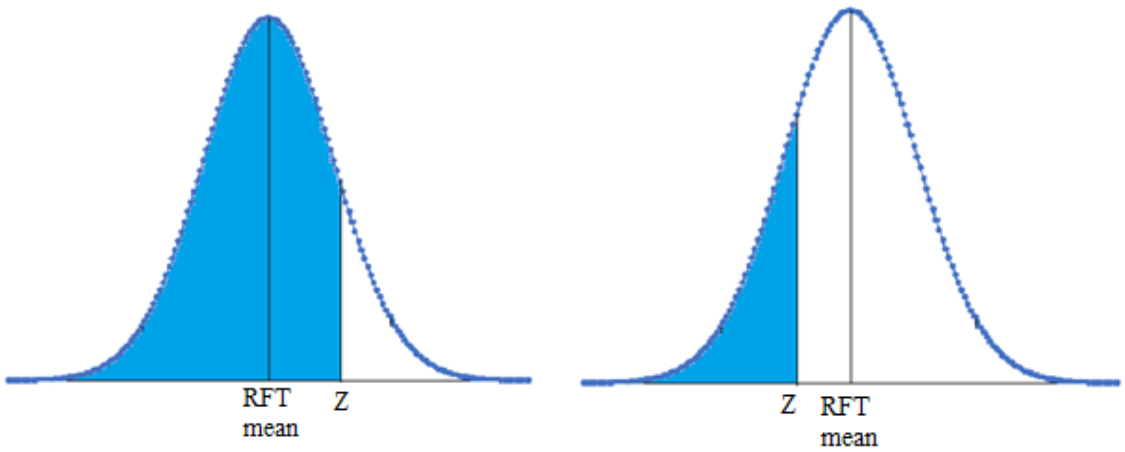

(a) (b)

Figure 2. Location of z-value in a normal distribution: (a) true cumulative t_d > RFT (b) true cumulative t_d < RFT

The general mathematical equation to calculate the total P_I value is shown in Equation 1.15 and can be simplified as Equation 1.16. In summary, the total P_I value of the PPS is the accumulation of the specific P_I values provided by every protection layer along the adversary path.

$$P_I = P_{(D_1)} \times P_{(C_1)} \times P_{(R|A_1)} + \sum_{i=2}^{n} P_{(D_i)} \times P_{(C_i)} \times P_{(R|A_i)} \times \prod_{i=1}^{i-1}\left(1 - P_{(D_i)}\right) \quad (1.15)$$

$$P_I = \sum_i^n specific\ P_{I_i} \quad (1.16)$$

The Probability of Neutralization (P_N) is the probability that the response force successfully neutralizes the adversary, given the interruption has been made. The Analytic System and Software for Evaluating Safeguards and Security (ASSESS) Neutralization Model is one of the computer code to simulate engagement between the postulated adversary and response force. It requires data on the adversary, such as number and type of the adversary, and weapon of the adversary. It also requires data on the response force, such as type and number of guards, and weapon owned by the guards. A Markov Chain is constructed to determine P_N as a function of successive volleys by both sides [8].

1.3. Previous Work

The EASI model has been used in many PPS evaluations and improvement studies. A.A Wadoud et al. used the single path EASI model to calculate the P_I value for two sabotage scenarios in a hypothetical research reactor facility [8]. The ASSESS code was used to calculate the P_N value for both scenarios to finally get the overall effectiveness (P_E) of the PPS using Equation 1.2. Based on the EASI model evaluation, they then modified the PPS design to achieve a higher and acceptable P_I value. Another PPS evaluation study has been done by O.D. Oyeyinka et al. They used the EASI model to calculate P_I value as the PPS effectiveness at a Nuclear Energy Centre (NEC) in Nigeria [9]. They demonstrated the use of the EASI model in PPS evaluation and performed sensitivity analysis. The EASI model was used for a single protected asset analysis, in which the most likely adversary path for each of the three main buildings had to be determined

manually through the target and site assessment process and was analyzed separately. Suggested upgrades to the security system of the facility were evaluated by calculating the improvement of P_I value in those three most likely adversary paths. Those two studies show that the EASI model is a single path analysis model which can only analyze one adversary path scenario at a time.

Several studies also have been done to improve or to use the EASI model for insider threat impact analysis on PPS effectiveness. Bowen Zou et al. proposed a novel method named "Estimate and Prevention of the Insider Threats (EPIT)" to estimate insider threat behaviors and the impact on the protection elements capability [10]. They used the Failure Mode and Effect Analysis (FMEA) to analyze PPS protections elements failure mode while taking human factor as the main external cause of the failure. Based on the role of staff in the PPS and the failure mode from the FMEA, Common Cause Failure (CCF) modeling and analysis were conducted which also included the impact of insiders to the PPS. The human factor impact to the detection and delay function of the protection element in PPS from the CCF analysis were then used to improve the EASI approach in the P_I value calculation. Another study from M. Hawila et al. demonstrated a methodology to evaluate the vulnerability of a PPS of a typical nuclear research reactor by considering an insider-outsider collusion threat to sabotage the reactor pump [11]. They used the Adversary Sequence Diagram (ASD) analysis to determine the Most Vulnerable Path (MVP) of the facility and then used the EASI model. The insider was assumed to be able to open two doors thus decreasing the delay time provided by these PPS protection elements along the adversary path. The P_I value substantially decreased by 29.9% in this case. In another similar work by M. Hawila and S. Chirayath, insider-outsider collusion was assumed to sabotage a power reactor spent fuel pool [12]. The P_I would drop by 16.9% if the insider opens the door with the highest delay time value and would drop by 39.3% if the insider can open another door along the most vulnerable path. These

studies show that the impact of insider threat is an important aspect to be considered in developing a methodology to evaluate the effectiveness of a PPS design.

N. Terao and M. Suzuki devised a new calculation method for three components in the EASI model: P_{Di}, P_{Ci}, and $P_{(R|A)i}$ [13]. For a specific type of sensor, such as infra-red or microwave, they expressed the uncertainty and variability as a probability distribution. In their work, uncertainty stands for the incompleteness of knowledge, such as failure to set condition or wrong operation procedures, while variability stands for the fluctuations in nature, such as weather and environmental conditions, or the presence of wild animals. P_C value is expressed using a human error probability distribution without the consideration of insider threat or sabotage possibilities. They used Poisson distribution to represent $P_{(R|A)}$ instead of the normal distribution as used in the EASI model. The P_{Di}, P_{Ci}, and $P_{(R|A)i}$ values in their method are expressed in a distribution of 5,000 values each, in which generated by the Monte Carlo method. By using those various values of P_D, P_C, and $P_{(R|A)}$ in the EASI principle, Equation 1.15 was used to get the P_I value distribution.

Meanwhile, there are also various methods that have been and are being developed besides the EASI model. One of the first developed methodologies to assess PPS vulnerabilities is the Systematic Analysis of Vulnerability to Intrusion (SAVI). It is said that SAVI can provide estimates of protection system effectiveness against a spectrum of outsider threats, including collusion with an insider adversary [14]. SAVI calculates P_I values of all potential paths of theft or sabotage attempt at the target. The model consists of the following four main parts. First, a graphic representation of the facility called the ASD. Second, a database of the component delay and detection values. Third, a threat and response force time specification. The last part is the algorithm to calculate the P_I value of the possible adversary paths and their ranks. For a threat including collusion with an insider, the appropriate protection element values are selected by the

analyst. For example, if a guard badge check is used where the guard is postulated as an insider threat, then the probability of detection would be set as zero (P_D=0). Another example is in which the insider compromises an emergency door which has panic bars. In this example, the delay time provided by the door should be selected as zero (t_d=0). This process relies on the analyst's understanding and assumption to postulate the insider's act in the SAVI simulation.

The SAVI algorithm is based on the adversary path timeline from the start until the target as shown in Figure 3. The algorithm then determines the Critical Detection Point (CDP) based on the RFT and the delay time provided by the protection elements. The P_I value is obtained by accumulating the detection probabilities from the CDP to the off-site area. At the end of the analysis, the SAVI code lists and ranks the first ten most vulnerable paths based on each P_I value from high to low.

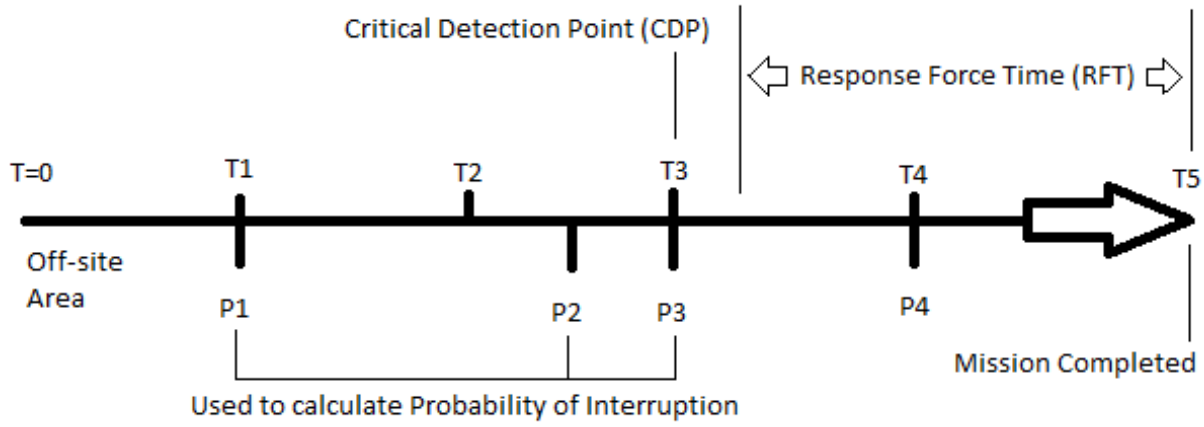

Figure 3. The SAVI adversary path timeline

Systematic Analysis of Physical Protection Effectiveness (SAPE) is another method developed in South Korea, mainly by researchers in the Korea Institute of Nonproliferation and Control (KINAC) [15]. They also used the same EASI principle, as shown in Equation 1.15, to

calculate the P_I value of the PPS. The difference from the EASI model is that, instead of using the ASD, they used a 2D map of the facility. The map was then divided into a grid of small individual meshes containing protection element information within the map. The mesh grid of the facility map provides a bird's eye view of the facility and the PPS elements in it. It is also representing the relative distance between the protection elements and the adversary. The relative distance is used to model the decrease of the protection element capability. In order to find the most vulnerable path, a path with the lowest P_I value, they used generalized A* algorithm. Moreover, SAPE also has a sensitivity analysis on the P_I value considering all protection elements along the evaluated path, which is calculated by using Equation 1.17 below.

$$S_{detect_i} = \frac{\partial P_I}{\partial P_{Di}} \text{ and } S_{delay_i} = \frac{\partial P_I}{\partial t_{di}} \tag{1.17}$$

Based on the literature survey, there is no work cited for multi-path analysis model to estimate uncertainty in P_I value. There is also no work cited in the literature to analyze various strategies used by the adversary, including the insider's collusion. The work by Norichika Terao and Mitsutoshi Suzuki shows a way to use Monte Carlo method in modeling the uncertainty of PPS components which gives uncertainty to the P_I value in the EASI model. However, Terao and Suzuki's study is still limited to a single path analysis and does not model various possible adversary path in a facility and insider's collusion. SAPE method by the KINAC is a facility-level analysis model to calculate P_I value and its sensitivity to the deviation P_D and t_d. But it does not yet model the various possible adversary path based on the penetration strategy nor the involvement of the insider. Therefore, the main purpose of this study is to develop a multi-path (facility level) analysis model to calculate P_I value, which is also able to model the performance

uncertainty of PPS component, various adversary path based on the penetration strategy, and the insider's involvement in adversary's intrusion that produce uncertainty value of the P_I value.

1.4. Objectives

This study is to develop a multi-path analysis methodology to evaluate the P_I value of a PPS at a facility using a stochastic approach (Monte Carlo) instead of the deterministic approach used in EASI model. The stochastic approach presented here can comprehensively assess the whole Adversary Sequence Diagram (ASD) of the facility and the PPS's protection elements instead of limiting it to adversary's single path analysis approach in the EASI model. The proposed stochastic approach of evaluating P_I will be able to analyze the strategic choices made by the adversary to reach the target based on their knowledge of the facility and the security system. These strategies include rushing strategy to the target, covert strategy, deep penetration strategy, etc. The proposed stochastic approach is also able to model the insider's involvement in assisting the outsider adversary's intrusion. At last, the stochastic approach is also applied in modeling the performance of P_D value of the PPS in P_I value calculation. The aim is to obtain a more realistic value for P_I and the corresponding uncertainty value of P_I. Another objective is to do a sensitivity analysis of P_I value with regards to P_D and t_d value, to see their relationship and estimate the change of the P_I value due to a deviation of P_D and t_d value in facility analysis.

1.5. Scope of Work

The scope of this work is limited to the evaluation of Probability of Interruption (P_I) value of the PPS, as one reflection of PPS's effectiveness, given that the performance value of each

protection element is available. This work does not include the process of determining the performance value of the protection element, such as P_D and t_d, instead, those values from the literature are used. Related to the response force time, it is assumed that the Probability of Communication (P_C) about the assessed alarm to the response force is the same for all of the protection elements (P_C=0.95). Evaluation of the Probability of Neutralization (P_N) is not in the scope of this work. This work expands the single path EASI model to be used in the multi-path level of adversary path analysis by using the Monte Carlo technique, as a stochastic approach, to obtain P_I distribution values and hence the uncertainty in P_I value.

This work does not include the discussion of adversary's attributes or the probability of the adversary attack. It does not calculate the probability of insider's involvement or the probability of success of insider action in helping the adversary. Instead, this work tries to model the insider's involvement in the moment of the adversary's intrusion to the facility, and the effect on the P_I value. Both the attributes of the adversary and the insider have to be postulated by the user in the stochastic approach proposed.

The method developed in this work assumes the intrusion of the adversary with or without the insider's help. It is not developed to measure the effectiveness of the PPS against the insider threat alone. Furthermore, the method developed is to automatically analyze a sabotage scenario using the user-supplied input file. The analyst has the option to analyze a theft scenario by modifying the input file.

2. DEVELOPMENT OF EASI-BASED INPUT FILE AND SOFTWARE CODE

2.1. Development of Facility Design for the Input File

2.1.1. Facility Description

A hypothetical facility, named the Nusantara Atomic Research Institute (NARI), was created for its PPS analysis, specifically for evaluating P_I value. Three hypothetical facility description documents obtained from the website of the International Training Course (ITC) on PPS of Nuclear Facilities and Materials by Sandia National Laboratories (SNL) were used as references to build NARI facility. The hypothetical facilities used as references were:

- The Lone Pine Nuclear Power Plant (LPNPP) [16]
- The Hypothetical Atomic Research Institute (HARI) [17]
- The Lagassi Institute of Medicine and Physics (LIMP) [18]

In short, NARI facility is the only research reactor facility owned by a hypothetical country named the Republic of Nusantara. Since the country decided to build nuclear power plant soon, there is a lot of joint research being conducted with faculty and students from an advanced university nearby the NARI facility. It also gained popularity and publication in which people can get a lot of information about NARI facility from open sources, such as newspaper, website, science and technology magazine, and academic literature. Knowing the importance of the NARI facility, organized crime group related to oil and gas business in the country may try to sabotage the reactor in NARI facility, possibly by colluding with the terrorist or criminal groups who have bad sentiments to the western countries supporting the nuclear energy program in the country. The terrorist and criminal group in the country have criminal record which indicates that they have the

capability and human resources to sabotage the NARI facility. Major damage to the reactor due to the external attack will demonstrate to the public the country's inability to safely and securely operate a nuclear facility while also causing a radiological hazard to the public and delaying the country's pursuit of nuclear energy. Appendix A provides a more detailed background of the country, facility, and the threats.

2.1.2. PPS Design of the NARI Facility

A PPS has been implemented at the NARI facility not long after the western countries came and assisted the country in nuclear energy research and development. Figure 4 shows the layout of the secured facility since then. The outer fence is 2.5-m chain fence with multiple sensors. The main gate is usually locked with a high-security padlock at night and is monitored by a surveillance camera nearby. At night, there is a guard who usually patrols around the limited access area of the facility.

The controlled area is surrounded by a double 2.5-m chain fence link, in which a vibration sensor is attached to each fence. Also, between the two fences, there is an infrared sensor. Figure 5 shows the layout of the personnel portal room. Both room doors, which connect the room to the controlled area and the limited access area, are locked and equipped with a balanced magnetic switch (BMS). There are also 4 steel turnstiles coupled with a badge and Personal Identification Number (PIN) system inside the personnel portal room itself. On the other side, the vehicle gate is a double chain link gate, which is locked by a high-security padlock at night. It is also enforced by the same infrared sensor system which serves the controlled double fences. The controlled area is usually patrolled by two guards randomly.

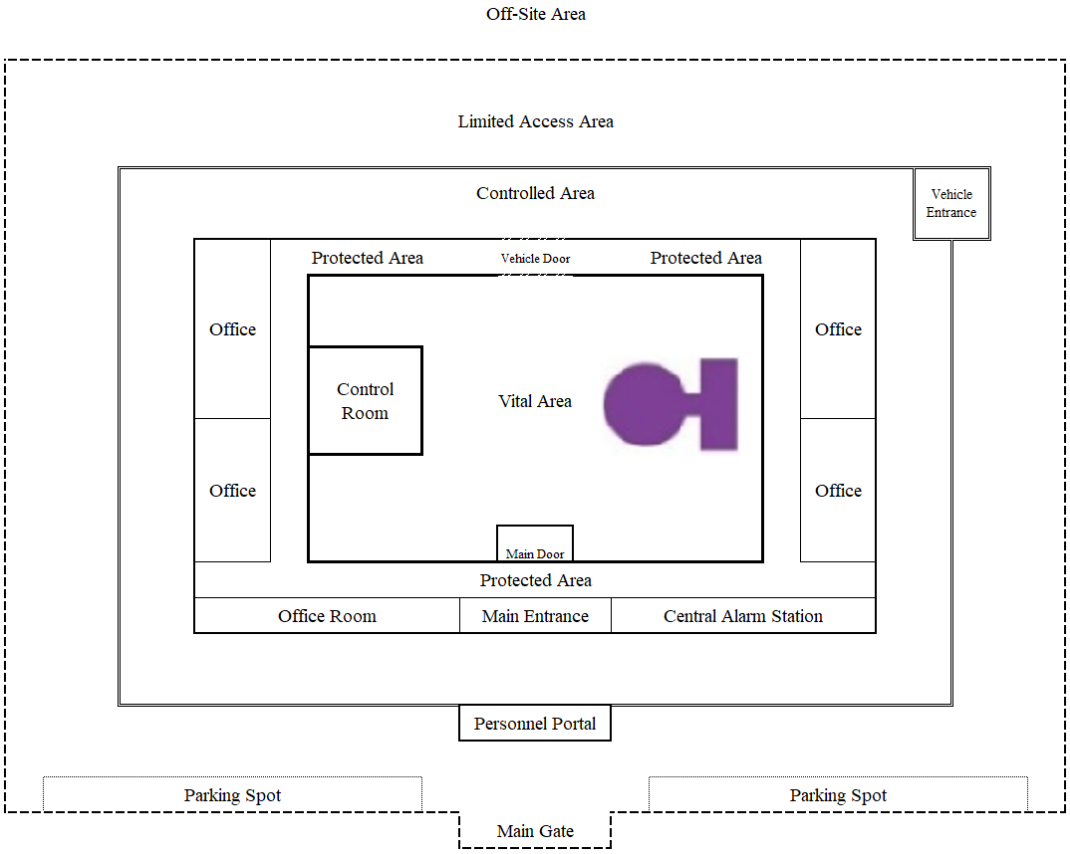

Figure 4. The NARI facility layout

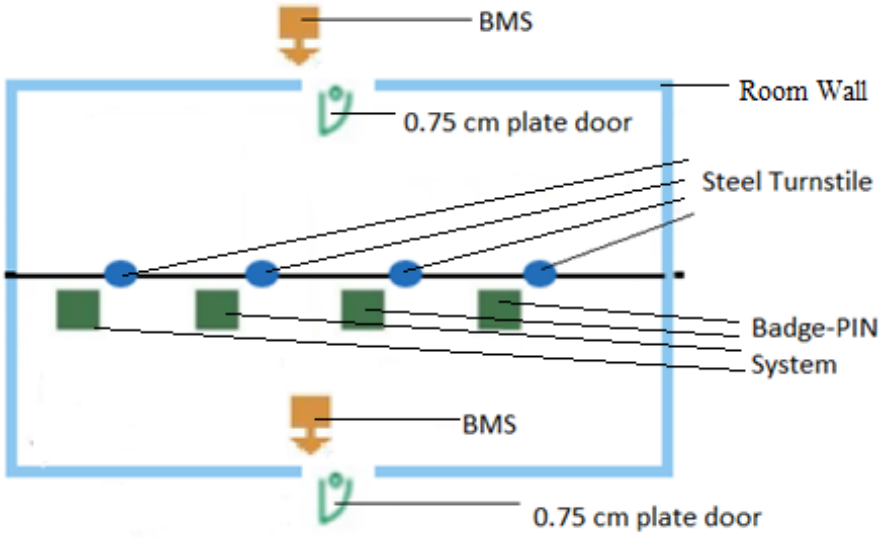

Figure 5. The personnel portal room layout

The building itself is built with a 20-cm thick concrete wall, which is then equipped with a vibration sensor. The building's main entrance room has an outer door which is equipped with a BMS. A steel turnstile coupled with badging and PIN system is installed inside the main entrance room for anyone to get through. The main entrance room layout is shown in Figure 6. There is also a metal detector inside the main entrance room but is only used in the daytime for non-employee visitors. The office rooms inside the facility building have windows which are equipped with glass break sensor, while the door to the protected area inside the building in each office room is equipped with position switch sensor. The central alarm station (CAS) room has windows to the controlled area as well. The CAS room windows are equipped with glass break sensors, while the CAS room is closed by a steel door to the protected area, which has a BMS on it. On the backside of the facility building, there is a 30-cm concrete and steel rolling door, to enable a transport vehicle to get into the building for the purposes bringing in any material or equipment.

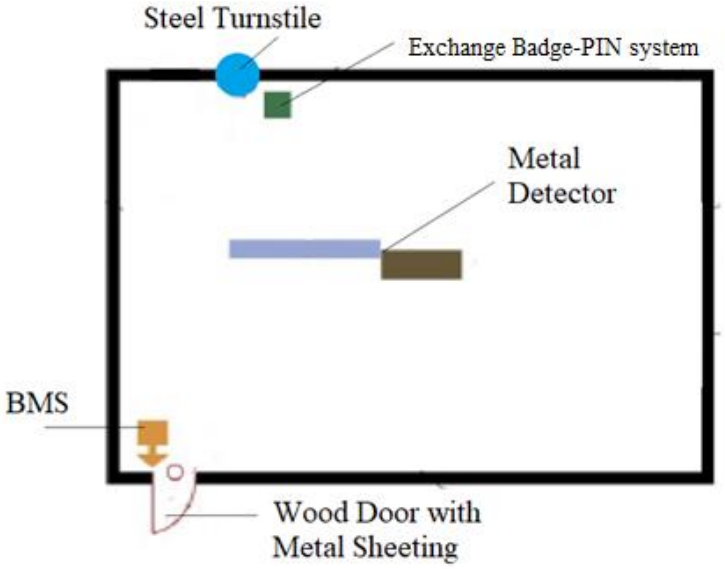

Figure 6. The main entrance room layout

The vital area, reactor hall, is surrounded by 60-cm concrete wall equipped with the vibration sensor as well. Personnel can get inside the vital area through the main door, which is made of steel, or through the vehicle door. Both doors are equipped with BMS and coupled to a badge-PIN system. At night during the maintenance period, multiple complement interior sensors monitor the area surrounding the reactor hall and the reactor core.

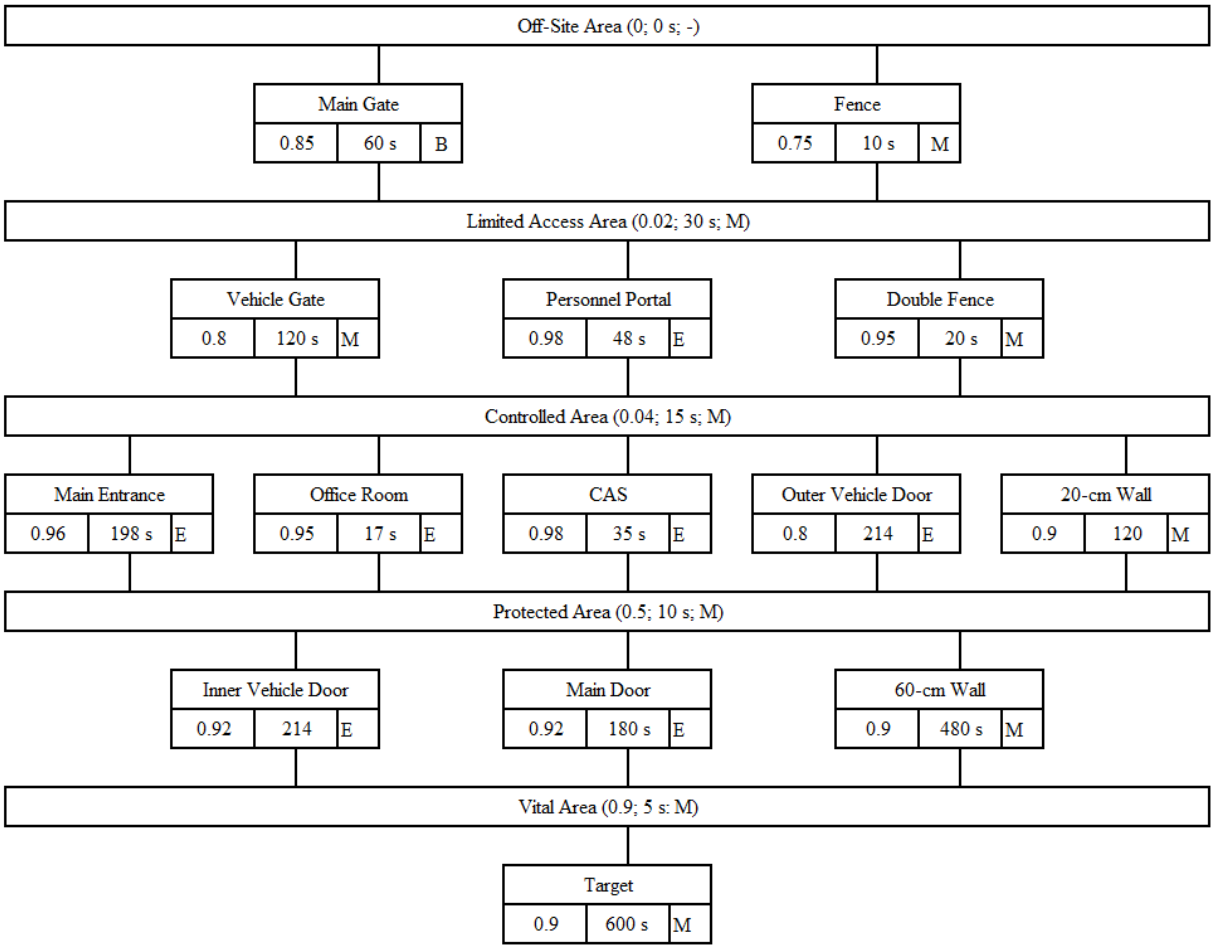

Figure 7. The Adversary Sequence Diagram (ASD) of the NARI facility

2.1.3. Adversary Sequence Diagram (ASD) and the Input File

From the facility and layout descriptions, the Adversary Sequence Diagram (ASD) of the facility's PPS can be made. The ASD in Figure 7 shows all the possible path options from the off-site area to the target for the adversary. For each path option, there are at least three pieces of information that need to be provided. The first one is the detection probability of the protection element in the path, commonly noted as P_D with a value from 0 to 1. The second information is the delay time provided by the protection element in the path, commonly noted as t_d with value in second or minute. The third one is the location of the detection point along the delay time in the path, either at the beginning (B), the middle (M), or the end (E). The HARI hypothetical facility document by SNL [17] provides all P_D and t_d values for NARI facility's ASD. Appendix B provides a detailed description of NARI facility's ASD development.

Generally, in a PPS, there are multiple protection elements to detect and delay the adversary along a path. To get the combined P_D value for a path option, the P_{ND} value of each detection element must be calculated using Equation 1.3. Then the combined P_D for that path option can be determined using Equation 2.1. As for the combined t_d value from several delay elements, Equation 2.2 is used to calculate the combined t_d for that path option. Equations 2.3 and 2.4 show an example of calculating the combined P_D value of a path option with three detection elements.

$$P_D = 1 - (P_{ND1} \times P_{ND2} \times P_{ND3}) \tag{2.1}$$

$$t_d = t_{d1} + t_{d2} + t_{d3} \tag{2.2}$$

$$P_{ND} \begin{cases} entering\ door\ BMS: P_{ND_1} = 1 - 0.8 = 0.2 \\ badge - PIN\ system: P_{ND_2} = 1 - 0.6 = 0.4 \\ exiting\ door\ BMS: P_{ND_3} = 1 - 0.8 = 0.2 \end{cases} \tag{2.3}$$

$$P_D = 1 - (0.2 \times 0.4 \times 0.2) = 1 - 0.016 = 0.984 \quad (2.4)$$

It is more complicated to estimate the location of the detection point of a path option with three detection elements in different locations. There is no general rule to follow and it depends on the user's intuition. One approach is to set the location of the detection point to the device which has the highest P_D value. Another approach used in this study is a conservative approach which sets the detection location to the last detection opportunity among those detection elements, thus, providing the minimum true t_d of that path option. For example, as shown in Figure 8a, there are three devices to detect the adversary, one at the beginning of the path, one at the middle of the path, and one at the end of the path. Therefore, the detection location will be set as 'E' if the user takes the conservative approach. Another example is if the latest 2 devices detect the adversary at the middle of the path element, as shown in Figure 8b, then the detection location will be set as 'M'.

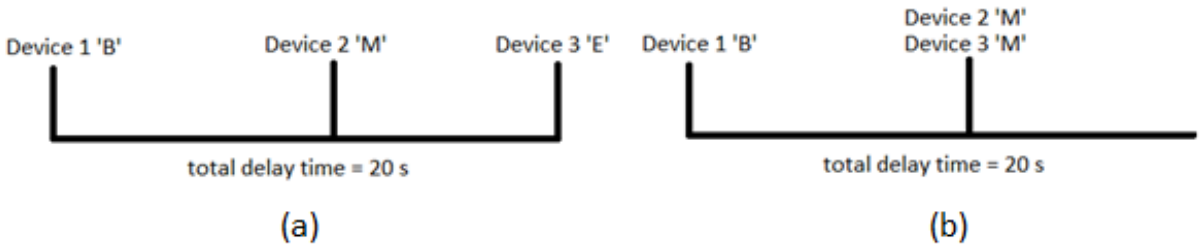

Figure 8. Detection location in a path element: (a) At the beginning, the middle, and the end. (b) At the beginning and the middle.

After the adversary sequence diagram is made, the input file for the software code can be prepared in a Microsoft Excel sheet file as shown in Figure 9. In this EASI model, the P_C value in cell E6 of the input file is same for all detection devices. And for this hypothetical facility, the P_C

value is set as 0.95, as most of the system operates at P_C=0.95 based on the SNL's system design evaluations [3]. However, the hypothetical response force team is located quite far from the facility. It takes around 11-12 minutes, 700 seconds precisely, for the postulated adequate response force team to interrupt the adversary. As a conservative approach based on tests at SNL, the standard deviation of the RFT can be estimated at 30% of the mean value [3].

In Figure 9, from row 10 and so on, one line represents one path option in a protection layer. Some information to be provided for each path option are:

- P_D value in column E
- σ_{P_D} value in column F
- Detection location in column G
- t_d value in column H
- σ_{t_d} value in column I
- Type of Delay information in column J

The type of delay component is an additional information of the delay feature of the path element, whether an authorized access might reduce the t_d of the path drastically, in which t_d=0. For example, the insider might leave the door and window unlocked for the adversary to get in the facility building through the office room, which is therefore set as 'A' for available. Meanwhile, the insider cannot use his access to reduce the delay time of the 60-cm vital area wall or the time needed by the adversary to travel the area, which is therefore set as 'NA" for not available.

In this study, it is assumed that the P_D value in a path option has 10% standard deviation in its performance. Meanwhile, the t_d standard deviation is 30% of the delay time mean value, due to

the same reason with the RFT standard deviation. Another important thing is that the user has to precisely enter the correct number of the protection layer because the largest number entered in Column B indicates the total number of protection layer in the PPS, which is used as an index in the software code's iteration.

A	B	C	D	E	F	G	H	I	J
2			Modified EASI-Monte Carlo	Probability of Alarm Communication		Response Force Time (RFT)			
3									
4									
5						Mean	Standard Deviation		
6				0.95		700	210		
7									
8									
9	Layer No	Attempt Options Description:		P(Detection)	Pdet std	Location	Delay Time Mean	Delay Time std	Type of Delay
10		a	Penetrate Main Gate	0.85	0.085	B	60	18.0	A
11		b	Penetrate Fence	0.75	0.075	M	10	3.0	NA
12	1	c							
13		d							
14		e							
15		a	Run through limited access area	0.02	0.002	M	30	9.0	NA
16		b							
17	2	c							
18		d							
19		e							
20		a	Penetrate Double Fences	0.95	0.095	M	20	6.0	NA
21		b	Penetrate Vehicle Gate	0.8	0.08	M	120	36.0	A
22	3	c	Penetrate Personnel Portal	0.98	0.098	E	48	14.4	A
23		d							
24		e							
25		a	Run through controlled area	0.04	0.004	M	15	4.5	NA
26		b							
27	4	c							
28		d							
29		e							
30		a	Penetrate Office Room	0.95	0.095	E	17	5.1	A
31		b	Penetrate CAS Room	0.98	0.098	E	35	10.5	A
32	5	c	Penetrate Outer Vehicle Door	0.8	0.08	E	214	64.2	A
33		d	Pentrate Main Entrance	0.96	0.096	E	198	59.4	A
34		e	Penetrate 20-cm Wall	0.9	0.09	M	120	36.0	NA
35		a	Run through Protected Area	0.5	0.05	M	10	3.0	NA
36		b							
37	6	c							
38		d							
39		e							
40		a	Penetrate Main Door	0.92	0.092	E	180	54.0	A
41		b	Penetrate Inner Vehicle Door	0.92	0.092	E	214	64.2	A
42	7	c	Penetrate 60-cm Wall	0.9	0.09	M	480	144.0	NA
43		d							
44		e							
45		a	Run through vital area to target	0.9	0.09	M	5	1.5	NA
46		b							
47	8	c							
48		d							
49		e							
50		a	Sabotage target	0.9	0.09	M	600	180.0	NA
51		b							
52	9	c							
53		d							
54		e							

Figure 9. The Microsoft Excel sheet file as the input for the software code

2.2. Development of the EASI-based Software Code

As discussed in section 1.2, EASI model is used widely to calculate P_I value of a PPS based on the protection elements (detection and delay elements) that must be encountered by the adversary along the path from offsite area to the target. In this study, the EASI model methodology is modified to implement the stochastic approach of calculating the P_I value from a numerous simulation. Figure 10 shows the general flowchart of the software code developed in this study.

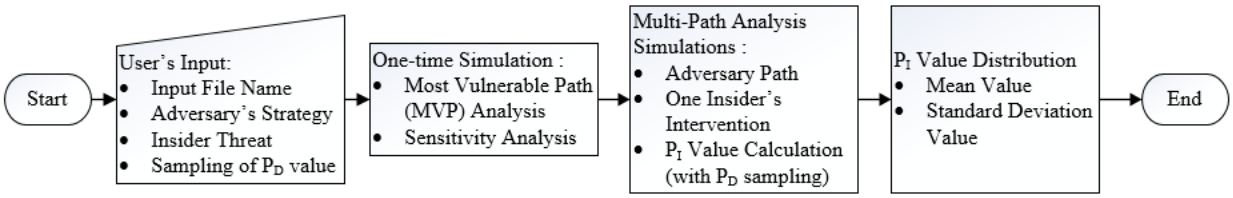

Figure 10. General flowchart of the software code

In the beginning, some information must be provided to the software code. They are the name of the MS Excel input file to be analyzed (as can be seen in Figure 9), the adversary's strategy to be assumed in the simulation to construct the adversary path, the existence and capability of the insider to be modeled in the simulation, the sampling process of P_D value along the adversary path in the simulation, and number of simulation to be done by the software code. The software code then continues to analyze the PPS information from the input file to find the Most Vulnerable Path (MVP) based on the concept of Critical Detection Point (CDP) in a one-time simulation. Also, the software code does the sensitivity analysis of P_I value with regards to P_D and t_d value, using the MVP as the base case scenario. Section 3 provides more detail about the MVP and sensitivity analysis.

After that, the software code does numerous simulation (as indicated by the user) of multi-path analysis. For every simulation, the software code constructs an adversary path by a stochastic approach based on the user's input about the adversary's strategy. The software code also uses a stochastic approach to model the insider's intervention to the PPS in assisting the adversary in in every simulation. After the adversary path and insider's intervention have been modeled, the software code calculates the P_I value using the EASI (as explained in section 1.2), in which the P_D value of every protection layer might be sampled in a stochastic process depending on the user's input for the simulation. The stochastic approach in constructing the adversary path and modeling the insider's intervention are discussed in section 4. The implementation of EASI model to do multiple simulations in the software code is discussed in sections 2.2.1, 2.2.2, 2.2.3, and 2.2.4. The stochastic approach to sampling the P_D of every protection layer is discussed in the last part of section 2.2.1 and the result of that stochastic approach to sampling P_D value is discussed in section 2.3.

2.2.1. Detection Function

This section shows the detection function calculation section built in the software code. As a reminder, there are several detection-related terms in the P_I calculation using EASI model. First, the Probability of Detection (P_D) of a protection layer is the probability that the adversary's intrusion is detected by the protection element in that protection layer, which includes the sensing, transmitting, and assessing processes. The second one is the Probability of Non-Detection (P_{ND}) of a protection layer. P_{ND} is the probability that the adversary's intrusion is not detected by the detection element in that protection layer. The third one is the Probability of No Detection (P_{NDet}) of a protection layer. It is the probability that the adversary's intrusion is not detected in any

protection layer from the starting point until the protection layer of interest. The fourth one is the Probability of First Detection (P_{FDet}) of a protection layer. It is the probability that the adversary's intrusion is not detected in any previous protection layer but then is detected for the first time in that protection layer of interest. The P_D, P_{ND}, P_{NDet}, P_{FDet} values are expressed mathematically in Equations 1.1, 1.3, 1.4, 1.5 respectively.

After the adversary path has been constructed, the software code continues with P_I calculation simulation which starts with detection function calculation. Figure 11 shows the iteration process of the software code to calculate P_{ND}, P_{NDet}, P_{FDet} for every protection layer from the first layer until the last layer.

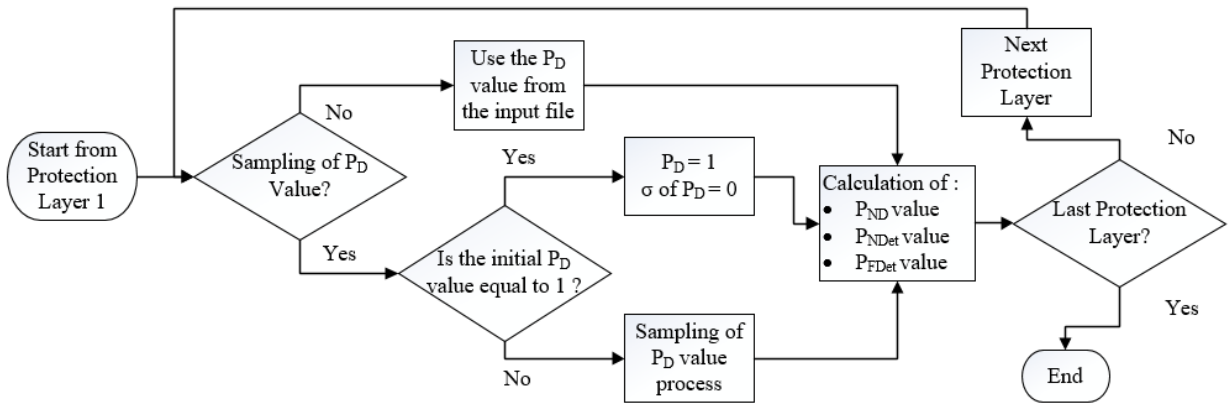

Figure 11. Detection function calculation process flowchart

Based on the user input at the beginning of the program, the software code checks whether the user wants to do sampling process for the P_D value of the adversary path to modeling the uncertainty and fluctuation of detection performance against the adversary's intrusion in the simulation. If the user indicates to not sampling the P_D value, the software code calculates the P_{ND},

P_{NDet}, P_{FDet} values based on the P_D value provided by the user in the MS Excel input file. If the user indicates to sampling the P_D value, the software code checks whether the P_D value of the protection layer in that iteration is equal to 1 or not. If it is equal to 1, the software code does not sample the P_D value for that protection layer, instead, goes straight to calculate the P_{ND}, P_{NDet}, P_{FDet} values based on P_D=1. If the P_D value of the protection layer in that iteration is not equal to 1, the software code does sample the P_D value for that protection layer through a process as shown in Figure 12.

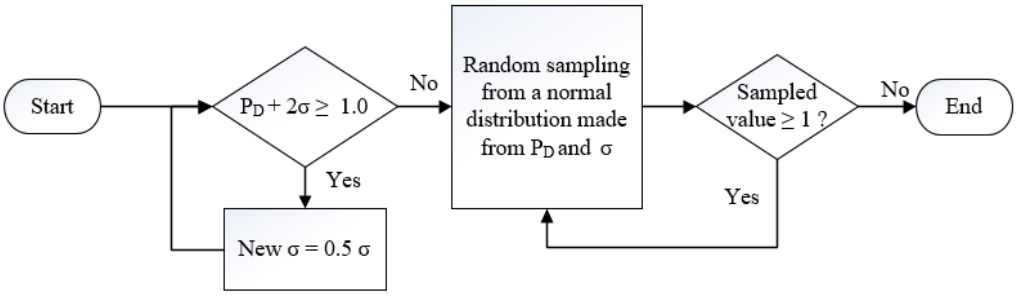

Figure 12. Sampling of P_D value process flowchart

First, the software code checks whether the $P_D + 2\sigma_{P_D}$ value of that protection layer is more than or equal to 1. If it is more than or equal to 1, the software code reduces the σ_{P_D} value of that protection layer by half until it meets the condition that $P_D + 2\sigma_{P_D}$ value is less than 1. Once that condition is met, the software code does the sampling process by generating a random number from a normal distribution which is made of the P_D value and the accepted σ_{P_D} value of that protection layer. If the sampled P_D value is equal or more than 1, the software code repeats the sampling process until it meets the condition that the sampled P_D value is less than one. Once the

sampled P_D value is meet that condition, the software code goes to calculate the P_{ND}, P_{NDet}, P_{FDet} values using that sampled P_D value for that protection layer as shown in Figure 11.

Those two conditions ($P_D + 2\sigma_{P_D}$ and the sampled P_D value have to be less than 1) have to be met to ensure that there is no P_D value is equal or more than 1 for any protection layer in which the initial P_D value provided by the user is not 1. These two conditions are also keeping the mean value of all sampled P_D values from numerous simulations, to not deviate far from the initial P_D value provided by the user for that protection layer.

2.2.2. Delay Function

This section shows the delay function calculation section built in the software code. As a reminder, there are several delay-related terms in the P_I calculation using EASI model. The first one is delay time (t_d), is an additional time provided by a protection element of the PPS, if the adversary chooses a certain path in the facility where the protection element is located. Or in other words, the amount of time needed by the adversary to overcome all protection elements in a certain path option of the protection layer of interest.

The second term is the true delay time value, which is the product of the t_d and the correction factor (C_F) with regards to the detection location. It indicates the amount of time has to be spent by the adversary after being detected for the first time in a protection layer of interest, before entering the next protection layer. For example, if the adversary has to spend 20 seconds to unlock the door in order to get through, thus, the t_d value of the door is 20 seconds. However, the detection mechanism installed on that door is that the sensor detects the adversary after the door is unlocked and opened. It means that the detection is made at the end of the delay mechanism, at end of the 20 seconds. That way, the true delay time of that path is 0 second since it provides no delay time after the first detection is made in that path. In the EASI model, the detection location information

is simplified as occurring in 3 possible ways, as expressed in Equation 1.8. Equations 1.9 and 1.10 show how the C_F affects to calculate true delay time and the true delay time variance.

The third term is the cumulative delay time. It is the total amount of delay time provided by the PPS that has to be spent by the adversary, from the beginning of the protection layer of interest until the adversary finishes their mission in the last protection layer. The fourth term is the true cumulative delay time. It is the total amount of delay time provided by the PPS that has to be spent by the adversary, from the detection location of the protection layer of interest until the adversary finishes their mission in the last protection layer. The difference between these two terms is due to the detection location (and its associated C_F) of the protection layer of interest. Equations 1.11 and 1.12 show how the C_F affects to calculate true cumulative delay time and the true cumulative delay time variance.

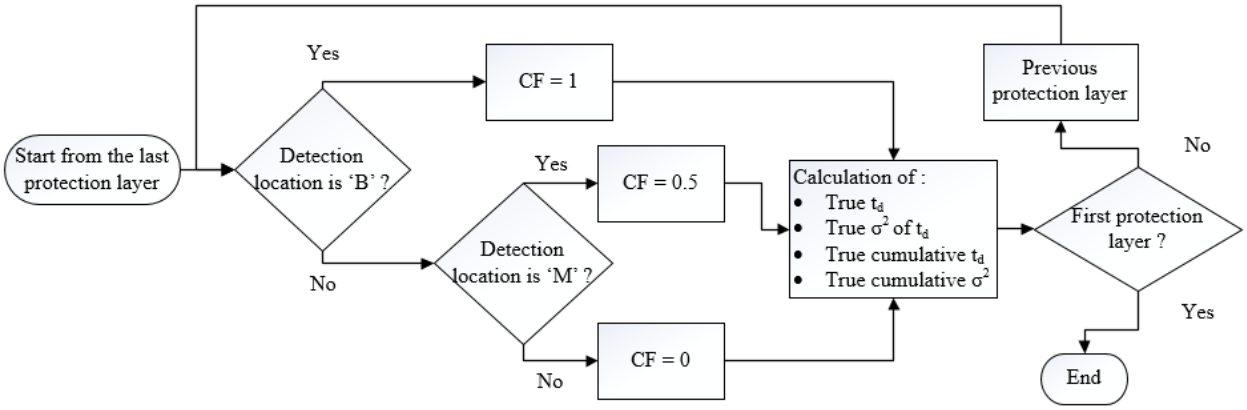

Figure 13. Delay function calculation process flowchart

After the detection function calculation process, the software code continues to delay function calculation process. Figure 13 shows the iteration process of the software code to determine the C_F of the protection layer of interest, to be used in calculating the true delay time

and true delay time variance, and also true cumulative delay time and true cumulative delay time variance of the protection layer of interest in that iteration.

The iteration process of the delay function calculation is a bit different than the detection function calculation. While the iteration of detection function calculation starts from the first protection layer, the iteration of the delay function calculation starts from the last protection layer. It is because to calculate true cumulative delay time of a protection layer, the cumulative delay time of the later protection layer has to be calculated first as shown in Equation 1.11. For example, in order to calculate the true cumulative delay time of the fifth protection layer, the cumulative delay time (Equation 1.6) for the sixth protection layer is needed. The same thing happens for the delay time variance value calculation.

2.2.3. Response Function

This section shows the response function calculation section built in the software code. After the detection function and the delay function calculations, the software continues to the response force function calculation process. As a reminder, there are several response-related terms in the P_I calculation using EASI model. The first term is the z-value, which is expressed in Equation 1.13. In general, z-value is the location of a certain value in the normal distribution indicated by how many standard deviations that value is from the mean of the normal distribution. In EASI model, given that the adversary is detected for the first time in a protection layer and based on how much time left for the adversary to complete the mission after that first detection (true cumulative delay time), how far is that time value from the RFT mean in the RFT normal distribution (made of RFT mean and standard deviation). The z-value is calculated for every protection layer in EASI model.

The second term is the Probability of Response Force Arrival ($P_{(R|A)}$) of a protection layer. It is the probability that the response force arrived before the end of adversary's mission, given the first alarm of intrusion is triggered by detection in that protection layer of interest (with its true cumulative delay time for the adversary to complete the mission). The $P_{(R|A)}$ value for every protection layer is approximated by integrating the probability density function from -∞ to the z-value of the protection layer of interest.

The third term is the specific Probability of Interruption (P_I) of a protection layer. It is the probability that the response force successfully interrupts the adversary, given the first alarm of intrusion is triggered in that protection layer of interest (with its true cumulative delay time for the adversary to complete the mission) and communicated to the response force. The specific P_I of every protection layer is the product of P_{FDet}, P_C, and ($P_{(R|A)}$) of the protection layer of interest as expressed by Equation 1.14. Finally, the total P_I value for the whole PPS's protection layers in the adversary path is the summation of all specific P_I values from every protection layer.

Figure 14 shows the flowchart of the software code to calculate z-value, $P_{(R|A)}$, and specific P_I value for every protection layer, before calculating the total P_I value of that one simulation.

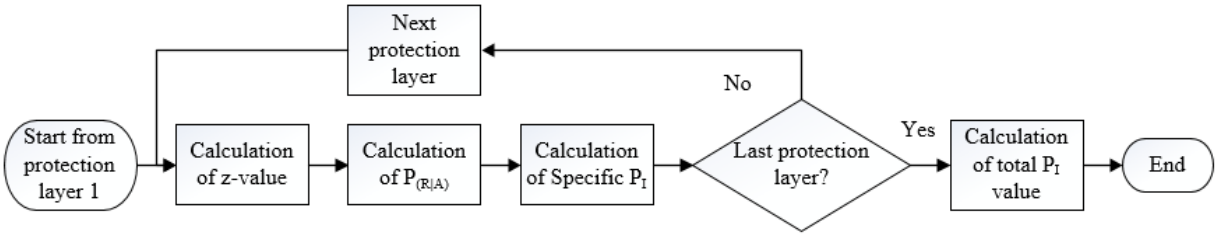

Figure 14. Response function calculation process flowchart

2.2.4. Multiple Simulations

As shown in Figure 10, the user has to provide information on how many simulations need to be done by the software code to do the multi-path analysis. For each simulation in the multi-path analysis, the software code does three main things as shown in Figure 15, which are the construction of adversary path (based on adversary's strategy), modeling the insider's intervention to the PPS, and P_I value calculation (including the sampling process of P_D values). The stochastic approach in those three processes differentiate details of one simulation from another simulation in the multiple simulations.

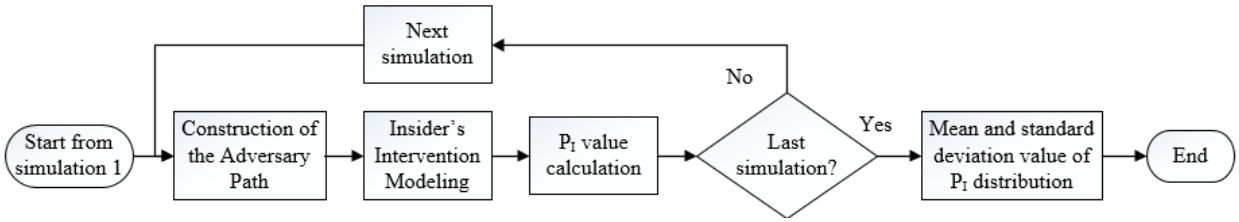

Figure 15. Multiple simulations of P_I calculation process flowchart

The software code records the P_I value for every simulation, along with some details for every simulation such as the adversary path, the P_D values, and the t_d values. The software code calculates the mean and standard deviation value of the P_I value distribution from multiple simulations.

2.3. Probability of Detection (P_D) Value Distribution

Figure 16 shows the distribution of P_D value of protection layer 1, 2, and 3 from the MVP simulation generated for a sample case. The distributions of P_D value of the other protection layers are provided in Appendix C.

For Figure 16a, the initial P_D value is 0.75 while the standard deviation is 0.075. From the sampling process, as explained in section 2.2.1, there are 100,000 P_D values of the first protection layer produced and used in 100,000 different MVP P_I calculation simulations. The distribution in Figure 16a has a mean value of 0.7495.

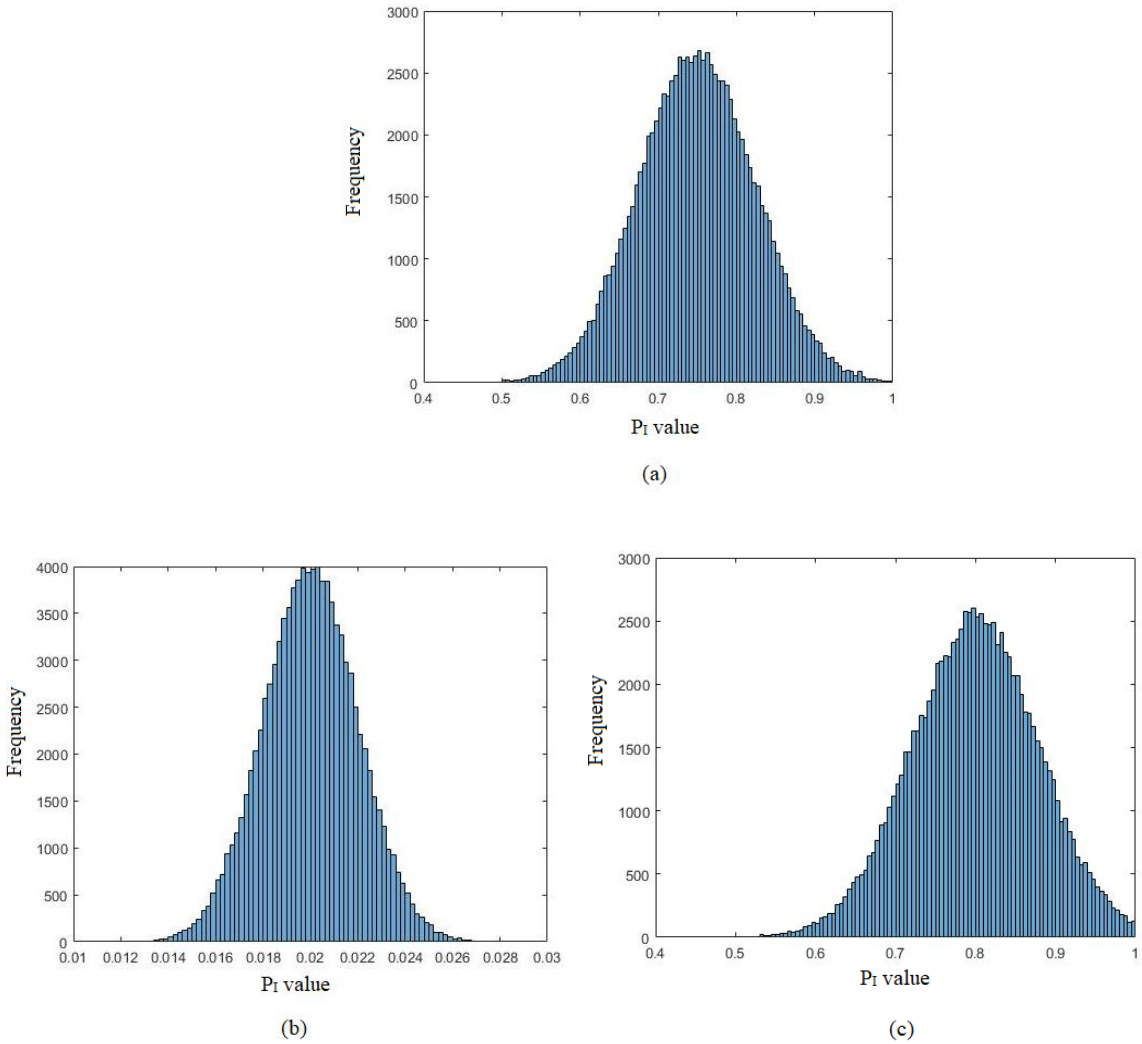

Figure 16. Distribution of P_D value for the MVP for the (a) first protection layer; (b) second protection layer; (c) third protection layer

For Figure 16b, the initial P_D value is 0.02 while the standard deviation is 0.002. From the sampling process, as explained in section 2.2.1, there are 100,000 P_D values of the second protection layer produced and used in 100,000 different MVP P_I calculation simulations. The distribution in Figure 16b has a mean value of 0.02.

For Figure 16c the initial P_D value is 0.8 while the standard deviation is 0.08. From the sampling process, as explained in section 2.2.1, there are 100,000 P_D values of the third protection layer produced and used in 100,000 different MVP P_I calculation simulations. The distribution in Figure 16c has a mean value of 0.7984.

From the distribution of P_D value for each protection layer produced by 100,000 MVP P_I calculation simulations, it can be seen that two conditions ($P_D + 2\sigma_{P_D}$ and the sampled P_D value have to be less than 1) set for the sampling process of P_D value are successfully creating a distribution of sampled P_D value used numerous simulations, in which the mean value is not far from the initial P_D value inputted by the user for the corresponding protection layer.

3. MOST VULNERABLE PATH (MVP) AND SENSITIVITY ANALYSIS

As shown in Figure 10 that the software code does a one-time simulation to analyze the PPS information the input file to find the MVP based on the CDP and does the sensitivity analysis of P_I value with regards to P_D and t_d value in that MVP. This section provides discussion on how the software code finds the MVP of the facility and does the sensitivity analysis.

3.1. Critical Detection Point (CDP) and Most Vulnerable Path (MVP)

The Most Vulnerable Path (MVP) is defined as the path to the target for which the effectiveness of the PPS, $P_E = P_I \times P_N$, is the lowest among all adversary paths [19]. Because the P_N value estimation is not part of the scope of this work, it is assumed that the MVP is the adversary path which has the lowest P_I value.

One most common approach to determine the MVP in EASI model is by utilizing the concept of Critical Detection Point (CDP). CDP is defined as the last detection point in the adversary path in which the remaining time for the adversary to complete the mission is still greater than the time for the response force to arrive (true cumulative delay time > RFT). If the detection is made before or at the CDP, the probability that the response force arrives before the end of adversary's mission is relatively higher (equal or greater than 0.5). If the detection is made after the CDP, the probability that the response force arrive before the end of adversary's mission is relatively low (lower than 0.5). Therefore, the time needed by the adversary from the CDP until the end of the mission, named as Time Remaining (TR), must be equal or more than the RFT.

Knowing the importance of this concept, the PPS designer should increase the delay function capability after the CDP, while also increasing the detection function capability before the CDP. On the other hand, the adversary might want to avoid being detected until a point, in which the remaining time for the adversary's fastest path to finish the mission is lower than the time for the response force to arrive (true cumulative delay time < RFT). PPS designer and analyst using the CDP as a reference point to determine the MVP from the ASD by choosing the path with the lowest t_d value from the bottom end until the CDP of the ASD and choosing the path with the lowest P_D value from the CDP until the top end of the ASD.

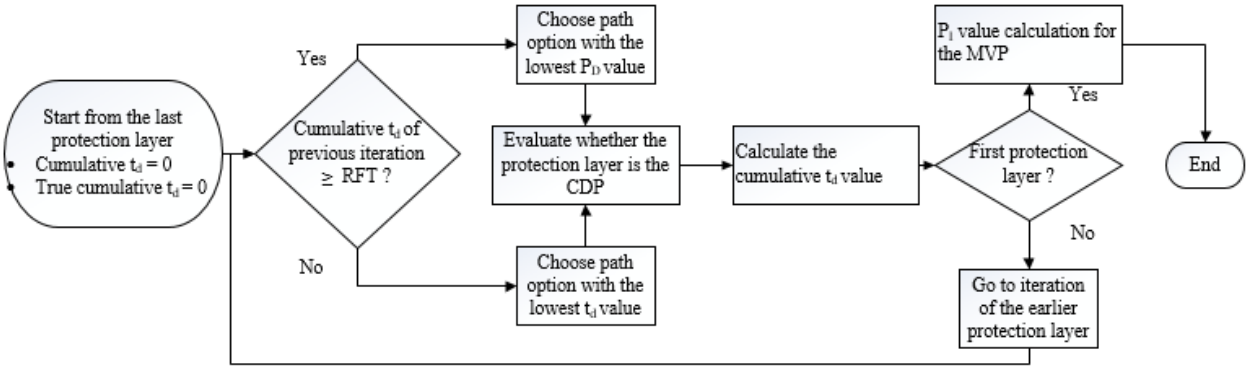

Figure 17. Overview of MVP analysis process flowchart

Figure 17 shows the iteration process of the software code in analyzing the ASD to determine the MVP and calculate the P_I value of the MVP. It shows that iteration process starts from the bottom end of the ASD towards the top end of the ASD in determining which path option in each protection layer is a part of the MVP. In every iteration, the software code evaluates whether the total cumulative delay time (not the true value) provided by the later protection layer (analyzed in previous iterations) is equal or more than the RFT value. If not equal or more than

the RFT, the software code goes to the process of choosing the path with the lowest delay capability of the protection layer in the present iteration (explained in section 3.1.1). If equal or more than the RFT, the software code goes to the process of choosing the path with the lowest detection capability of the protection layer in the present iteration (explained in section 3.1.2). After the path option has been chosen, the software code goes to the process of determining whether the protection layer in the present iteration is the location of the CDP or not. The software code also calculates the total cumulative delay time provided by all protection layer that has been analyzed by the MVP iteration process. The software code then determines whether the protection layer in the present iteration is the last to be analyzed or not. If not, it continues to the next iteration process. If yes, it calculates the P_I value of the MVP to end the process of the MVP analysis.

3.1.1. Choosing Path Option with the Lowest Delay Capability for the MVP

Figure 18 shows the process of the software code in choosing the path with the lowest delay capability. This process is done when analyzing protection layer from the bottom end of the ASD until the CDP has been found and determined in the iteration process of Figure 17. The maximum number of iteration is five since in this study the input file provides up to five path options in a protection layer.

In the first iteration, the software code takes first path option as the ‘temporary’ chosen path. In the next iteration, it will be compared with the second path option. The first comparison is the true delay time value. If the true t_d of the second path option is lower than the true t_d of the first path as the ‘temporary’ chosen path, the software code takes the second path option as the new ‘temporary’ chosen path, replacing the first path option to be compared in the next iteration. If the true t_d of the second path option is higher than the true t_d of the first path as the ‘temporary’

chosen path, the software code retains the first path option as the ‘temporary’ chosen path to be compared in the next iteration process.

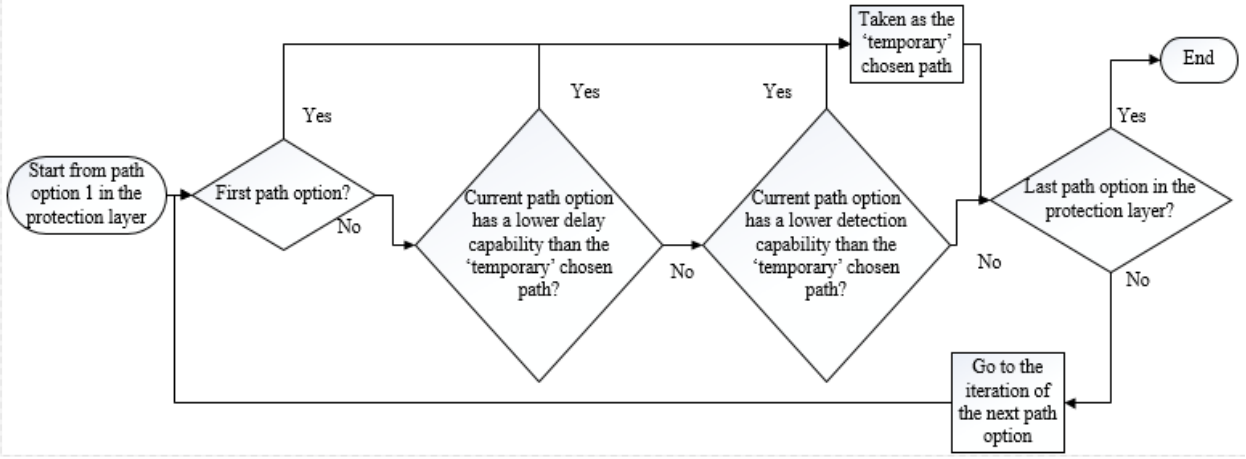

Figure 18. Path selection process flowchart for the later protection layer (CDP to end)

If the true t_d of the second path option is equal to the true t_d of the first path as the ‘temporary’ chosen path, the software code then compares the original t_d value of both path options to choose the path option with the lowest original t_d value. If both path options have the same original t_d value, the software code then compares P_D value of both path options to choose path option with the lowest P_D value. If even both path options have the same P_D value, the software code retains the first path option as the ‘temporary’ chosen path to be compared in the next iteration process. The similar comparison process is done for the rest of the iteration.

3.1.2. Choosing Path Option with the Lowest Detection Capability for the MVP

Figure 19 shows the process of the software code in choosing the path with the lowest detection capability. This process is done when analyzing protection layer from when the CDP has been found and determined in the iteration process of Figure 17, until the top end of the ASD. The maximum number of iteration is five since in this study the input file provides up to five path options in a protection layer.

In the first iteration, the software code takes first path option as the 'temporary' chosen path. In the next iteration, it will be compared with the second path option with regards to the P_D value. If the P_D of the second path option is lower than the P_D of the first path as the 'temporary' chosen path, the software code takes the second path option as the new 'temporary' chosen path, replacing the first path option to be compared in the next iteration. If the P_D of the second path option is higher than the P_D of the first path as the 'temporary' chosen path, the software code retains the first path option as the 'temporary' chosen path to be compared in the next iteration process.

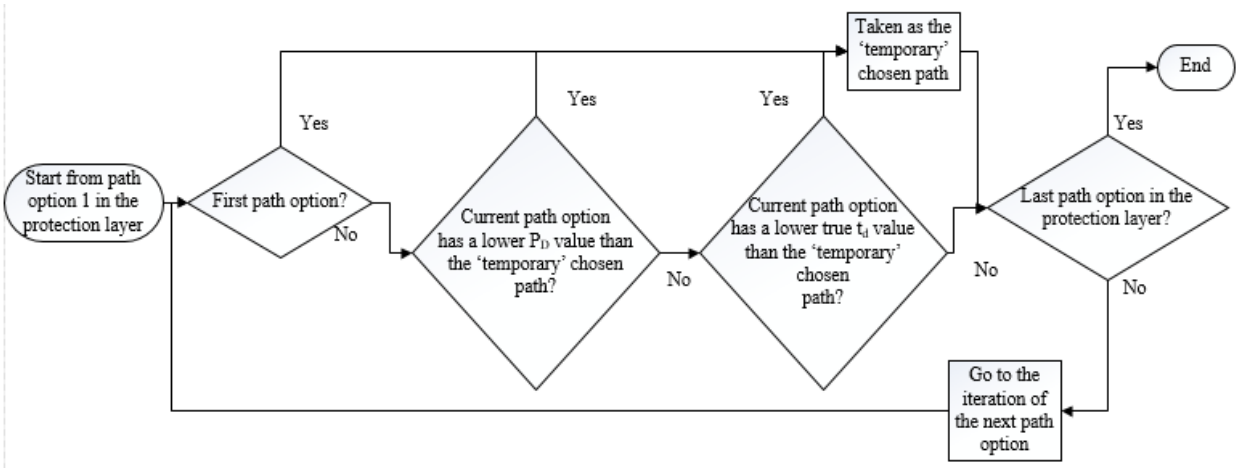

Figure 19. Path selection process flowchart for the earlier protection layer (start to CDP)

If both path options have the same P_D value, the software code then compares true t_d of both path options to choose path option with the lowest true t_d. If even both path options have the same true t_d value, the software code retains the first path option as the 'temporary' chosen path to be compared in the next iteration process. The similar comparison process is done for the rest of the iteration.

3.1.3. Determining the CDP Location of the MVP

As can be seen from Figure 17, that after a path option has been chosen in an iteration of a protection layer, from either the process in section 3.1.1 or section 3.1.2, the software code goes to the process of determining whether the CDP is in the protection layer of the present iteration or not.

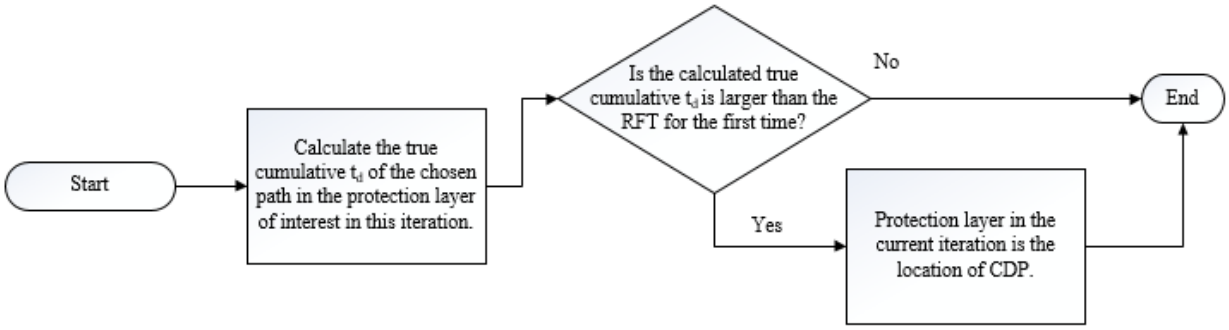

Figure 20. Flowchart of the process in determining the CDP location

Figure 20 shows the flowchart of determining the CDP by the software code. The software code adds the true t_d of the chosen path of the protection layer of interest in the present iteration, with the total cumulative delay time from the previous iteration, to get the true cumulative delay time of the protection layer (which is the remaining time for the adversary to complete the mission given is detected in this protection layer). If only this true cumulative delay time is the first to

equal or larger than the RFT mean, then the corresponding protection layer is the location of the CDP and the true cumulative delay time of that protection layer is the TR value of the CDP.

3.1.4. MVP Analysis Result of the NARI Facility

The MVP analysis of the NARI facility by the software code gives P_I=0.88. The CDP of the facility is at the sixth protection layer, which gives TR = 790 seconds until the adversary complete the mission. Table 1 shows the path information for every protection layer in the MVP of the NARI facility. It is seen that software code chooses the lowest P_D value from the first until sixth protection layer, then chooses the lowest t_d afterward. Figure 21 shows the MVP in the facility layout.

Table 1. Most Vulnerable Path (MVP) of the NARI facility

Layer	Path Option #	Description	P_D	Detection Location	Delay Time (Mean)	Type of Delay
1	2	Penetrate Fence	0.75	M	10	NA
2	1	Run through limited area	0.02	M	30	NA
3	2	Penetrate Vehicle Gate	0.8	M	120	A
4	1	Run through controlled area	0.04	M	15	NA
5	3	Penetrate Vehicle Door	0.8	E	214	A
6	1	Run through protected area	0.5	M	10	NA
7	1	Penetrate Main Door	0.92	E	180	A
8	1	Run through vital area	0.9	M	5	NA
9	1	Sabotage Target	0.9	M	600	NA

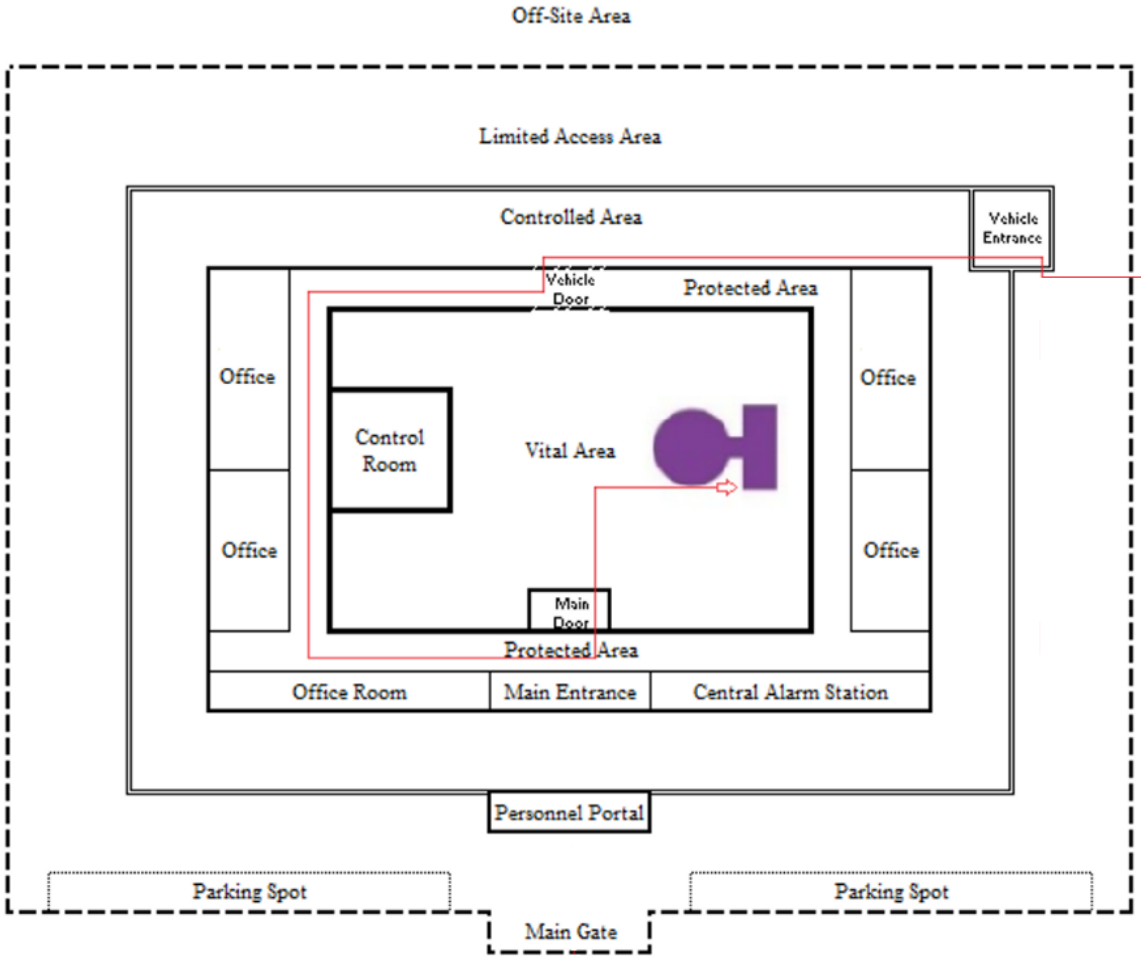

Figure 21. The layout of the MVP route as the result of the MVP analysis

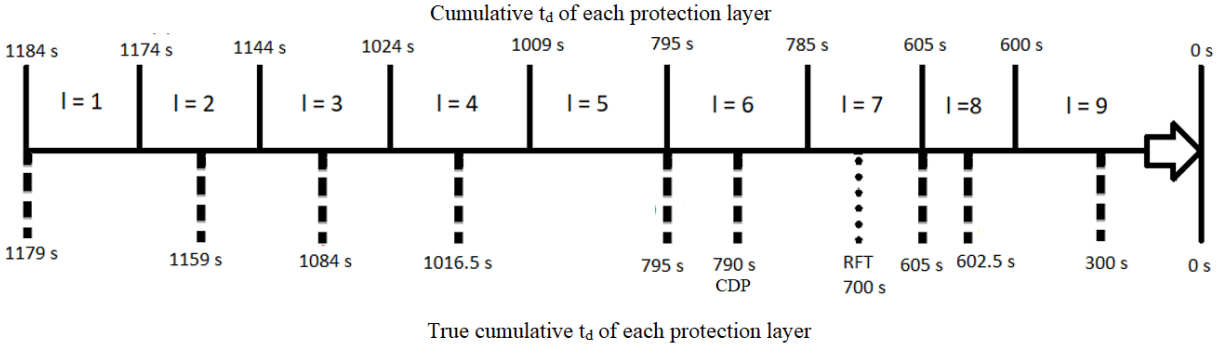

Figure 22. The adversary timeline of the MVP

Figure 22 shows the adversary timeline of the MVP for the NARI facility. However, the dimension scale between those lines does not precisely show the time distance between one protection layer to another. The upward solid line shows the cumulative delay time provided by the PPS from the target until the protection layer of interest. The downward dashed line indicates the true cumulative delay time from the target until the detection point protection layer of interest. The downward dotted line shows the response force time (RFT) of the PPS.

The MVP analysis states that the CDP is the sixth layer with TR=790 seconds, although the RFT itself is 700 seconds and falls in the bin of the seventh protection layer. However, as can be seen in the PPS description and input file in section 2.1, all protection elements in the seventh protection layer make detection at the end of penetration of the seventh protection layer. Thus, if the adversary is detected by any protection element of seventh protection layer, there are only 605 seconds left before the adversary reaches the target, as shown by true cumulative delay time at seventh protection layer in Figure 22. In that case, the response force does not have enough time to interrupt the adversary's intrusion. To prevent this from happening, the sixth protection layer must be set as the CDP, as this is the last chance for the PPS to detect the adversary while the response force still has time to interrupt the adversary's intrusion.

If each of all the path options in the seventh protection layer makes a detection at the beginning of the penetration of seventh protection layer, then the chosen path for seventh protection layer will stay the same, while the CDP will be at the seventh protection layer and the TR value is 785 seconds. That change is to fulfill the definition of CDP, as the first detection point before any point, in which cumulative delay time is equal to the RFT. Meanwhile, if only first path option of the seventh protection layer detects the adversary at the beginning of penetration to the

seventh protection layer, while the other path elements detect at the end, the software will choose third path option due to its smaller t_d value compared to the t_d value of second path option in the seventh layer. That will affect the cumulative delay time value from the seventh layer to the first layer.

3.2. Sensitivity Analysis

After the MVP analysis has been done, the software code continues with sensitivity analysis of P_I with regards to the P_D and t_d value in the MVP. Figure 23 shows the flowchart of the sensitivity analysis process by the software code, in which the iteration starts from the first until the last protection layer of the MVP. In every iteration process for each protection layer, there are 7 sub-iteration processes in which the first two sub-iterations are to get data points for sensitivity with regards to P_D value while the last five sub-iterations are to get data points for sensitivity with regards to t_d value.

In the first sub-iteration, the software code calculates P_I value for which the P_D value of the protection layer of interest in the present iteration is decreased by its σ_{P_D}. In the second sub-iteration, the software code calculates P_I value for which P_D value of the protection layer of interest in the present iteration is increased by its σ_{P_D}.

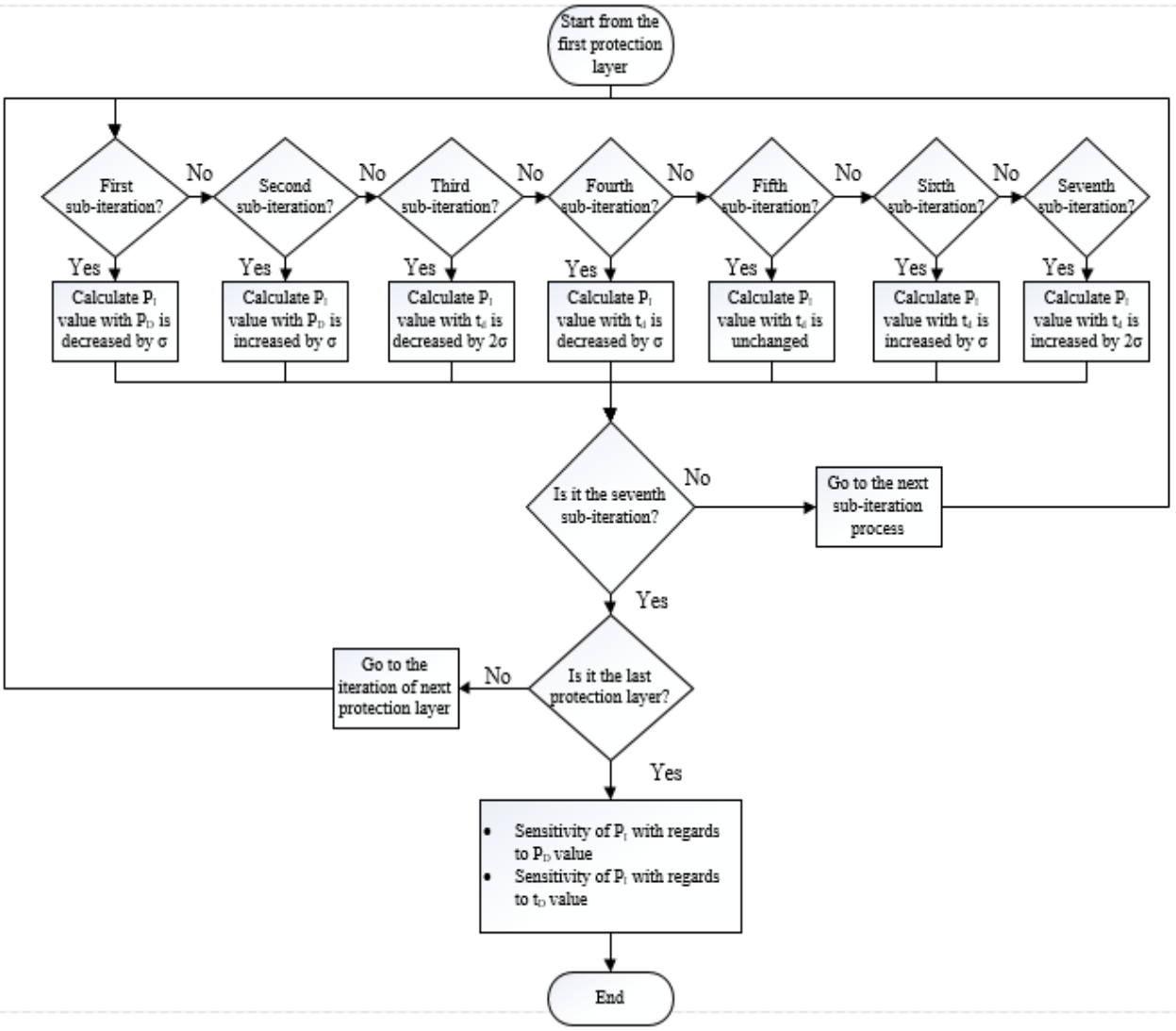

Figure 23. Sensitivity Analysis Process Flowchart

In the third sub-iteration, the software code calculates P_I value for which the t_d value of the protection layer of interest in the present iteration is decreased by two times its σ_{t_d}. In the fourth sub-iteration, the software code calculates P_I value for which the t_d value of the protection layer of interest in the present iteration is decreased by one times its σ_{t_d}. In the fifth sub-iteration, the software code calculates P_I value for which the t_d value of the protection layer of interest in the

present iteration is unchanged. In the sixth sub-iteration, the software code calculates P_I value for which the t_d value of the protection layer of interest in the present iteration is increased by one times its σ_{t_d}. In the seventh sub-iteration, the software code calculates P_I value for which the t_d value of the protection layer of interest in the present iteration is increased by two times its σ_{t_d}. In the sub-iteration in which the t_d is changed, the σ_{t_d} will be adjusted (30% of t_d) when calculating the P_I value.

After 7 sub-iterations have been done for every protection layer iteration, the software code continues with calculating the sensitivity of P_I with regards to the P_D and t_d value. From manual EASI calculation with five data points for the sensitivity analysis of P_I with regards to P_D value, it is found that the P_D has a linear relationship with the P_I value. Figure 24 shows the example of a linear relationship between P_D of first protection layer with P_I value. Therefore, the software code uses Equation 3.2 to predict how much the P_I will change if there is 0.1 absolute value deviation of P_D in any protection layer.

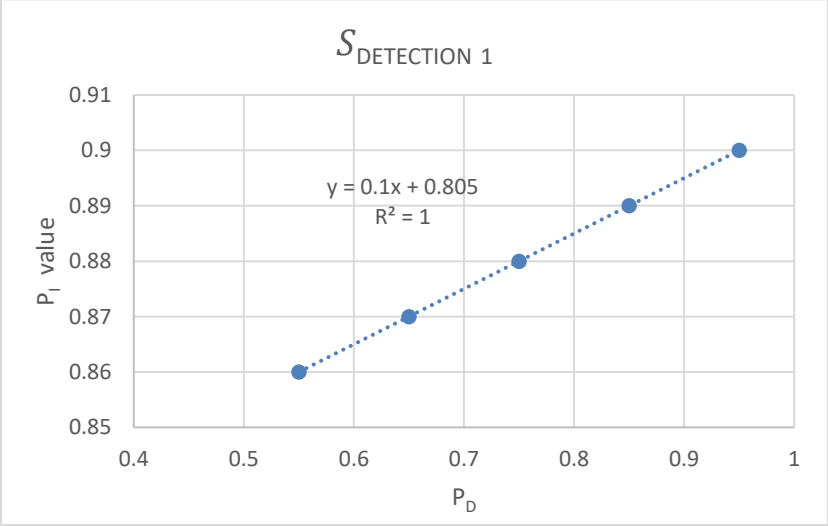

Figure 24. Relationship of P_D of the first protection layer with P_I value

$$S_{P_D} = 0.1 \times \frac{P_{I(P_D+\sigma_{P_D})} - P_{I(P_D-\sigma_{P_D})}}{(2\times\sigma_{P_D})} \quad (3.2)$$

Meanwhile, from manual EASI calculation with five data points for the sensitivity analysis of P_I with regards to t_d value, it is found that the t_d has a non-linear relationship with the P_I value, especially if t_d value is big and comparable to the RFT. For example, Figure 25 shows the non-linear relationship between the t_d of the ninth protection layer with the P_I value.

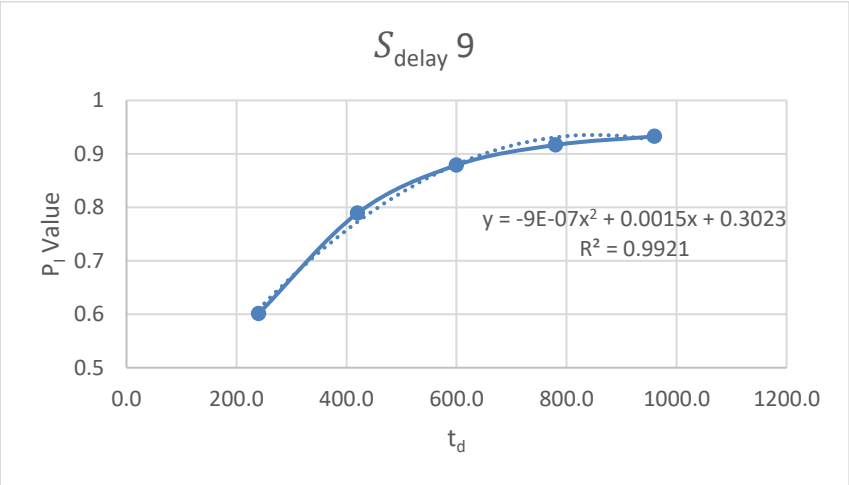

Figure 25. Relationship of t_d of the ninth protection layer with P_I value

The software cannot use the same principle as the detection case to predict the change of P_I value due to a deviation of t_d in any protection layer. Instead, the software code creates a polynomial equation with a degree of 2 as exampled by Equation 3.3, then used the coefficient 'a' and coefficient 'b' in Equation 3.4 to predict how much the P_I value will change if there is any 5 seconds deviation of t_d in the protection layer. Coefficient 'c' is not used because it is canceling each other in the derivation process to find the difference of coefficient 'y' from different 'x' values.

$$y = ax^2 + bx + c \tag{3.3}$$

$$S_{t_d} = a(10 \times t_d \times 25) + b(5) \tag{3.4}$$

3.2.1. Sensitivity Analysis with Regards to P_D Value

Table 2 summarizes the result of the P_I sensitivity analysis with respect to the P_{Ds} of the detection elements in the NARI facility's MVP (Table 1). From the sensitivity analysis, it can be inferred that the P_D in the first protection layer is one of the most sensitive points of the PPS, as it causes a change of 0.0094 (≈0.01) to the total P_I value if the P_D deviates by an absolute value of 0.1. It is followed by the P_D in the third protection layer, as it also causes a change of 0.0068 (≈0.01) in the total P_I value if P_D is deviated by an absolute value of 0.1. However, both changes are still insignificant to the base case P_I=0.88.

Table 2. Summary of sensitivity analysis of P_I with regards to P_D value

Base Case Probability of Interruption for MVP P_I = 0.88			
Layer	P_I for P_D - σ	P_I for P_D + σ	P_I Value change due to 0.1 deviation of P_D
1	0.87	0.89	0.01
2	0.88	0.88	0.00
3	0.87	0.88	0.01
4	0.88	0.89	0.00
5	0.88	0.88	0.00
6	0.88	0.88	0.00
7	0.88	0.88	0.00
8	0.88	0.88	0.00
9	0.88	0.88	0.00

Appendix D provides the calculation tables which show how the P_D value of a protection layer change affects the whole P_I value calculation. The calculation tables verify that the major contribution of the total P_I value comes from the specific P_I value of the first and the third protection layers as those two contribute 0.85 to the total P_I value.

3.2.2. Sensitivity Analysis with Regards to t_d Value

Table 3 shows the P_I values obtained by the software code for each protection layer, in cases that the t_d is decreased by 2 σ_{t_d}, decreased by 1 σ_{t_d}, unchanged, increased by 1 σ_{t_d}, increased by 2 σ_{t_d}. It also shows coefficients a, b, and c of the polynomial equation degree of 2 fitted for those five P_I values for each protection layer. Appendix E provides graphs of polynomial equation fitted for 5 data points for each NARI facility's MVP protection layer.

Table 3. Summary of sensitivity analysis of P_I with regards to t_d value

Layer	P_I Value for different t_d value in protection layer					a	b	c	P_I value change due to 5 seconds deviation
	$t_d - (2*\sigma)$	$t_d - (1*\sigma)$	t_d of MVP	$t_d + (1*\sigma)$	$t_d + (2*\sigma)$				
1	0.88	0.89	0.88	0.88	0.88	8.0E-07	0.0001	0.88	0.0006
2	0.87	0.88	0.88	0.88	0.88	-6.0E-07	0.0003	0.87	0.0012
3	0.85	0.87	0.88	0.89	0.90	-7.0E-07	0.0005	0.83	0.0015
4	0.88	0.88	0.88	0.88	0.88	-7.0E-07	0.0004	0.87	0.0018
5	0.82	0.85	0.88	0.90	0.91	-9.0E-07	0.0007	0.76	0.0017
6	0.88	0.88	0.88	0.88	0.88	-8.0E-07	0.0004	0.87	0.0020
7	0.82	0.86	0.88	0.90	0.91	-6.0E-07	0.0008	0.78	0.0020
8	0.88	0.88	0.88	0.88	0.88	-6.0E-06	0.0004	0.88	0.0021
9	0.60	0.79	0.88	0.92	0.93	-9.0E-07	0.0015	0.30	0.0022

Right end column in Table 3 shows the result of P_I sensitivity analysis due to 5 seconds deviation of any protection layer's t_d value of the NARI facility's MVP. There is a general trend

that the P_I is more sensitive to t_d value change at the deeper protection layers, although there are some anomalies in the fifth and seventh protection layer in this case. Those two layers have a smaller P_I value change than the previous protection layer because their detection locations are located at the end of the path (see Table 1). However, all P_I value changes are insignificant to the base case P_I value (0.88). It means that the NARI facility's MVP is not sensitive to 5 seconds deviation of any protection layer's t_d value.

4. THE ADVERSARY PATH AND THE INSIDER'S INTERVENTION OF PPS

As shown in Figure 10, the software code does numerous simulations of multi-path analysis based on the user's input about the adversary's strategy and insider's intervention. The software code uses stochastic (Monte Carlo) approach to construct the adversary path (and the P_D values in that path), model the insider's intervention for every simulation, and eventually calculates the P_I value for that simulation. The software code then estimates the mean and standard deviation values, as expressed by Equations 4.1 and 4.2 respectively, of the P_I value distribution obtained from numerous simulation.

$$\mu = \frac{1}{N}\sum_{i=1}^{N} x_i \tag{4.1}$$

$$\sigma = \sqrt{\frac{1}{N-1}\sum_{i=1}^{N} |x_i - \mu|^2} \tag{4.2}$$

There are five adversary's strategies developed in the software code to be used in the simulation, which are the random strategy, rushing strategy, covert strategy, deep penetration strategy, and MVP strategy. These strategies are explained in sections 4.1.1, 4.1.2, 4.1.3, 4.1.4, and 4.1.5. Those strategies are developed for multi-path analysis simulation, except the MVP strategy in which the software code uses a single path (the result from MVP analysis) in the simulation and only does the stochastic approach in modeling the insider's intervention and sampling the P_D values.

There are three insider's intervention models developed in the software code to be used in the simulation, which are the insider's intervention of P_D, insider's intervention of t_d, and insider's intervention of P_D and t_d. These three models are explained in sections 4.2.1, 4.2.2, 4.2.3.

Figure 26 shows the general flowchart of the software code in the process of constructing the adversary path and modeling the insider's intervention of the PPS. It starts by evaluating the user's input about the adversary's strategy. Depending on the user's input, the software code goes to a different algorithm for constructing the adversary path by using stochastic approach (except the MVP strategy). The software code then continues by evaluating the user's input about the insider in the simulation. Depending on the user's input, the software code goes to a different algorithm in modeling the insider's intervention of PPS in the adversary path by using stochastic approach.

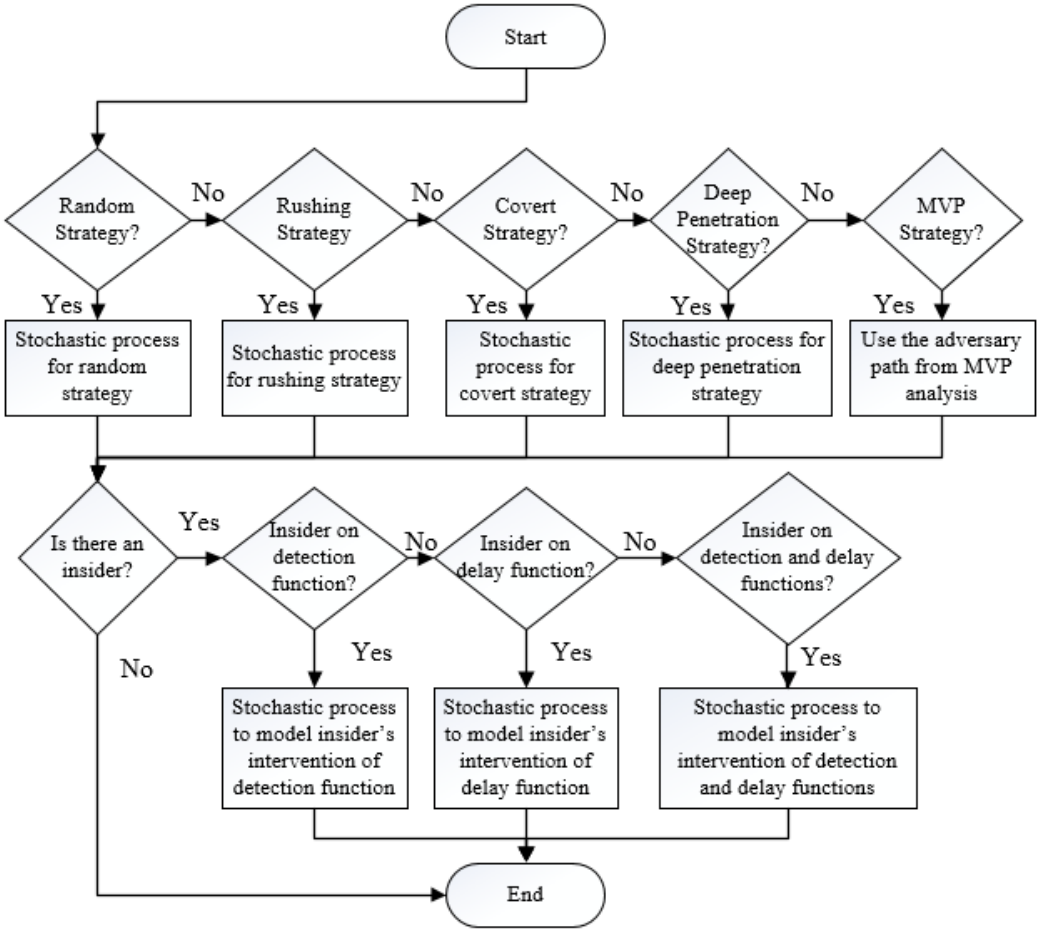

Figure 26. Adversary path and insider's intervention modeling process flowchart

4.1. The Adversary's Strategy

4.1.1. Random Strategy

The first adversary's strategy developed in the software code is the random strategy. It is an option for the user to assume that the adversary has no particular strategy in penetrating the facility, therefore, chooses the path randomly without much consideration about the existing PPS in the facility. This option can be used to simulate an adversary which does not have adequate knowledge about the existing PPS when penetrating the facility, thus, makes a spontaneous path choice based on any consideration and circumstance at the time.

Figure 27 shows the example of stochastic approach implementation in the software code, in modeling adversary's random strategy in choosing one path in a protection layer with three path options. The software code generates and assigns a random number (between 0 to 1) for every path option. The software code then normalizes those assigned numbers and create bins from 0 to 1 as shown in Figure 27. Lastly, the software code generates another random number (between 0 to 1) after the bins have been made. If the random number is between 0 and 0.3, the first path option is the chosen path for that protection layer. If the random number is between 0.3 and 0.75, the second path option is the chosen path for that protection layer. If the random number is between 0.75 and 1, the third path option is the chosen path for that protection layer. This process is being done for each protection layer, from first to last, by the software code in adversary's random strategy.

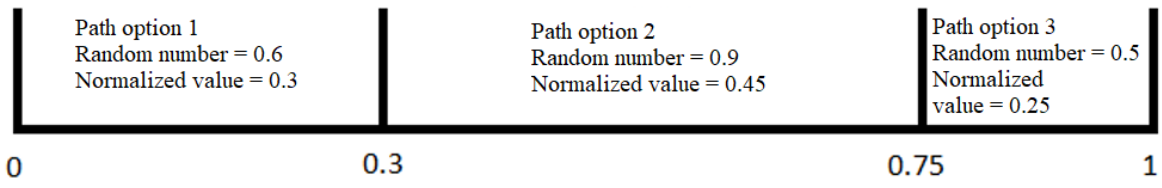

Figure 27. Example of bins for random strategy path selection process

Figure 28 shows the distribution of P_I values from 100,000 simulations for the adversary's random strategy in penetrating the NARI facility. The distribution is a result of the multi-path analysis, with the sampling of P_D values of the constructed adversary path in each simulation, without insider's intervention of any PPS's function. The mean value of the distribution is 0.86 with a standard deviation of 0.07.

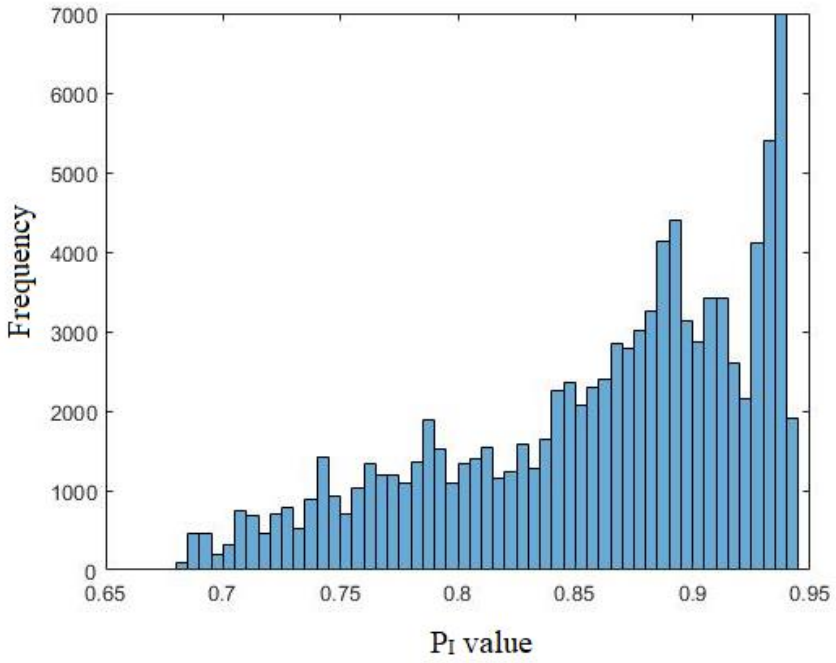

Figure 28. The P_I value distribution of the adversary's random strategy simulations

4.1.2. Rushing Strategy

The second adversary's strategy developed in the software code is the rushing strategy. It is an option for the user to assume that the adversary, for whatever reason, disregards the detection capability of the existing PPS. The adversary is assumed to tend to choose the faster way (path

option with the lower t_d value) in penetrating the facility. The adversary is assumed to know the layout of the facility and understand the t_d value of each path option in every protection layer.

$$'new' = 1 - normalized\ t_d \tag{4.3}$$

Figure 29 shows the example of stochastic approach implementation in the software code, in modeling adversary's rushing strategy in choosing one path in a protection layer with three path options. First, the software code normalizes the t_d value of each path option. Equation 4.3 is then used to get a 'new' assigned number for every path option. Those numbers are then normalized to be used by the software code to create bins from 0 to 1 as shown in Figure 29. By this process, path option with a lower t_d value will have a wider bin, which means more preferred to be chosen by the adversary. Lastly, the software code generates a random number (between 0 to 1) after the bins have been made. If the generated random number is between 0 and 0.4, the first path option is the chosen path for that protection layer. If the random number is between 0.4 and 0.65, the second path option is the chosen path for that protection layer. If the random number is between 0.65 and 1, the third path option is the chosen path for that protection layer. This process is being done for each protection layer, from first to last, by the software code in adversary's rushing strategy.

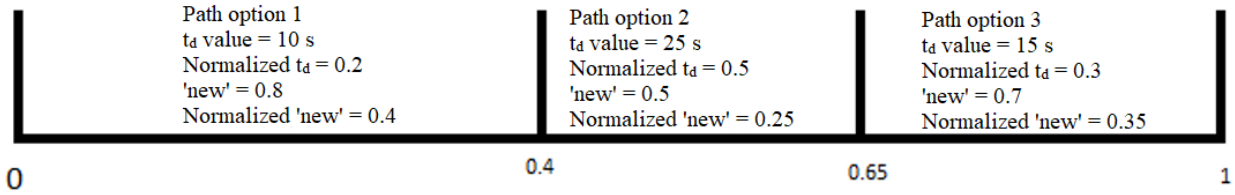

Figure 29. Example of bins for rushing strategy path selection process

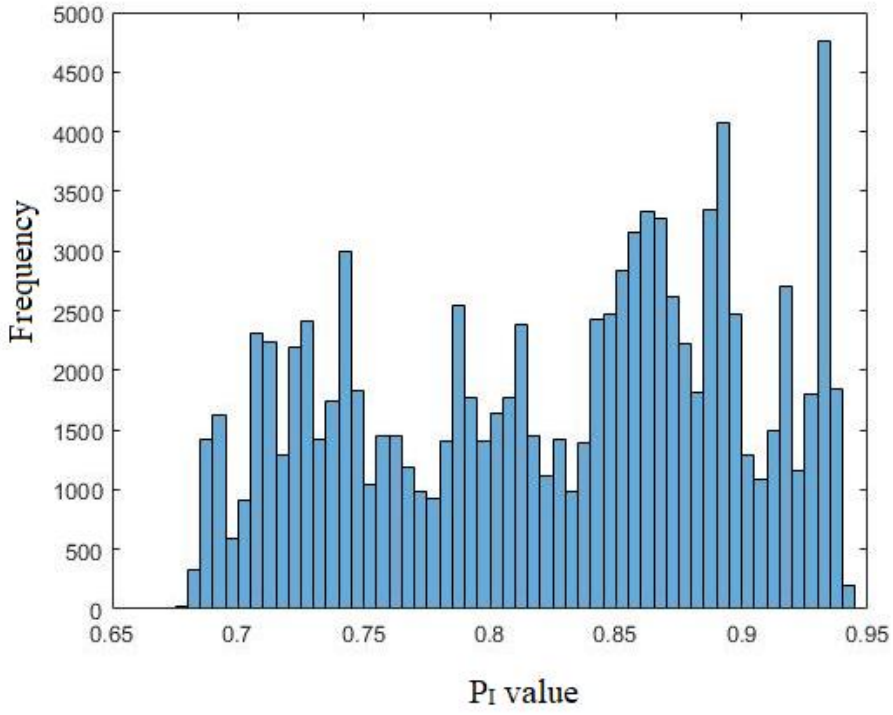

Figure 30. The P_I value distribution of the adversary's rushing strategy simulations

Figure 30 shows the distribution of P_I values from 100,000 simulations for the adversary's rushing strategy in penetrating the NARI facility. The distribution is a result of the multi-path analysis, with the sampling of P_D values of the constructed adversary path in each simulation, without insider's intervention of any PPS's function. The mean value of the distribution is 0.83 with a standard deviation of 0.07.

4.1.3. Covert Strategy

The third adversary's strategy developed in the software code is the covert strategy. It is an option for the user to assume that the adversary, for whatever reason, disregards the delay capability of the existing PPS. The adversary is assumed to tend to avoid being detected (path

option with the lower P_D value) in penetrating the facility. The adversary is assumed to know the layout of the facility and understand the P_D value of each path option in every protection layer.

Figure 31 shows the example of stochastic approach implementation in the software code, in modeling adversary's covert strategy in choosing one path in a protection layer with three path options. First, the software code uses Equation 1.3 to get the P_{ND} value for each path option. The software code then normalizes those P_{ND} values and creates bins from 0 to 1 as shown in Figure 31. Lastly, the software code generates a random number (between 0 to 1) after the bins have been made. If the generated random number is between 0 and 0.35, the first path option is the chosen path for that protection layer. If the random number is between 0.35 and 0.7, the second path option is the chosen path for that protection layer. If the random number is between 0.7 and 1, the third path option is the chosen path for that protection layer. This process is being done for each protection layer, from first to last, by the software code in adversary's covert strategy.

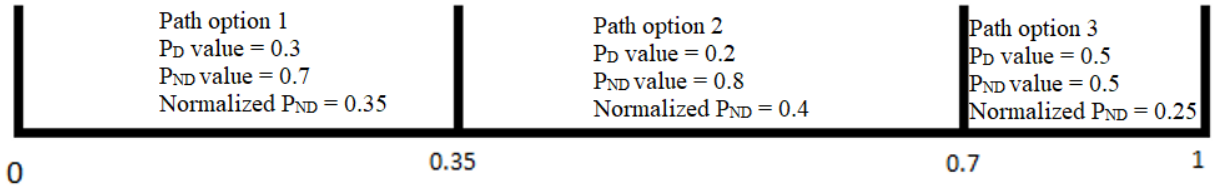

Figure 31. Example of bins for covert strategy path selection process

Figure 32 shows the distribution of P_I values from 100,000 simulations for the adversary's covert strategy in penetrating the NARI facility. The distribution is a result of the multi-path analysis, the with sampling of P_D values of the constructed adversary path in each simulation, without insider's intervention of any PPS's function. The mean value of the distribution is 0.89 with a standard deviation of 0.05.

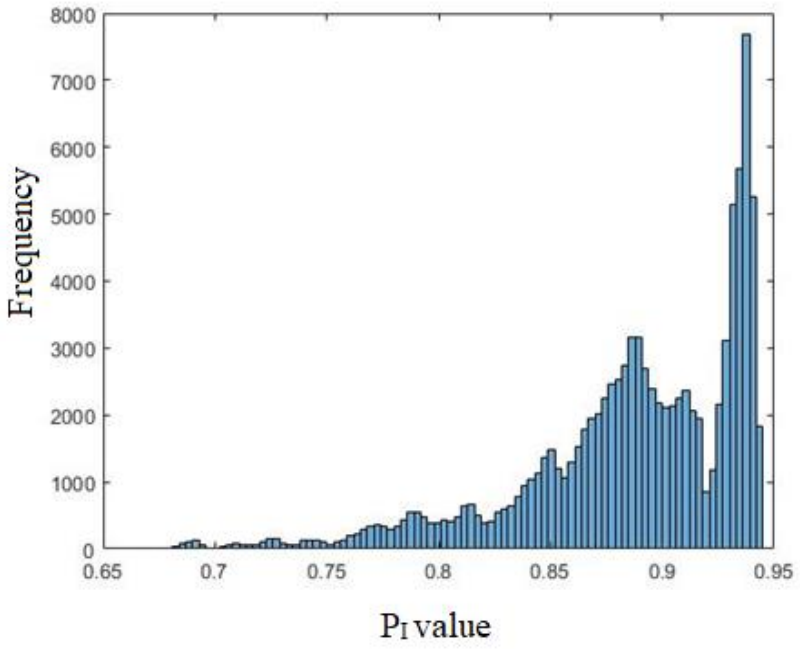

Figure 32. The P_I value distribution of the adversary's covert strategy simulations

4.1.4. Deep Penetration Strategy

The fourth adversary's strategy developed in the software code is the deep penetration strategy. It is an option for the user to assume that the adversary has a lot of knowledge of the facility layout and the PPS of the facility, and understands the concept of the detection, delay, and response functions of the PPS, as well as the CDP of the facility. Therefore, it is assumed that the adversary tries to penetrate the facility as deep as possible by choosing path option with the lower P_D value before the CDP and choosing path option with the lower t_d value after the CDP.

Figure 33 shows the flowchart of the software code modeling the adversary's deep penetration strategy in constructing the adversary path. The software code uses the CDP resulted from the MVP analysis as a reference protection layer. If the protection layer of interest is before or at the CDP's protection layer, the software code uses the algorithm of covert strategy (lower P_D value) in choosing path option in that protection layer. If the protection layer of interest is after the

CDP's protection layer, the software code uses the algorithm of rushing strategy (lower t_d value) in choosing path option in that protection layer. This process is being done for each protection layer, from first to last, by the software code in adversary's deep penetration strategy.

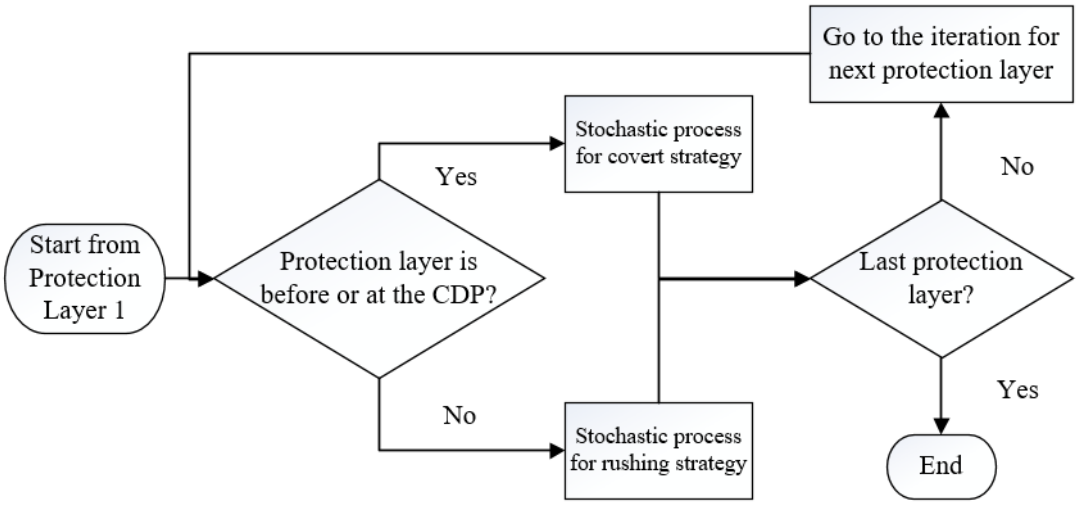

Figure 33. Flowchart of modeling the adversary's deep penetration strategy in path selection process

Figure 34 shows the distribution of P_I values from 100,000 simulations for the adversary's deep penetration strategy in penetrating the NARI facility. The distribution is a result of the multi-path analysis, with the sampling of P_D values of the constructed adversary path in each simulation, without insider's intervention of any PPS's function. The mean value of the distribution is 0.88 with a standard deviation of 0.05.

There is a sharp drop in the area between 0.91 and 0.93 in Figure 34. It is because the fact most of the path combinations with deep penetration strategy resulted in the area around 0.87 and around 0.94, while their P_D value sampling process is rarely resulting P_I value between 0.91 and 0.93. There are only few path combinations with P_I value in the area between 0.91 and 0.93.

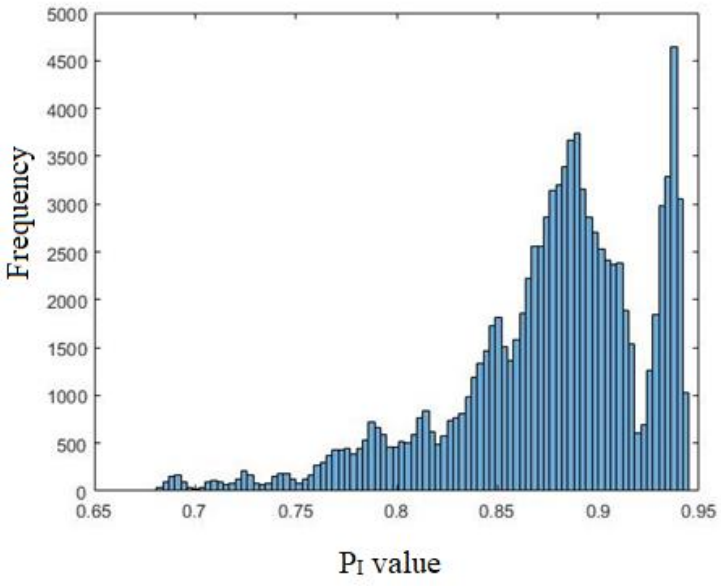

Figure 34. The P_I value distribution of the adversary's deep penetration strategy simulations

4.1.5. MVP Strategy

The fifth adversary's strategy developed in the software code is the MVP strategy. It is an option for the user to assume that the adversary has a full knowledge of the facility layout, the PPS, and the CDP of the facility. The adversary then has chosen the MVP of the facility, as explained in section 3.1, to be the only determined path in penetrating facility.

Figure 35 shows the distribution of P_I values from 100,000 simulations for the adversary's random strategy in penetrating the NARI facility. The distribution is a result of the multi-path analysis, with the sampling of P_D values of the constructed adversary path in each simulation, without insider's intervention of any PPS's function. The mean value of the distribution is 0.88 with a standard deviation of 0.01. Unexpectedly, random strategy and rushing strategy have a lower P_I value than deep penetration strategy and MVP strategy. This unexpected result is discussed in section 5.

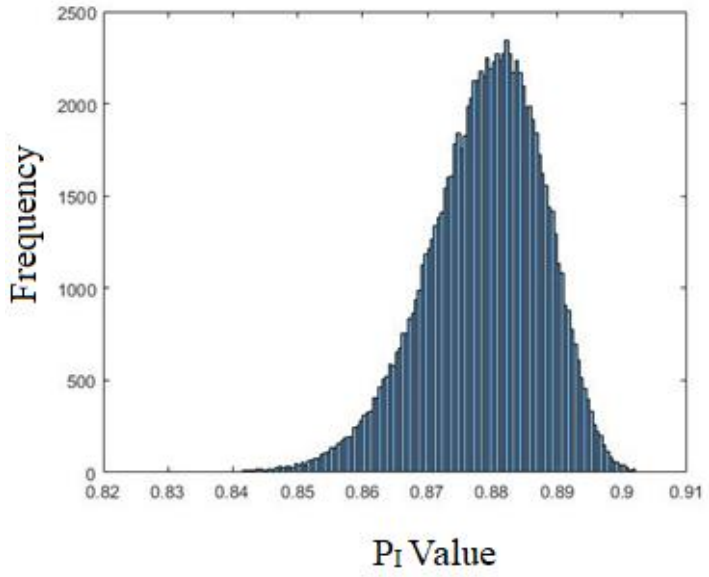

Figure 35. The P_I value distribution of the adversary's MVP strategy simulations

4.2. The Insider's Intervention of PPS

As mentioned before, there are three models developed for insider's intervention in the software code. It is seen from Figure 26 that after the adversary path has been constructed, the software code goes to the process of modeling the insider's intervention. However, if the user indicates that there is no insider in the simulation, the software code goes straight to P_I calculation after the adversary path has been constructed. The following insider's intervention models are based on the single path MVP simulations, as shown in section 4.1.5 to clearly show the impact of the insider in the simulations.

4.2.1. Insider's Intervention to the Detection Function

The first insider's intervention model developed in the software code is the intervention of detection function. In this model, it is assumed that the insider manages to disable detection function at any protection layer in the constructed adversary path.

Figure 36 shows the flowchart how the software code models the insider's intervention to the detection function. The software code generates a pseudo-random integer number ranges from one to the total number of protection layer in the analyzed facility. The generated integer number is taken to indicate which protection layer that the insider intervenes with. For example, if the generated number is '6', then the P_D and σ_{P_D} values of the sixth protection layer in the constructed adversary path are set as '0'.

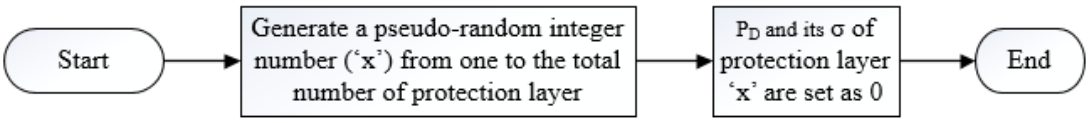

Figure 36. Flowchart of modeling the insider's intervention of detection function of the PPS

Figure 37 shows the distribution of P_I values from 100,000 simulations for insider's intervention of detection function combined with the adversary's MVP strategy (and sampling of P_D values) in penetrating the NARI facility. The mean value of the distribution is 0.86 with a standard deviation of 0.03. It is seen that some simulations have P_I values below 0.8, which does not exist in the case without insider (Figure 35).

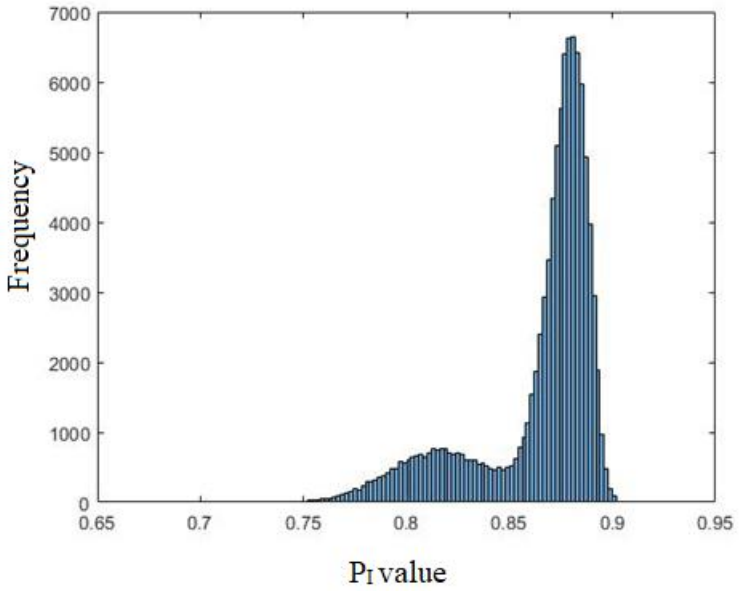

Figure 37. The P_I value distribution of the adversary's MVP with insider's intervention of detection function

4.2.2. Insider's Intervention to the Delay Function

The second insider's intervention model developed in the software code is the intervention of delay function. In this model, it is assumed that the insider manages to disable delay function at any protection layer in the constructed adversary path, in which the delay function of that path option is available to be reduced by the insider's capability as indicated in the input file by the user (Figure 9).

Figure 38 shows the flowchart how the software code models the insider's intervention of the delay function. The software code generates a pseudo-random integer number from one up to the total number of protection layer in the analyzed facility. The generated integer number is taken to indicate which protection layer that the insider intervenes with. The software code evaluates whether the protection layer in the constructed adversary path is a path with 'Type of Delay'

information ‘A’ in the input file (Figure 9). If the ‘Type of Delay’ information of that path is ‘NA’ given by the user, the software code repeats the pseudo-random integer number generating process until it meets the condition where the variable ‘type’ of the path element is ‘A’. For example, given the MVP of the NARI facility (Table 1) is used in the simulation. If the generated pseudo-random integer number is ‘6’, in which the path of the sixth protection layer is an area to be traversed by the adversary (‘Type of Delay’ is ‘NA’), then the software code has to repeat the pseudo-random integer number generation process. If the next generated number is ‘7’, in which the path of the seventh protection layer is a door (‘Type of Delay’ is ‘A’), then the t_d and σ_{t_d} values of the seventh protection layer in that constructed adversary path are set as ‘0’. However, there might be a case where the constructed adversary path has no path of protection layer with ‘Type of Delay’ information ‘A’. In that case, after a number of times of checking, the simulation continues without reducing any t_d and σ_{t_d} value.

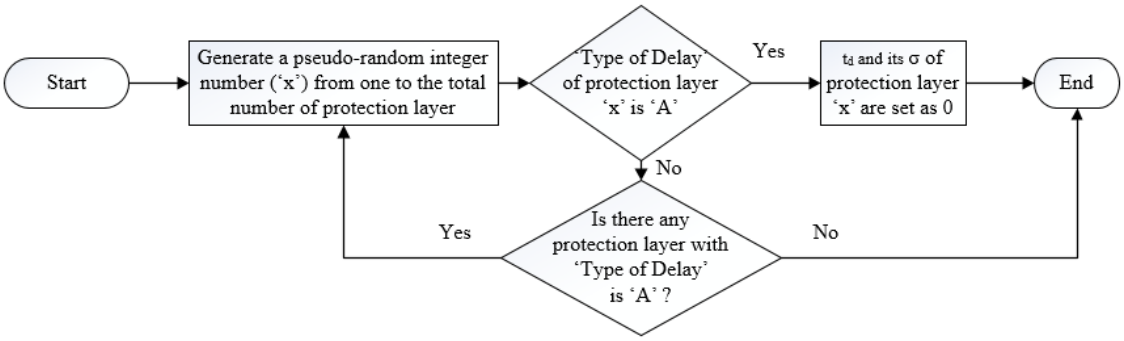

Figure 38. Flowchart of modeling the insider’s intervention of delay function of the PPS

Figure 39 shows the distribution of P_I values from 100,000 simulations for insider’s intervention of detection function combined with the adversary’s MVP strategy (and sampling of

P_D values) in penetrating the NARI facility. The mean value of the distribution is 0.79 with a standard deviation of 0.03.

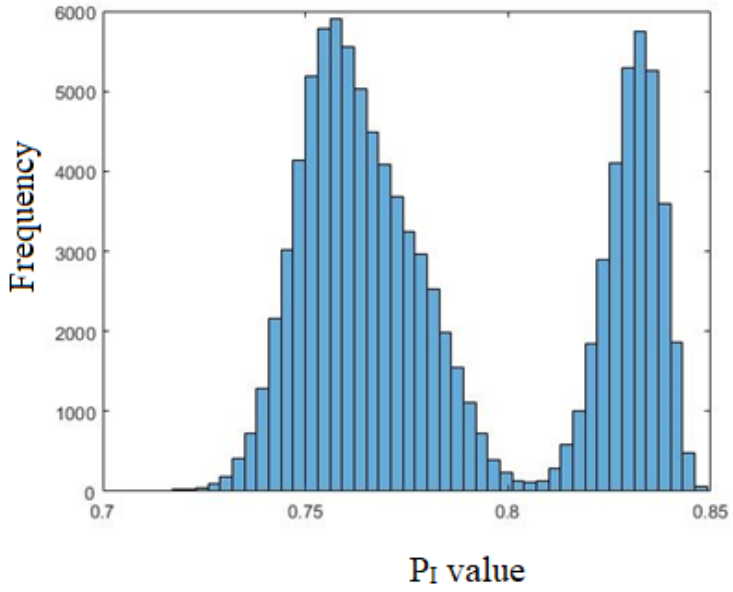

Figure 39. The P_I value distribution of the adversary's MVP with insider's intervention of delay function

The distribution in Figure 39 has two peaks due to the characteristic of the MVP of NARI facility which is used in the simulation of insider's intervention of delay function here. In Table 1, it is seen that the MVP of NARI facility has only three protection layers in which the path has a delay function can be disabled by the insider ('Type of Delay' information is 'A'). The software code simulates one insider disables delay function of one protection layer in every simulation. Insider's intervention of delay function in the third protection layer resulted in P_I=0.83. Insider's intervention of delay function in the fifth protection layer resulted in P_I=0.75. This P_I value is the lowest one due to the highest decrease in delay time (214 seconds) compared to the other intervention. Insider's intervention of delay function in the seventh protection layer resulted in

P_I=0.77. The sampling of P_D values in the MVP simulation gives a distribution around those three P_I values.

4.2.3. Insider's Intervention to the Detection and Delay Functions

The third insider's intervention model developed in the software code is the intervention of detection and delay functions. In this model, it is assumed that the insider manages to disable both detection and delay functions at any protection layer in the constructed adversary path, in which the delay function of that path option is available to be reduced by the insider's capability as indicated in the input file by the user (Figure 9).

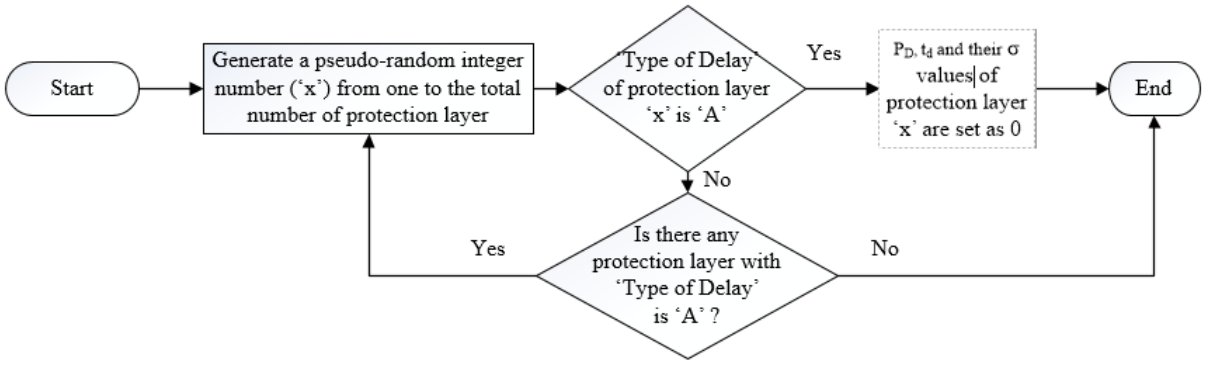

Figure 40. Flowchart of modeling the insider's intervention of detection and delay functions of the PPS

Figure 40 shows the flowchart how the software code models the insider's intervention of detection and delay functions. Basically, it has the similar process with the insider's intervention of delay function, except that the P_D and σ_{P_D} are also set as '0' beside the t_d and σ_{t_d} values.

Figure 41 shows the distribution of P_I values from 100,000 simulations for insider's intervention of detection and delay functions combined with the adversary's MVP strategy (and

sampling of P_D values) in penetrating the NARI facility. The mean value of the distribution is 0.77 with a standard deviation of 0.02. It is seen that most simulations have P_I values below 0.8, which does not exist in the case without insider (Figure 35).

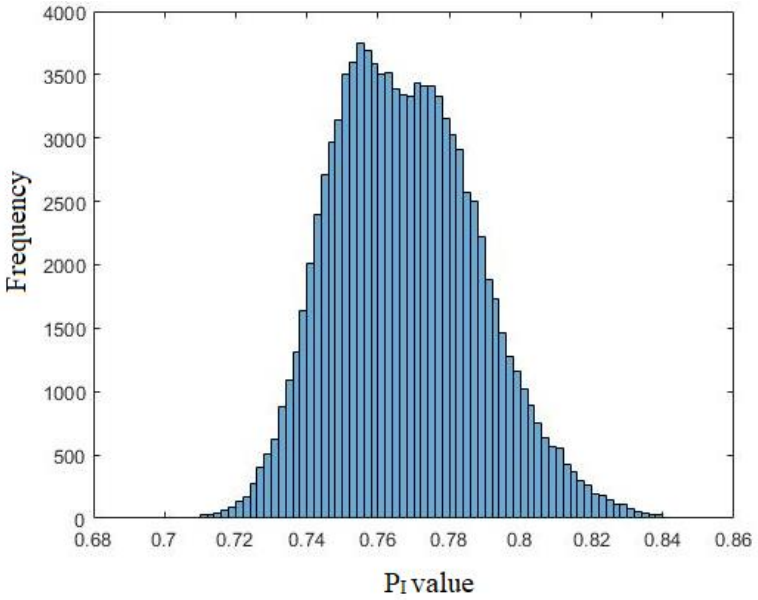

Figure 41. The P_I value distribution of the adversary's MVP with insider's intervention of detection and delay functions

5. RESULTS, DISCUSSION AND RECOMMENDATION

Results from the P_D value distribution, and MVP and sensitivity analysis are summarized in this section. Moreover, the discussion of results from the simulations for the adversary's various intrusion strategies including insider support or no support is presented in this section. This section also provides suggestions on the improvements on calculating EASI-based P_I values from a more realistic approach.

Table 4 shows the comparison between the initial and sampled P_D values for every protection layer along the MVP constructed by the CDP approach in section 3.1. It is seen that the distribution of sampled P_D values for every path option in the protection layer does have a mean value in the range of the initial standard deviation from initial P_D value provided in the Microsoft Excel input file.

Table 4. Comparison of the initial and the distribution of P_D value

Protection Layer	Description	Initial P_D Value	Initial Standard Deviation of P_D value	Mean Value of Sampled P_D Values Distribution	Standard Deviation of Sampled P_D Values Distribution
1	penetrate the fence	0.75	0.075	0.7495	0.075
2	run through limited access area	0.02	0.002	0.02	0.002
3	penetrate vehicle gate	0.8	0.08	0.7984	0.078
4	run through controlled area	0.04	0.004	0.04	0.004
5	penetrate outer vehicle door	0.8	0.08	0.7986	0.079
6	run through protected area	0.5	0.05	0.5002	0.050
7	penetrate main door	0.92	0.092	0.9201	0.023
8	run through vital area	0.9	0.09	0.8986	0.043
9	sabotage the target	0.92	0.092	0.8984	0.043

$$\sigma_u = u\sqrt{\left(\frac{\sigma_x}{x}\right)^2 + \left(\frac{\sigma_y}{y}\right)^2 + \cdots} \quad (5.1)$$

However, as mentioned in section 2.1. as well, the standard deviation of initial P_D value in the input file is 10% of the P_D value of the path element, which usually consists of several detection devices with different type to each other The P_D for every path in this software code will be more realistic and accurate if the P_D value and its standard deviation for every detection device in the path element modeled and calculated, as exampled by the work of Norichika Terao and Mitsutoshi Suzuki. The combined standard deviation for the path can be calculated by Equation 5.1.

Table 5. Results of the sensitivity analysis

Protection Layer	Description	Sensitivity of 0.1 P_D Deviation	Sensitivity of 5 Seconds t_d Deviation
1	Penetrate the fence	0.01	0.00
2	Run through limited access area	0.00	0.00
3	Penetrate vehicle gate	0.01	0.00
4	Run through controlled area	0.00	0.00
5	Penetrate outer vehicle door	0.00	0.00
6	Run through protected area	0.00	0.00
7	Penetrate main door	0.00	0.00
8	Run through vital area	0.00	0.00
9	Sabotage the target	0.00	0.00

Table 5 summarizes the results of the P_I sensitivity with regards to the P_D and t_d values of the NARI facility's MVP. It can be seen that the NARI facility's MVP is not sensitive either to the

fluctuation of P_D performance (up to an absolute value of 0.1) or the adversary's outperforming the delay element (up to 5 seconds faster). There is no significant change in the total P_I value due to 0.1 absolute value change in P_D value or 5 seconds change in t_d value in any protection layer. As for the sensitivity due to t_d, it is believed that 5 seconds change is negligible to the RFT (700 seconds) in this case. However, it is found in this study that the P_I value has a linear relationship with P_D value and has a non-linear relationship with the t_d value.

Table 6 shows the result (mean and standard deviation of P_I value distribution) of 100,000 simulations for every combination of adversary's strategy and insider's intervention in the NARI facility. Unexpectedly, the analysis gives that the rushing strategy approach by the adversary results in a path with lowest P_I value, followed by the random strategy as the second lowest. From single path calculation table of adversary's rushing strategy in Appendix D, it is seen that rushing strategy approach drastically reduce the cumulative delay time of the adversary path, thus, drastically reduce the z-value and the $P_{(R|A)}$ of protection layers, especially the first and the third protection layers as the main contributors to the total P_I value. Even though the adversary path of rushing strategy has higher P_D values, the reduction due to the decreased cumulative delay time in the adversary path is not compensated.

In short, the PPS of the NARI facility is unbalanced. There are path options with similar P_D value but have very different t_d value. It makes the adversary benefits more in choosing a path with the lowest t_d value, regardless of the P_D value, especially from the starting point until the CDP in penetrating the NARI facility. This means that the CDP approach to determine the MVP has failed to find the path with the lowest P_I value for the NARI facility case.

Table 6. Results of the P_I calculation simulations with combination of the adversary's strategy and the insider's intervention of the NARI facility

P_I value and standard deviation	No insider	Insider intervenes P_D	Insider intervenes t_d	Insider intervenes P_D and t_d
Random	0.86 ± 0.07	0.85 ± 0.07	0.79 ± 0.14	0.77 ± 0.11
Rushing	0.82 ± 0.07	0.82 ± 0.08	0.73 ± 0.13	0.72 ± 0.13
Covert	0.89 ± 0.05	0.88 ± 0.06	0.82 ± 0.10	0.81 ± 0.09
Deep Penetration	0.88 ± 0.05	0.87 ± 0.06	0.80 ± 0.10	0.78 ± 0.09
MVP	0.88 ± 0.01	0.86 ± 0.03	0.79 ± 0.03	0.77 ± 0.02

Another hypothetical nuclear facility case based on the work reported by Hawila et. al. [10] is used to compare the P_I value distribution obtained for NARI facility analysis presented here. Hawila's work analyzed a sabotage case at a nuclear power plant for which the ASD is shown in Appendix F. By using the same CDP approach as explained at the beginning of section 3.1, the MVP of that facility is determined and analyzed by using the single path EASI P_I calculation table. The result shows that the P_I value for MVP is 0.89. Then, by using the rushing strategy of the adversary, the P_I value for the adversary path increased to 0.95. The calculation tables for this nuclear power plant facility considering the MVP and the rushing strategy approach are provided in Appendix F. In Hawila's case, the CDP approach successfully produced an MVP with lower P_I value compared to the rushing strategy (0.89 vs 0.95).

It is found that the CDP approach works to find the MVP of a facility with a balanced PPS design, in which the adversary does not have many path options with a wide range of P_D and t_d values. However, there might be a lot of facilities with an unbalanced PPS. Therefore, the CDP approach cannot be bluntly applied for the analysis and finding the path with the lowest P_I value.

In summary, from the comparison of P_I value calculation of two hypothetical facilities, it can be concluded that the software code developed in this study can provide understanding about the balance of the PPS design.

It should be noted that the NARI facility in this study is a more open facility, with relatively less focus on the delay function of the PPS to reduce the hindrance for the visitors, compared to the nuclear power plant in Hawila's study, However, if the country seriously need to secure the facility major changes in the delay function should be done. The PPS of the NARI facility can be strengthened by modifying the protection elements of the PPS as follows:

- For the first protection layer, substitute the fence by a 60-cm wall which can provide a delay time of 480 seconds just like the vital area building. Equip the wall with a seismic buried cable sensor system with $P_D = 0.5$. As for the main gate, make it a double gate with a high security padlock each, thus, increase t_d to 120 s in total.
- For the third protection layer, substitute the double fence also with a 20-cm wall with delay time of 120 s and vibration sensor with $P_D = 0.9$. Enhance the vehicle gate to provide $t_d = 214$ s like the vehicle door at the entry to the vital area.
- For the fifth protection layer, substitute the window of the CAS and office rooms with a wall as a protection element. Thus, those rooms will have the same P_D and t_d value as that of the building wall.

Table 7 shows the result (mean and standard deviation of P_I value distribution) of 100,000 simulations for every combination of adversary's strategy and insider's intervention of the improved PPS design of NARI facility. It can be noted from the P_I values in Table 7 that the improved PPS is more balanced, both the rushing and the covert strategy approaches do not result

in a lower mean P_I value compared to the deep penetration or the MVP strategies. However, the PPS design is still sensitive to the decrease of the delay time caused by the insider. Lowering the RFT value is one solution to further improve the resilience of the PPS.

There is another issue if multi-path analysis is used for PPS evaluation even using a stochastic (Monte Carlo) approach. That is the mean and standard deviation values from P_I distribution from the simulations may not lead to produce a conservative PPS design. For example, in section 4.2.2, the mean value of the distribution is 0.79, while there are many P_I values in the distribution which is less than 0.79. For a conservative PPS design, the analyst may be interested in the lowest P_I value. Therefore, an analysis on the P_I value distribution is presented next.

Table 7. Results of P_I calculation simulations to the improved PPS design of NARI facility

P_I Value and Standard Deviation	No Insider	Insider intervenes P_D	Insider intervenes t_d	Insider intervenes P_D and t_d
Random	0.91 ± 0.03	0.89 ± 0.04	0.86 ± 0.07	0.84 ± 0.07
Rushing	0.91 ± 0.02	0.90 ± 0.04	0.86 ± 0.06	0.84 ± 0.06
Covert	0.90 ± 0.03	0.89 ± 0.05	0.86 ± 0.07	0.83 ± 0.07
Deep Penetration	0.90 ± 0.03	0.88 ± 0.05	0.84 ± 0.06	0.81 ± 0.06

Figure 42 shows the frequency of P_I values from 100,000 simulations of the original NARI facility's MVP without insider's collusion, in 5 bins of ranges where the P_I values vary from 0.5 to 0.6, 0.6 to 0.7, 0.7 to 0.8, 0.8 to 0.9, 0.9 to 1. Each bin has a mean P_I value. It is seen that for the MVP base case, all the P_I values are concentrated in the bin range 0.8 to 0.9, with mean value 0.88.

Figure 43 shows the frequency of P_I value from 100,000 simulations of adversary's random strategy and rushing strategy in penetrating the original NARI facility without insider's collusion. It is seen that in the random strategy, there are around 20,000 simulations (around 20% of total simulations) with P_I values less than 0.8. In the rushing strategy, there are more than 30,000 simulations (more than 30% of total simulations) with P_I value less than 0.8.

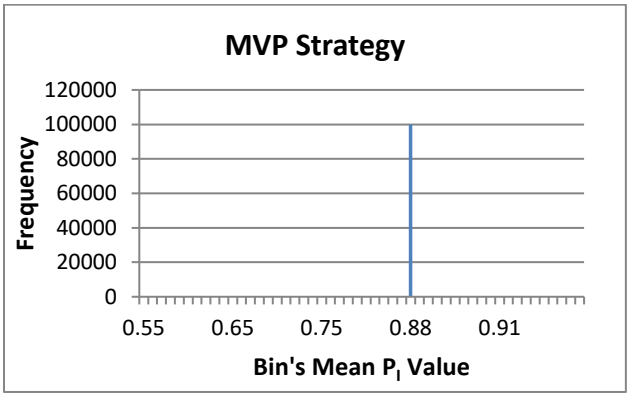

Figure 42. Frequency of P_I value in five bins of MVP strategy for NARI facility

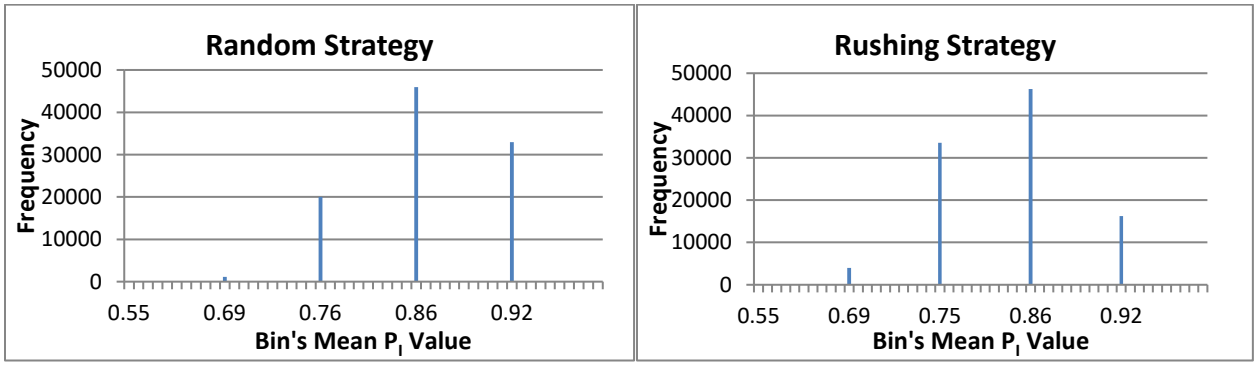

Figure 43. Frequency of P_I value in five bins of random strategy and rushing strategy for NARI facility

Figure 44 shows the frequency of P_I value from 100,000 simulations of adversary's covert strategy and deep penetration strategy in penetrating the original NARI facility without insider's collusion. It is seen that in the covert strategy, there are around 5,000 simulations (5% of total

simulations) with P_I value less than 0.8. In the deep penetration strategy, there are around 8,000 simulations (8% of total simulations) with P_I value less than 0.8. In all of those strategies, there are small number of simulations in which the P_I value is less than 0.7.

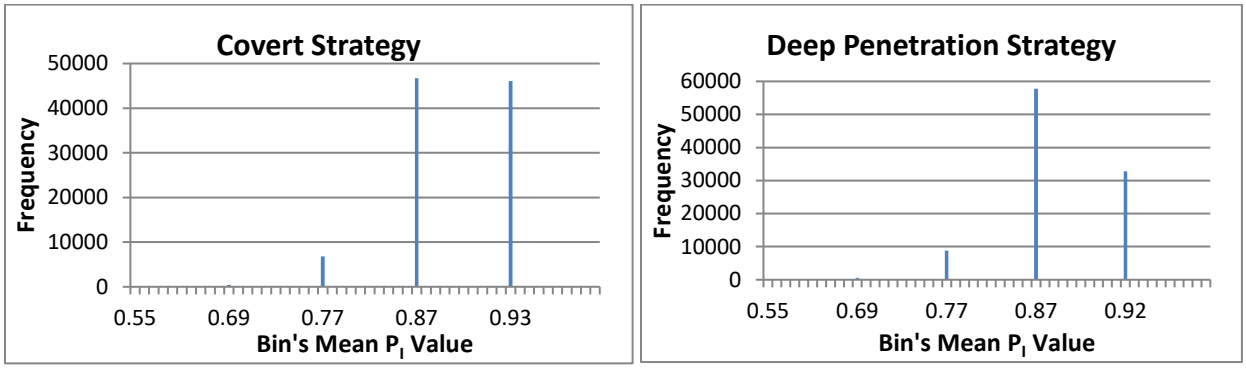

Figure 44. Frequency of P_I value in five bins of covert strategy and deep penetration strategy for NARI facility

Figure 45 shows the frequency of P_I value from 100,000 simulations of adversary's MVP strategy combined with insider's intervention in penetrating the original NARI facility's MVP. There are a few numbers of simulation in the insider's intervention of detection function case with P_I value less than 0.8. However, in the case of insider's intervention of delay function, more than half (65%) of the simulations have P_I value less than 0.8. In the case of insider's intervention of detection and delay functions, more than 80% of the simulations have P_I value less than 0.8. The frequency analysis is valuable in the multi-path analysis from numerous simulation, rather than just depending on the mean and standard deviation values from the distribution.

Frequency analysis in the multi-path analysis shows a drastic change of P_I value distribution in several bins due to various adversary strategies and insider's collusion. The adversary's rushing strategy (in Figure 43), among other strategies, has the highest percentage of

simulations resulting lower P_I value (below 0.8) compared with the base case of single path MVP (Figure 42) of the NARI facility. The insider's intervention of detection and delay functions, among other insider's collusions, has the highest percentage of simulations resulting lower P_I value (below 0.8).

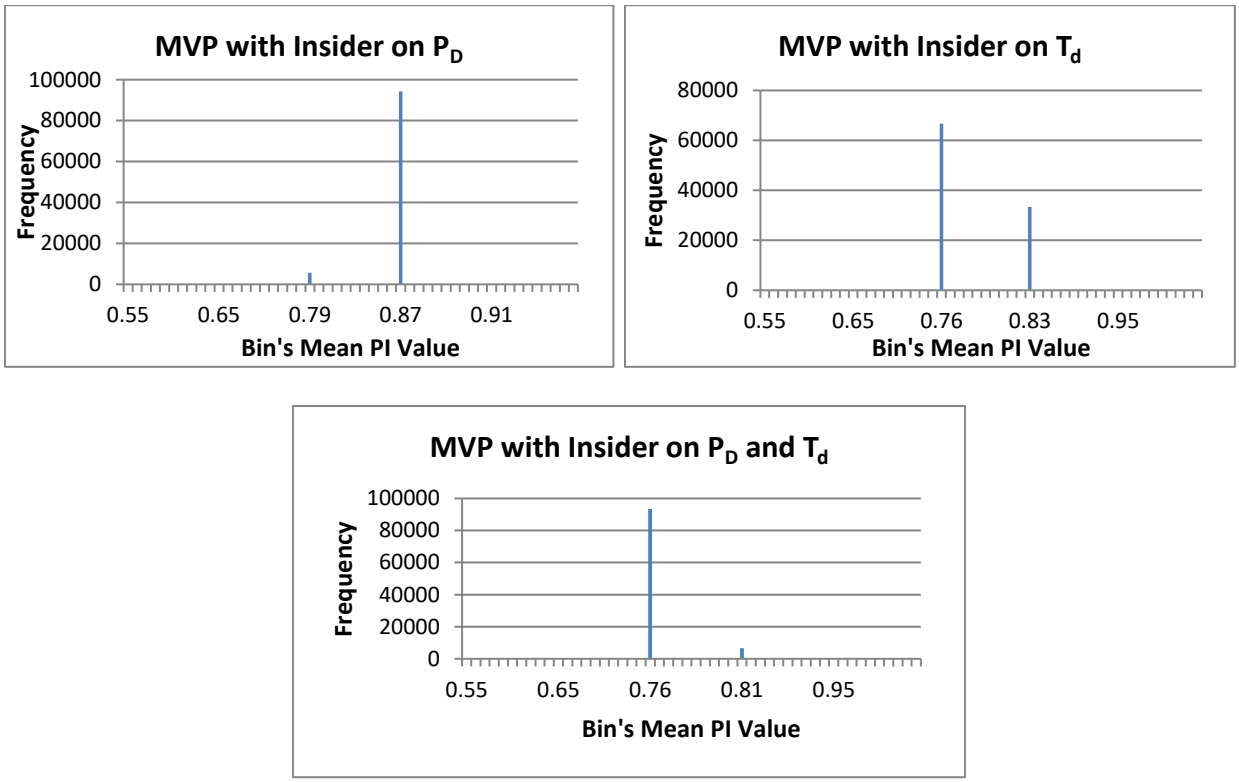

Figure 45. Frequency of P_I value in five bins NARI facility's MVP with various insider's intervention of PPS's function

Further recommendations based on this work for the adversary path modeling is that analyzing various adversary strategies and the insider's malicious involvement are very important. The hypothetical facilities used in this study are considered as simple facilities with less complicated PPS. They do not have jump mechanism which allows the adversary to surpass one

or two protection layers along the path to the target. This jump strategy analysis is not a capability of the developed software code. Also, modeling of theft-case scenario cannot be analyzed completely by this software code. Currently, the detail of insider's act to reduce the delay time cannot be analyzed in the software code. There is also a room for improvement in modeling how the insider intervenes with the protection element in a path element of the PPS, especially if the protection element in each path option can be modeled in more detail.

6. CONCLUSION

A stochastic (Monte Carlo) approach developed and implemented in the Estimate of Adversary Sequence Interruption (EASI) model as part of this study is presented. The approach is capable of analyzing the effectiveness of a Physical Protection System (PPS) by estimating Probability of Interruption (P_I) value and the uncertainty in P_I value. The implementation is done by developing a software code. The software code is tested by analyzing a hypothetical facility by estimating the P_I values considering the characteristics [Probability of Detection (P_D) and delay time (t_d)] of the protection elements in the PPS, uncertainties in the P_D and t_D values and various adversary strategies including collusion with an insider. Sensitivity analysis of P_I value with regards to P_D and t_d values is performed for the Most Vulnerable Path (MVP) of the facility by considering the Critical Detection Point (CDP) of the facility's Adversary Sequence Diagram (ASD).

Sensitivity analysis of P_I value estimation shows that the relationship between P_D and P_I is linear, however the relationship between t_d and P_I is non-linear. The implementation of stochastic (Monte Carlo) approach successfully produces P_I value distribution from which the mean and standard deviation values are estimated. The P_I value is the lowest in the simulations where the insider act is included, whether the insider acts on the detection or delay function or both simultaneously. The lowest mean value of P_I distribution is for the rushing strategy, among the other adversary strategies analyzed. This is due to an unbalanced PPS design of the analyzed hypothetical facility.

In addition, the multi-path analysis in this software code was complemented by a frequency distribution analysis of P_I values manually. This is needed because the mean and standard deviation values alone could mislead the user to overlook simulations with much lower P_I value than the mean. Frequency analysis performed on the P_I values is found to be valuable in modifying the PPS design instead of just using the mean value of the P_I distribution and its standard deviation in multi-path analysis. This is because the P_I value frequency distribution analysis shows a drastic change of P_I value when categorized in to several bins, especially for various adversary strategies and insider's collusion compared to the base case. The adversary's rushing strategy, among other strategies, has the highest percentage of the distribution resulting in lower P_I values (below 0.8). The insider's intervention of detection and delay functions, among other insider's collusions, has the highest percentage of the distribution resulting in lower P_I values (below 0.8).

The implementation of the stochastic (Mote Carlo) method is valuable in modeling the P_D values in the EASI model and in the estimation of P_I value distribution and the uncertainty associated, especially in modeling the adversary path including the collusion of an insider for multi-path analysis. The insider collusion is found to reduce the P_I value of the PPS drastically.

In the future, it is valuable to add to the software the theft and jump case scenarios. It would be good to add to the software code an automatic analysis of the P_I value frequency distribution. Detailed modeling of detection and delay elements in a path can be a future work too.

REFERENCES

[1] INTERNATIONAL ATOMIC ENERGY AGENCY, "*Convention on the Physical Protection of Nuclear Material"* INFCIRC/274/Rev.1, Vienna, (1980).

[2] INTERNATIONAL ATOMIC ENERGY AGENCY, "*The Physical Protection of Nuclear Material and Nuclear Facilities",* INFCIRC/225/Rev.4, Vienna, (1999).

[3] GARCIA M.L., "*The Design and Evaluation of Physical Protection System",* Butterworth-Heinemann, Burlington (2001).

[4] U.S. CONGRESS: OFFICE OF TECHNOLOGY ASSESSMENT, "*Technology Against Terrorism: Structuring Security"*, OTA-ISC-511, Washington, D.C., (1992).

[5] FERGUSON C., POTTER W., "*Four Faces of Nuclear Terrorism"*, Center for Nonproliferation Studies, Monterey (2004).

[6] INTERNATIONAL ATOMIC ENERGY AGENCY, "*Development, Use and Maintenance of the Design Basis Threat",* IAEA Nuclear Security Series No. 10, Vienna, (2009)

[7] BENNET H., "EASI – An Evaluation Method for Physical Security System", *Nuclear Materials Management*, Vol. 6, No. 3, 371-379, (1977).

[8] Wadoud A.A., Adail A.S., Saleh A.A., "Physical Protection Evaluation Process for Nuclear Facility via Sabotage Scenarios", *Alexandria Engineering Journal*, 1-9, (2017). https://doi.org/10.1016/j.aej.2017.01.045

[9] OYEYINKA O.D., DIM L.A., ECHETA M.C., KUYE A.O., "Determination of System Effectiveness for Physical Protection System of a Nuclear Energy Centre", *Science and Technology*, Vol. 4, No. 2, 9-16, (2014).

[10] ZOU, B., YANG M., GUO J., BENJAMIN E., et al., "Insider Threats of Physical Protection Systems in Nuclear Power Plants: Prevention and Evaluation", *Progress in Nuclear Energy*, 1-8, (2017). http://dx.doi.org/10.1016/j.pnucene.2017.08.006

[11] HAWILA M., CHIRAYATH S., CHARLTON W., "Nuclear Security Risk Evaluation Using Adversary Pathway Analysis Methodology for an Insider-Outsider Collusion Scenario", *INMM Annual Meeting Proceedings*, Vol 56, 1-8, (2015).

[12] HAWILA, M., CHIRAYATH, S., "Nuclear Security Risk Analysis: An Insider-Outsider Collusion Scenario," *International Journal of Nuclear Security*, Vol. 2, No. 2, Article 7, (2016). http://dx.doi.org/10.7290/V7B56GNN

[13] TERAO N., SUZUKI M., "A Probabilistic Extension of the EASI Model", *Journal of Physical Security*, Vol. 7, No. 2, 12-29, (2014).

[14] WINBLAD A.E., "The SAVI Vulnerability Assessment Model", *INMM Annual Meeting Proceedings*, Vol. 16, 24-28, (1987).

[15] JANG S. S., KWAK S., YOO, H., KIM J., YOON W. K., "Development of a Vulnerability Assessment Code for a Physical Protection System: Systematic Analysis of Physical Protection Effectiveness (SAPE)", *Nuclear Engineering and Technology*, Vol. 41, No. 5, 747-752, (2009).

[16] SANDIA NATIONAL LABORATORIES, "Hypothetical Facility Exercise Data: Hypothetical Atomic Research Institute", The Twenty-Sixth International Training Course, Albuquerque, (2016).

[17] SANDIA NATIONAL LABORATORIES, "Hypothetical Facility Exercise Data: The Lone Pine Nuclear Power Plant", The Twenty-Sixth International Training Course, Albuquerque, (2016).

[18] SANDIA NATIONAL LABORATORIES, "Hypothetical Facility Exercise Data: The Lagassi Institute of Medicine and Physics", The Twenty-Sixth International Training Course, Albuquerque, (2016).

[19] SANDIA NATIONAL LABORATORIES, "20. Multipath Analysis: Outsider Analysis with the Path Analysis (MP VEASI) Model", The Twenty-Sixth International Training Course, Albuquerque, (2016).

APPENDIX A

COUNTRY, FACILITY, AND THREAT DESCRIPTION

The NARI facility is located in the outskirt of hypothetical City, Nusa, the capital city of the hypothetical Republic of Nusantara, a developing country in the Southeast Asia region. It is operated by the country's National Science and Technology Institute (NSTI) and engages in many research activities with one of the advanced universities in the country, the University of Nusantara (UNUS), which is also located near NARI. It has served as the country's premier research facility in nuclear science and technology for about 15 years. The country has decided to start the construction of a nuclear power plant in 2025. The country has increased the amount of joint research being conducted with the faculties and students from the UNUS. The NARI facility has gained attention in the media. The media spotlights the facility and its research activities frequently, since the country's 'go nuclear' decision was made just before the Japanese Fukushima Nuclear Accident in 2011. All of the NARI facility publicity given by the media, UNUS, and NSTI have made the NARI facility and its activities transparent. People can get a lot of information about NARI facility from open sources, such as newspaper, website, science and technology magazine, and academic literature.

The Republic of Nusantara was well-known as an oil-exporter in the 1970s and 1980s, but it has turned into a net oil-importer country since mid-late 1990's to fulfill their energy needs. It is well known that there are a lot of oil and gas businessmen and organized crime network in the country, who were unhappy with the country's decision to pursue nuclear energy, which threaten their oil and gas business. There were protests happening in many occasions, such as during the

nuclear-related conferences and summits in the city, nuclear-related visits by researchers and businessmen from other countries. The protesters are highly suspected to be supported by the oil and gas businessmen and by the organized crime network. Not only nuclear energy, there were several cases of sabotage of renewable energy installation plant, such as small to mid-level of solar and wind farm. Sabotage mainly happened in an area which is highly dependent on oil energy.

Meanwhile, the country is also a nest of some terrorist and criminal groups. Since the economic crisis in the late 1990s, there is no rapid economy progression that satisfies the mid to low-income group people in the country. Those mid to low income group people showed their dissatisfaction and opposition to the government through crime and terrorism. There have been several major bombings in the country those took place during occasions related to western cultural events. Apparently, the country's main partners in the nuclear research and development are developed western countries, considered enemies by the terrorist and criminal groups.

Since the partnership began two years ago, the western countries have funded the implementation of a security system in the NARI facility. Based on the facility target analysis, the highest consequence is when there is a sabotage that causes major damage to the reactor. The worst outcome is that it may cause unacceptable radiological release. Meanwhile, as the country's one and only nuclear research and development facility, major damage to the facility will delay the country's pursuit of nuclear energy. It will also show the public of the country's inability to safely and securely operate a nuclear facility, given the existence of the terrorist and criminal groups in the country. Even people who are currently pro-nuclear might oppose to the country's plan to use nuclear energy, due to the threat of radiological release in from a nuclear accident or sabotage. Based on the analysis of the reactor, the fastest way to cause considerable damage to the reactor is

to sabotage the control rod drive bridge during the maintenance of the reactor. It will take around 10 minutes to cause the damage.

Knowing the importance of the facility for the country's early nuclear regime, people who oppose the plan might want to create damage to the reactor. The oil and gas businessmen and the people from the organized crime network are among the most probable ones. In some of the cases of renewable energy plant sabotage, the culprits have proven to be related to the oil and gas business. Therefore, it is highly possible that the organized crime would find a way to try sabotage the reactor in NARI facility, possibly with support from the terrorist or criminal groups. They are assumed to have enough material and resources and from the past incidents it is clear that the terrorist and criminal groups have the capability and human resources to do the sabotage.

The postulated threat for the NARI facility can be described as follows. The adversary's motivation comes from a mix of anti-western, anti-government, and anti-nuclear energy sentiments. The adversary's intention is to sabotage the nuclear reactor inside NARI facility. The adversary has enough funding to acquire the required materials, tools, and human resources to execute their sabotage plan at the NARI reactor. The adversary team, which consists of four to five people, will all be equipped with at least one rifle and one pistol. Limited explosive materials will be available for the adversary to penetrate one or two steel doors or concrete wall and to sabotage the reactor. Portable mechanical tools are also possessed by the adversary team, but not high-tech advanced tools. They communicate to each other by using the cellular phone and two-way radio system. The adversary team has a land transportation vehicle which can only deliver the team undetected until the offsite area just before entering the limited access area of the NARI facility. The adversary has enough technical skill to use those materials, tools, equipment, and weapons

combined with stealth and force tactic. The adversary has no sophisticated cyber skills. Although very unlikely, there is still a possibility of an insider assisting the adversary.

APPENDIX B

DEVELOPMENT OF ADVERSARY SEQUENCE DIAGRAM (ASD) OF NARI FACILITY

The HARI hypothetical facility document by SNL [17] provides all P_D and t_d values to construct the ASD of the NARI hypothetical facility. From the offsite area, there is no protection element used to detect or to delay an adversary. Therefore, it has P_D=0 value and t_d=0 value. For the next step, there are two options for the adversary to enter the limited access area from the off-site area: either through the main gate or through the fence surrounding the limited access area. For the adversary to pass through the fence, the P_D value is 0.75 since the fence is equipped with multiple sensors. The multiple sensors might detect the adversary in the middle of action in passing through the fence, in which case the detection location is set as 'M'. But, it will take only approximately 10 seconds for the adversary to pass through the fence. As for the main gate, the adversary will take approximately 60 seconds to open or break the high security padlock. The addition of the camera to monitor the main gate will give the P_D value 0.85 in detecting the adversary once they have arrived at the main gate to unlock the padlock, thus, the detection location is set as 'B'.

The average distance from the facility's outer fence to the controlled area's double fence is 300 meters. It will take 30 seconds for the adversary to traverse the limited access area. A guard patrolling in a scheduled time gives the limited access area a P_D value of 0.02 and might detect the adversary in the middle of the path. In order to get into the controlled area, the adversary has three options. The first option is through the double fence, which has 20 seconds delay time value. Since each fence has a vibration sensor and an infrared sensor system in between the fence, Equation 1.3

and Equation 2.1 are used to calculate the combined P_D value of those sensors. From the reference [17], the fence vibration sensor gives P_D value 0.5 for each fence, while the exterior infrared sensor gives P_D value of 0.8. Therefore, the combined P_D value of the double fence is 0.95. Those sensors are likely to detect the adversary in the middle of the action to pass through the double fence. Therefore, this path's detection location is set as 'M'. The second option to enter the controlled area is through the vehicle gate which is locked with high security padlocks on both sides of the gate, which give a delay time of this path element of 120 seconds. The infrared sensor used in the double fence goes through this vehicle gate as well, which will detect the adversary in the middle of the path element with P_D value of 0.8.

The third option is to go through the personnel portal. Both doors to get in and to get out of the personnel portal are 0.75-cm steel plate doors. Each door gives approximately 30 seconds delay time for the postulated adversary. The steel turnstile inside the room gives an additional delay time of 18 seconds for this path element. BMS in both doors give P_D value 0.8 each, while the badge-PIN system of the turnstile gives P_D value 0.6. Therefore, the combined P_D value for the personnel portal room is 0.98, obtained by using Equations 1.3 and 2.1. Once the adversary is in the controlled area, the adversary must take at least 15 seconds to travel before penetrating the protected area. Two random patrol guards in the controlled area contribute to combined P_D value of 0.04 by applying Equations 1.3 and 2.1, in which the detection location is in the middle of the adversary path in passing through the area.

In order to penetrate the protected area, the adversary has five options to get through. The first option is through the main entrance of the building. The 10-cm wood door with metal sheeting gives 180 seconds delay time, while the steel turnstile gives 18 seconds delay time, therefore 198

seconds in total. The BMS with P_D=0.8 attached at the front door and the exchange badge-PIN system at the steel turnstile with P_D=0.8 contribute to P_D value of 0.96 in total. The last detection opportunity is if the adversary somehow breaks through the turnstile right before they enter the protected area, thus, the detection location is set as 'E'. The second option is to penetrate the window of the office room, then break through the door. There is a glass break sensor attached to every window with P_D=0.9 and a position switch sensor attached to the door with P_D=0.5. It gives P_D=0.95 in total for the office room by utilizing Equations 1.3 and 2.1. However, 5 seconds delay time of the window and 12 seconds delay time of the wood door only give 17 seconds delay time in total for the office room. The detection location of the office room is set as 'E' as the BMS of the office door is the last detection opportunity before entering the protected area.

The third option is through the Central Alarm Station (CAS) room. The window for the CAS room also has the glass break sensor with P_D=0.9 and delay time of 5 seconds, while its door is made of steel with a delay time of 30 seconds where the BMS with P_D=0.8 is attached to. In total, the CAS room has P_D value of 0.98 and delay time of 35 seconds, and the detection location is also set as 'E' with regards to the BMS at the door. The fourth option is through the outer-side 30-cm concrete and steel rolling vehicle door at the backside of the building. The outsider might spend approximately 214 seconds to use explosives to break the lock of the door. The BMS with P_D=0.8 equipped to the door will detect the adversary once the door just before the protected area is opened and entry is made. Thus, the detector location for this path element is set as 'E'. The last option is by penetrating through the building wall directly. It would take approximately 120 seconds to use explosives to break the 20-cm concrete wall and enter the protected area. However, the building wall is equipped with a vibration sensor which has P_D value of 0.9 to detect the

explosion vibration. Thus, the detection location is set as 'M'. In the protected area itself, the video motion sensor is applied in several spots insider the administration building hall with P_D value of 0.5. It might detect the adversary movement in the middle of the path element. The average time for the adversary to go through the administration hall to start penetrating the vital area is approximately 10 seconds.

From the protected area, there are three options to get into the vital area. First option is through inner-side vehicle door from the back of the building. The delay time provided by this inner side door is same with the outer vehicle rolling door, 214 seconds by explosive to break the door. But, this rolling door is equipped with a badge-PIN system with P_D=0.6 and BMS with P_D=0.8. These sensors will detect the adversary after the lock is broken, and the door is opened. These sensors give the combined P_D value of 0.92 to this path element. The second option is through the main door. It has the same detection BMS and badge-PIN system feature with the inner-sider vehicle door which gives the combined P_D of 0.92 and detection location is set as 'E'. However, since it is a 30-cm wooden door with metal sheeting, it has a lower delay time value, 180 seconds, for a penetration using explosives. The third option is through the vital area building wall. It is a 60-cm concrete wall with a vibration sensor, thus, giving this path element a P_D value of 0.9, detection location set as 'M', and delay time of 480 seconds if the adversary uses explosives. The vital area and the target are equipped by multiple complementary sensors with P_D=0.9 for each of them. It will take approximately not more than five seconds needed by the adversary to penetrate the vital area to reach the target. And as stated in the target identification before, it will take approximately 600 seconds to sabotage the control rod drive bridge until the adversary desired level of damage. Those multiple complementary sensors in many parts of the of the vital area and

around the reactor most likely detect the adversary in the middle of their progress in the path element, therefore detection location ‘M’ is given for both path elements in the ASD.

APPENDIX C

DISTRIBUTION OF DETECTION PROBABILITY VALUE OF THE NARI FACILITY

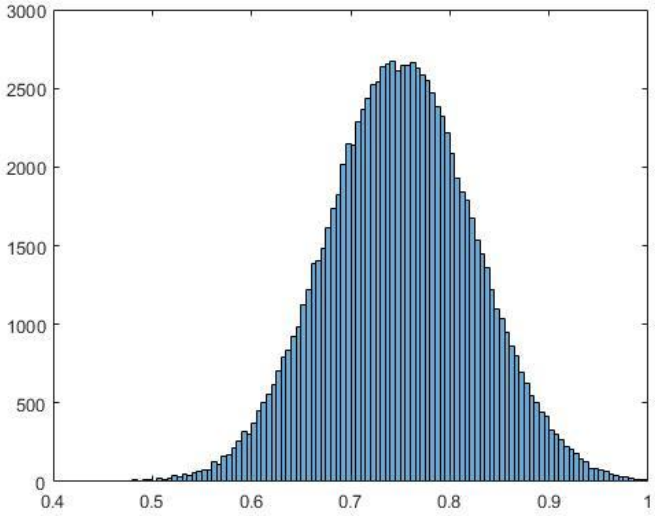

P_D value distribution of the first protection layer

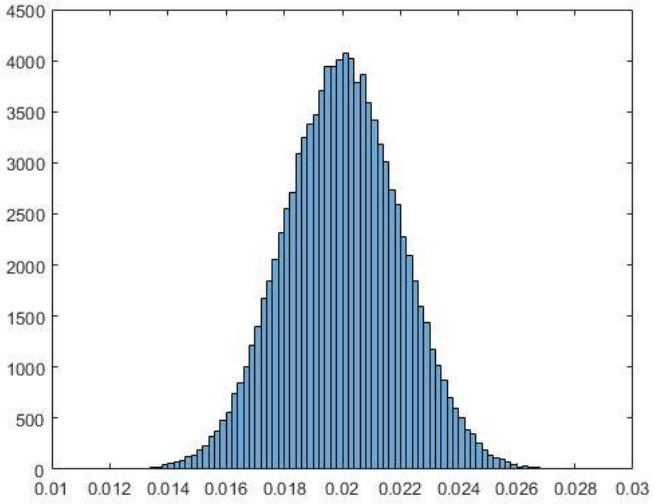

P_D value distribution of the second protection layer

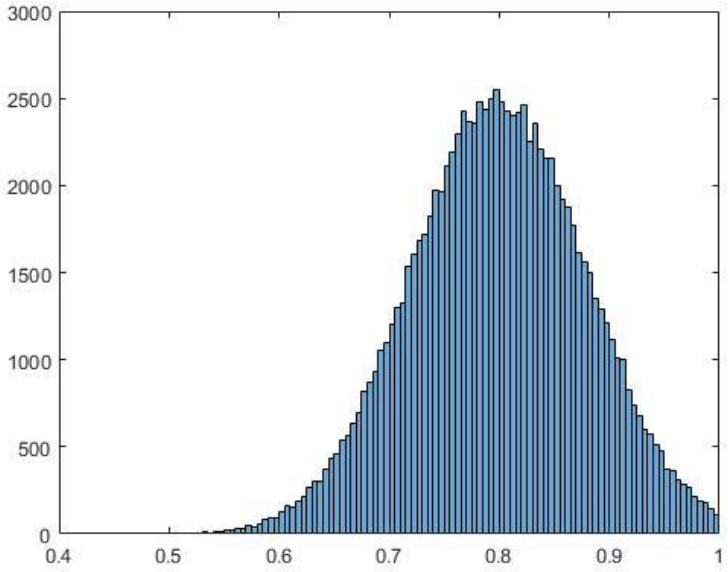

P_D value distribution of the third protection layer

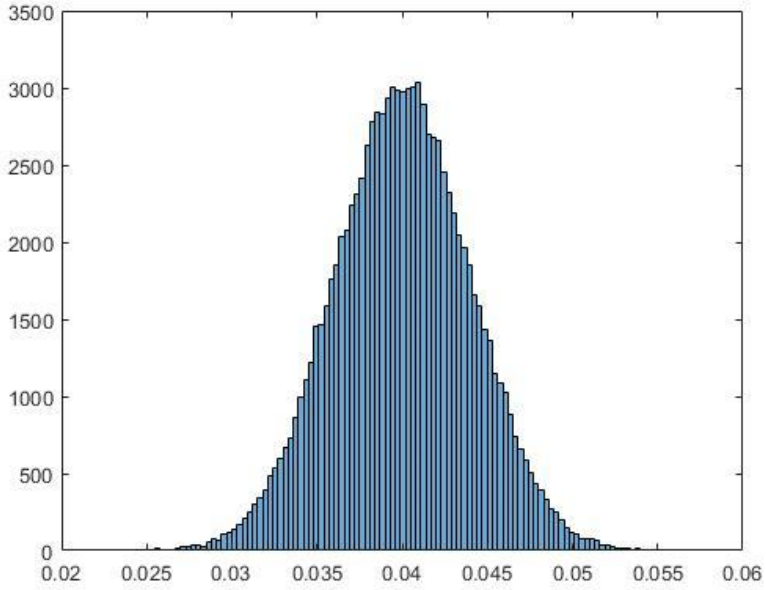

P_D value distribution of the fourth protection layer

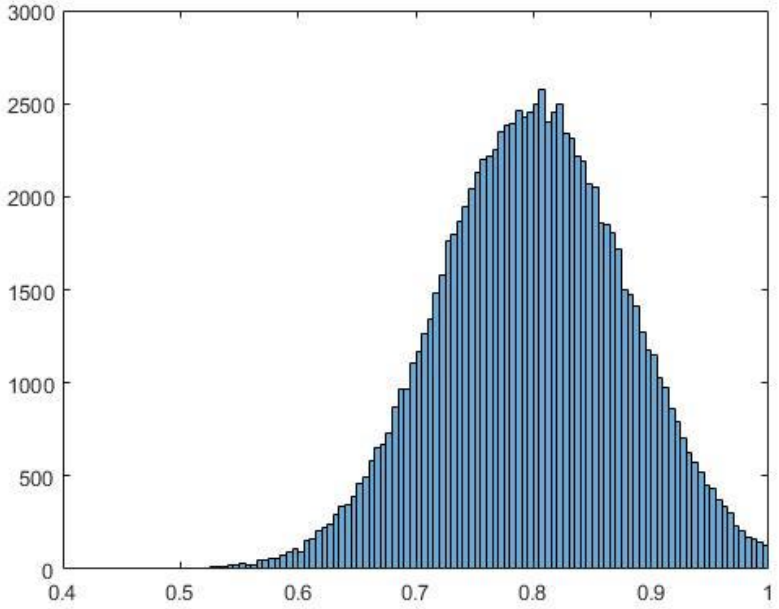

P_D value distribution of the fifth protection layer

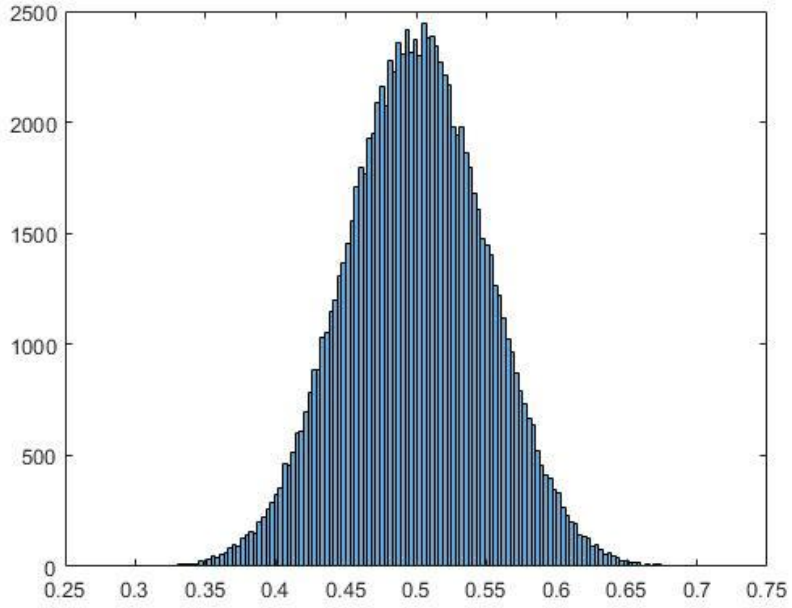

P_D value distribution of the sixth protection layer

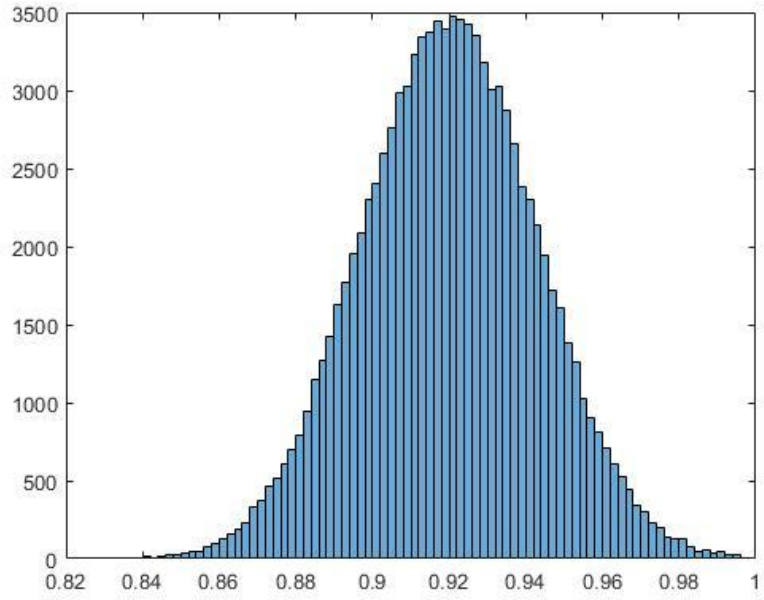

P_D value distribution of the seventh protection layer

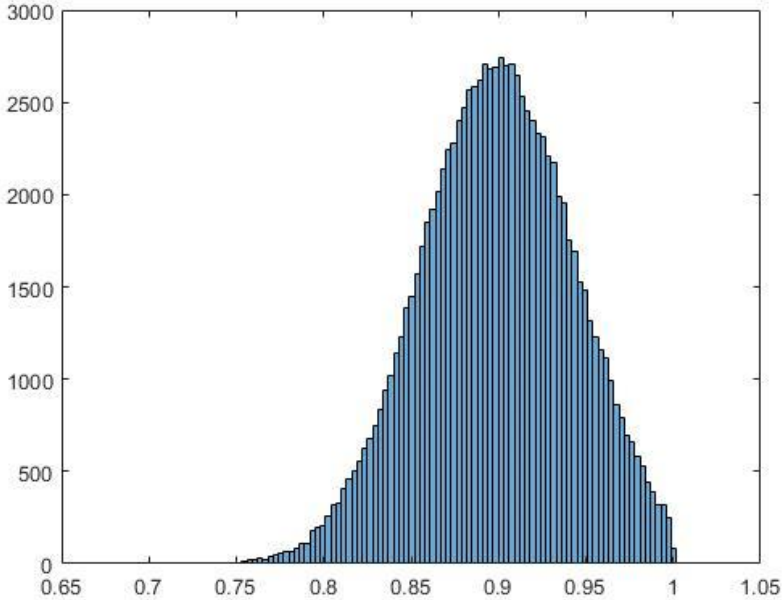

P_D value distribution of the eighth protection layer

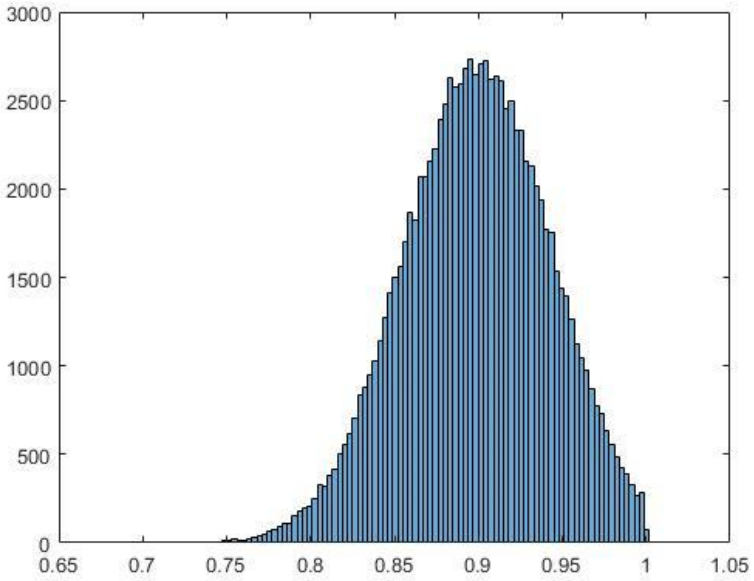

P_D value distribution of the ninth protection layer

APPENDIX D

SINGLE PATH EASI CALCULATION TABLE FOR SENSITVITY ANALYSIS

Sensitivity Analysis due to P_D change

	1	RFT	700	210	Detection			Delay				Probability of Interruption		0.8883
PC	0.95											Response		
Layer	Detection Probability	Location	Delay Time Mean	Delay Time STD	Probability of Detection	Probability of No Detection	Probability of First Detection	Cumulative Delay Time	Cumulative Variance	True Cumulative Delay Time	True Cumulative Variance	z-value	Response Force Arrival Probability	Specific Probability of Interruption
1	0.85	M	10	3.0	0.85	0.1500	0.8500	1184	40855.14	1179	40848.39	1.6435	0.9499	0.7670
2	0.02	M	30	9.0	0.02	0.1470	0.0030	1174	40846.14	1159	40785.39	1.5754	0.9424	0.0027
3	0.8	M	120	36.0	0.8	0.0294	0.1176	1144	40765.14	1084	39793.14	1.3258	0.9075	0.1014
4	0.04	M	15	4.5	0.04	0.0282	0.0012	1024	39469.14	1016.5	39453.953	1.0949	0.8632	0.0010
5	0.8	E	214	64.2	0.8	0.0056	0.0226	1009	39448.89	795	35327.25	0.3371	0.6320	0.0136
6	0.5	M	10	3.0	0.5	0.0028	0.0028	795	35327.25	790	35320.5	0.3194	0.6253	0.0017
7	0.92	E	180	54.0	0.92	0.0002	0.0026	785	35318.25	605	32402.25	-0.3435	0.3656	0.0009
8	0.9	M	5	1.5	0.9	0.0000	0.0002	605	32402.25	602.5	32400.563	-0.3525	0.3622	0.0001
9	0.9	M	600	180.0	0.9	0.0000	0.0000	600	32400	300	8100	-1.7508	0.0400	0.0000

	1	RFT	700	210	Detection			Delay				Probability of Interruption		0.8811
PC	0.95											Response		
Layer	Detection Probability	Location	Delay Time Mean	Delay Time STD	Probability of Detection	Probability of No Detection	Probability of First Detection	Cumulative Delay Time	Cumulative Variance	True Cumulative Delay Time	True Cumulative Variance	z-values	Response Force Arrival Probability	Specific Probability of Interruption
1	0.75	M	10	3.0	0.75	0.2500	0.7500	1184	40855.14	1179	40848.39	1.6435	0.9499	0.6768
2	0.12	M	30	9.0	0.12	0.2200	0.0300	1174	40846.14	1159	40785.39	1.5754	0.9424	0.0269
3	0.8	M	120	36.0	0.8	0.0440	0.1760	1144	40765.14	1084	39793.14	1.3258	0.9075	0.1517
4	0.04	M	15	4.5	0.04	0.0422	0.0018	1024	39469.14	1016.5	39453.9525	1.0949	0.8632	0.0014
5	0.8	E	214	64.2	0.8	0.0084	0.0338	1009	39448.89	795	35327.25	0.3371	0.6320	0.0203
6	0.5	M	10	3.0	0.5	0.0042	0.0042	795	35327.25	790	35320.5	0.3194	0.6253	0.0025
7	0.92	E	180	54.0	0.92	0.0003	0.0039	785	35318.25	605	32402.25	-0.3435	0.3656	0.0013
8	0.9	M	5	1.5	0.9	0.0000	0.0003	605	32402.25	602.5	32400.5625	-0.3525	0.3622	0.0001
9	0.9	M	600	180.0	0.9	0.0000	0.0000	600	32400	300	8100	-1.7508	0.0400	0.0000

	1	RFT	700	210	Detection			Delay				Probability of Interruption		0.8857
PC	0.95											Response		
Layer	Detection Probability	Location	Delay Time Mean	Delay Time STD	Probability of Detection	Probability of No Detection	Probability of First Detection	Cumulative Delay Time	Cumulative Variance	True Cumulative Delay Time	True Cumulative Variance	z-values	Response Force Arrival Probability	Specific Probability of Interruption
1	0.75	M	10	3.0	0.75	0.2500	0.7500	1184	40855.14	1179	40848.39	1.6435	0.9499	0.6768
2	0.02	M	30	9.0	0.02	0.2450	0.0050	1174	40846.14	1159	40785.39	1.5754	0.9424	0.0045
3	0.9	M	120	36.0	0.9	0.0245	0.2205	1144	40765.14	1084	39793.14	1.3258	0.9075	0.1901
4	0.04	M	15	4.5	0.04	0.0235	0.0010	1024	39469.14	1016.5	39453.9525	1.0949	0.8632	0.0008
5	0.8	E	214	64.2	0.8	0.0047	0.0188	1009	39448.89	795	35327.25	0.3371	0.6320	0.0113
6	0.5	M	10	3.0	0.5	0.0024	0.0024	795	35327.25	790	35320.5	0.3194	0.6253	0.0014
7	0.92	E	180	54.0	0.92	0.0002	0.0022	785	35318.25	605	32402.25	-0.3435	0.3656	0.0008
8	0.9	M	5	1.5	0.9	0.0000	0.0002	605	32402.25	602.5	32400.5625	-0.3525	0.3622	0.0001
9	0.9	M	600	180.0	0.9	0.0000	0.0000	600	32400	300	8100	-1.7508	0.0400	0.0000

	1	RFT	700	210	Detection			Delay				Probability of Interruption	0.8801
PC	0.95											Response	
Layer	Detection Probability	Location	Delay Time Mean	Delay Time STD	Probability of Detection	Probability of No Detection	Probability of First Detection	Cumulative Delay Time	Cumulative Variance	True Cumulative Delay Time	True Cumulative Variance	z-values	Response Force Arrival Probability	Specific Probability of Interruption
1	0.75	M	10	3.0	0.75	0.2500	0.7500	1184	40855.14	1179	40848.39	1.6435	0.9499	0.6768
2	0.02	M	30	9.0	0.02	0.2450	0.0050	1174	40846.14	1159	40785.39	1.5754	0.9424	0.0045
3	0.8	M	120	36.0	0.8	0.0490	0.1960	1144	40765.14	1084	39793.14	1.3258	0.9075	0.1690
4	0.14	M	15	4.5	0.14	0.0421	0.0069	1024	39469.14	1016.5	39453.9525	1.0949	0.8632	0.0056
5	0.8	E	214	64.2	0.8	0.0084	0.0337	1009	39448.89	795	35327.25	0.3371	0.6320	0.0202
6	0.5	M	10	3.0	0.5	0.0042	0.0042	795	35327.25	790	35320.5	0.3194	0.6253	0.0025
7	0.92	E	180	54.0	0.92	0.0003	0.0039	785	35318.25	605	32402.25	-0.3435	0.3656	0.0013
8	0.9	M	5	1.5	0.9	0.0000	0.0003	605	32402.25	602.5	32400.5625	-0.3525	0.3622	0.0001
9	0.9	M	600	180.0	0.9	0.0000	0.0000	600	32400	300	8100	-1.7508	0.0400	0.0000

	1	RFT	700	210	Detection			Delay				Probability of Interruption	0.8795
PC	0.95											Response	
Layer	Detection Probability	Location	Delay Time Mean	Delay Time STD	Probability of Detection	Probability of No Detection	Probability of First Detection	Cumulative Delay Time	Cumulative Variance	True Cumulative Delay Time	True Cumulative Variance	z-values	Response Force Arrival Probability	Specific Probability of Interruption
1	0.75	M	10	3.0	0.75	0.2500	0.7500	1184	40855.14	1179	40848.39	1.6435	0.9499	0.6768
2	0.02	M	30	9.0	0.02	0.2450	0.0050	1174	40846.14	1159	40785.39	1.5754	0.9424	0.0045
3	0.8	M	120	36.0	0.8	0.0490	0.1960	1144	40765.14	1084	39793.14	1.3258	0.9075	0.1690
4	0.04	M	15	4.5	0.04	0.0470	0.0020	1024	39469.14	1016.5	39453.9525	1.0949	0.8632	0.0016
5	0.9	E	214	64.2	0.9	0.0047	0.0423	1009	39448.89	795	35327.25	0.3371	0.6320	0.0254
6	0.5	M	10	3.0	0.5	0.0024	0.0024	795	35327.25	790	35320.5	0.3194	0.6253	0.0014
7	0.92	E	180	54.0	0.92	0.0002	0.0022	785	35318.25	605	32402.25	-0.3435	0.3656	0.0008
8	0.9	M	5	1.5	0.9	0.0000	0.0002	605	32402.25	602.5	32400.5625	-0.3525	0.3622	0.0001
9	0.9	M	600	180.0	0.9	0.0000	0.0000	600	32400	300	8100	-1.7508	0.0400	0.0000

	1	RFT	700	210	Detection			Delay				Probability of Interruption	0.8791
PC	0.95											Response	
Layer	Detection Probability	Location	Delay Time Mean	Delay Time STD	Probability of Detection	Probability of No Detection	Probability of First Detection	Cumulative Delay Time	Cumulative Variance	True Cumulative Delay Time	True Cumulative Variance	z-values	Response Force Arrival Probability	Specific Probability of Interruption
1	0.75	M	10	3.0	0.75	0.2500	0.7500	1184	40855.14	1179	40848.39	1.6435	0.9499	0.6768
2	0.02	M	30	9.0	0.02	0.2450	0.0050	1174	40846.14	1159	40785.39	1.5754	0.9424	0.0045
3	0.8	M	120	36.0	0.8	0.0490	0.1960	1144	40765.14	1084	39793.14	1.3258	0.9075	0.1690
4	0.04	M	15	4.5	0.04	0.0470	0.0020	1024	39469.14	1016.5	39453.9525	1.0949	0.8632	0.0016
5	0.8	E	214	64.2	0.8	0.0094	0.0376	1009	39448.89	795	35327.25	0.3371	0.6320	0.0226
6	0.6	M	10	3.0	0.6	0.0038	0.0056	795	35327.25	790	35320.5	0.3194	0.6253	0.0034
7	0.92	E	180	54.0	0.92	0.0003	0.0035	785	35318.25	605	32402.25	-0.3435	0.3656	0.0012
8	0.9	M	5	1.5	0.9	0.0000	0.0003	605	32402.25	602.5	32400.5625	-0.3525	0.3622	0.0001
9	0.9	M	600	180.0	0.9	0.0000	0.0000	600	32400	300	8100	-1.7508	0.0400	0.0000

Sensitivity Analysis due to t_d change

td1	1	RFT	700	210	Detection			Delay				Probability of Interruption	0.879474154
PC	0.95											Response	
Layer	Detection Probability	Location	Delay Time Mean	Delay Time STD	Probability of Detection	Probability of No Detection	Probability of First Detection	Cumulative Delay Time	Cumulative Variance	True Cumulative Delay Time	True Cumulative Variance	z-value	Response Force Arrival Probability	Specific Probability of Interruption
1	0.75	M	15	4.5	0.75	0.25	0.75	1189	40866.39	1181.5	40851.2025	1.6520	0.9507	0.713049975
2	0.02	M	30	9.0	0.02	0.245	0.005	1174	40846.14	1159	40785.39	1.5754	0.9424	0.004712101
3	0.8	M	120	36.0	0.8	0.049	0.196	1144	40765.14	1084	39793.14	1.3258	0.9075	0.177878224
4	0.04	M	15	4.5	0.04	0.04704	0.00196	1024	39469.14	1016.5	39453.9525	1.0949	0.8632	0.001691928
5	0.8	E	214	64.2	0.8	0.009408	0.037632	1009	39448.89	795	35327.25	0.3371	0.6320	0.023782424
6	0.5	M	10	3.0	0.5	0.004704	0.004704	795	35327.25	790	35320.5	0.3194	0.6253	0.00294128
7	0.92	E	180	54.0	0.92	0.00037632	0.00432768	785	35318.25	605	32402.25	-0.3435	0.3656	0.0015823
8	0.9	M	5	1.5	0.9	3.7632E-05	0.00033869	605	32402.25	602.5	32400.5625	-0.3525	0.3622	0.000122682
9	0.9	M	600	180.0	0.9	3.7632E-06	3.3869E-05	600	32400	300	8100	-1.7508	0.0400	1.35456E-06

td2	1	RFT	700	210	Detection			Delay				Probability of Interruption		0.880078801
PC	0.95											Response		
Layer	Detection Probability	Location	Delay Time Mean	Delay Time STD	Probability of Detection	Probability of No Detection	Probability of First Detection	Cumulative Delay Time	Cumulative Variance	True Cumulative Delay Time	True Cumulative Variance	z-value	Response Force Arrival Probability	Specific Probability of Interruption
1	0.75	M	10	3.0	0.75	0.25	0.75	1189	40884.39	1184	40877.64	1.6603	0.9516	0.713681569
2	0.02	M	35	10.5	0.02	0.245	0.005	1179	40875.39	1161.5	40792.7025	1.5839	0.9434	0.004716977
3	0.8	M	120	36.0	0.8	0.049	0.196	1144	40765.14	1084	39793.14	1.3258	0.9075	0.177878224
4	0.04	M	15	4.5	0.04	0.04704	0.00196	1024	39469.14	1016.5	39453.9525	1.0949	0.8632	0.001691928
5	0.8	E	214	64.2	0.8	0.009408	0.037632	1009	39448.89	795	35327.25	0.3371	0.6320	0.023782424
6	0.5	M	10	3.0	0.5	0.004704	0.004704	795	35327.25	790	35320.5	0.3194	0.6253	0.00294128
7	0.92	E	180	54.0	0.92	0.00037632	0.00432768	785	35318.25	605	32402.25	-0.3435	0.3656	0.0015823
8	0.9	M	5	1.5	0.9	3.7632E-05	0.00033869	605	32402.25	602.5	32400.5625	-0.3525	0.3622	0.000122682
9	0.9	M	600	180.0	0.9	3.7632E-06	3.3869E-05	600	32400	300	8100	-1.7508	0.0400	1.35456E-06

td3	1	RFT	700	210	Detection			Delay				Probability of Interruption		0.880284263
PC	0.95											Response		
Layer	Detection Probability	Location	Delay Time Mean	Delay Time STD	Probability of Detection	Probability of No Detection	Probability of First Detection	Cumulative Delay Time	Cumulative Variance	True Cumulative Delay Time	True Cumulative Variance	z-value	Response Force Arrival Probability	Specific Probability of Interruption
1	0.75	M	10	3.0	0.75	0.25	0.75	1189	40965.39	1184	40958.64	1.6595	0.9515	0.713621909
2	0.02	M	30	9.0	0.02	0.245	0.005	1179	40956.39	1164	40895.64	1.5915	0.9443	0.004721284
3	0.8	M	125	37.5	0.8	0.049	0.196	1149	40875.39	1086.5	39820.7025	1.3342	0.9089	0.178149853
4	0.04	M	15	4.5	0.04	0.04704	0.00196	1024	39469.14	1016.5	39453.9525	1.0949	0.8632	0.001691928
5	0.8	E	214	64.2	0.8	0.009408	0.037632	1009	39448.89	795	35327.25	0.3371	0.6320	0.023782424
6	0.5	M	10	3.0	0.5	0.004704	0.004704	795	35327.25	790	35320.5	0.3194	0.6253	0.00294128
7	0.92	E	180	54.0	0.92	0.00037632	0.00432768	785	35318.25	605	32402.25	-0.3435	0.3656	0.0015823
8	0.9	M	5	1.5	0.9	3.7632E-05	0.00033869	605	32402.25	602.5	32400.5625	-0.3525	0.3622	0.000122682
9	0.9	M	600	180.0	0.9	3.7632E-06	3.3869E-05	600	32400	300	8100	-1.7508	0.0400	1.35456E-06

td4	1	RFT	700	210	Detection			Delay				Probability of Interruption		0.880618945
PC	0.95											Response		
Layer	Detection Probability	Location	Delay Time Mean	Delay Time STD	Probability of Detection	Probability of No Detection	Probability of First Detection	Cumulative Delay Time	Cumulative Variance	True Cumulative Delay Time	True Cumulative Variance	z-value	Response Force Arrival Probability	Specific Probability of Interruption
1	0.75	M	10	3.0	0.75	0.2500	0.7500	1189	40870.89	1184	40864.14	1.6605	0.9516	0.7137
2	0.02	M	30	9.0	0.02	0.2450	0.0050	1179	40861.89	1164	40801.14	1.5924	0.9444	0.0047
3	0.8	M	120	36.0	0.8	0.0490	0.1960	1149	40780.89	1089	39808.89	1.3429	0.9103	0.1784
4	0.04	M	20	6.0	0.04	0.0470	0.0020	1029	39484.89	1019	39457.89	1.1036	0.8651	0.0017
5	0.8	E	214	64.2	0.8	0.0094	0.0376	1009	39448.89	795	35327.25	0.3371	0.6320	0.0238
6	0.5	M	10	3.0	0.5	0.0047	0.0047	795	35327.25	790	35320.50	0.3194	0.6253	0.0029
7	0.92	E	180	54.0	0.92	0.0004	0.0043	785	35318.25	605	32402.25	-0.3435	0.3656	0.0016
8	0.9	M	5	1.5	0.9	0.0000	0.0003	605	32402.25	602.5	32400.56	-0.3525	0.3622	0.0001
9	0.9	M	600	180.0	0.9	0.0000	0.0000	600	32400	300	8100.00	-1.7508	0.0400	0.0000

td5	1	RFT	700	210	Detection			Delay				Probability of Interruption		0.880452523
PC	0.95											Response		
Layer	Detection Probability	Location	Delay Time Mean	Delay Time STD	Probability of Detection	Probability of No Detection	Probability of First Detection	Cumulative Delay Time	Cumulative Variance	True Cumulative Delay Time	True Cumulative Variance	z-value	Response Force Arrival Probability	Specific Probability of Interruption
1	0.75	M	10	3.0	0.75	0.2500	0.7500	1189	41049.99	1184	41043.24	1.6587	0.9514	0.7136
2	0.02	M	30	9.0	0.02	0.2450	0.0050	1179	41040.99	1164	40980.24	1.5908	0.9442	0.0047
3	0.8	M	120	36.0	0.8	0.0490	0.1960	1149	40959.99	1089	39987.99	1.3415	0.9101	0.1784
4	0.04	M	15	4.5	0.04	0.0470	0.0020	1029	39663.99	1021.5	39648.8025	1.1109	0.8667	0.0017
5	0.8	E	219	65.7	0.8	0.0094	0.0376	1014	39643.74	795	35327.25	0.3371	0.6320	0.0238
6	0.5	M	10	3.0	0.5	0.0047	0.0047	795	35327.25	790	35320.5	0.3194	0.6253	0.0029
7	0.92	E	180	54.0	0.92	0.0004	0.0043	785	35318.25	605	32402.25	-0.3435	0.3656	0.0016
8	0.9	M	5	1.5	0.9	0.0000	0.0003	605	32402.25	602.5	32400.5625	-0.3525	0.3622	0.0001
9	0.9	M	600	180.0	0.9	0.0000	0.0000	600	32400	300	8100	-1.7508	0.0400	0.0000

td6	1	RFT	700	210	Detection			Delay				Probability of Interruption		0.880879653
PC	0.95											Response		
Layer	Detection Probability	Location	Delay Time Mean	Delay Time STD	Probability of Detection	Probability of No Detection	Probability of First Detection	Cumulative Delay Time	Cumulative Variance	True Cumulative Delay Time	True Cumulative Variance	z-value	Response Force Arrival Probability	Specific Probability of Interruption
1	0.75	M	10	3.0	0.75	0.25	0.75	1189	40866.39	1184	40859.64	1.6605	0.9516	0.713694828
2	0.02	M	30	9.0	0.02	0.245	0.005	1179	40857.39	1164	40796.64	1.5925	0.9444	0.004721805
3	0.8	M	120	36.0	0.8	0.049	0.196	1149	40776.39	1089	39804.39	1.3429	0.9104	0.178429506
4	0.04	M	15	4.5	0.04	0.04704	0.00196	1029	39480.39	1021.5	39465.2025	1.1122	0.8670	0.001699253
5	0.8	E	214	64.2	0.8	0.009408	0.037632	1014	39460.14	800	35338.5	0.3548	0.6386	0.024032945
6	0.5	M	15	4.5	0.5	0.004704	0.004704	800	35338.5	792.5	35323.3125	0.3282	0.6286	0.002957067
7	0.92	E	180	54.0	0.92	0.00037632	0.00432768	785	35318.25	605	32402.25	-0.3435	0.3656	0.0015823
8	0.9	M	5	1.5	0.9	3.7632E-05	0.00033869	605	32402.25	602.5	32400.5625	-0.3525	0.3622	0.000122682
9	0.9	M	600	180.0	0.9	3.7632E-06	3.3869E-05	600	32400	300	8100	-1.7508	0.0400	1.35456E-06

td7	1	RFT	700	210	Detection			Delay				Probability of Interruption		0.88074435
PC	0.95											Response		
Layer	Detection Probability	Location	Delay Time Mean	Delay Time STD	Probability of Detection	Probability of No Detection	Probability of First Detection	Cumulative Delay Time	Cumulative Variance	True Cumulative Delay Time	True Cumulative Variance	z-value	Response Force Arrival Probability	Specific Probability of Interruption
1	0.75	M	10	3.0	0.75	0.2500	0.7500	1189	41019.39	1184	41012.64	1.6590	0.9514	0.7136
2	0.02	M	30	9.0	0.02	0.2450	0.0050	1179	41010.39	1164	40949.64	1.5910	0.9442	0.0047
3	0.8	M	120	36.0	0.8	0.0490	0.1960	1149	40929.39	1089	39957.39	1.3417	0.9102	0.1784
4	0.04	M	15	4.5	0.04	0.0470	0.0020	1029	39633.39	1021.5	39618.20	1.1111	0.8667	0.0017
5	0.8	E	214	64.2	0.8	0.0094	0.0376	1014	39613.14	800	35491.50	0.3545	0.6385	0.0240
6	0.5	M	10	3.0	0.5	0.0047	0.0047	800	35491.50	795	35484.75	0.3368	0.6318	0.0030
7	0.92	E	185	55.5	0.92	0.0004	0.0043	790	35482.50	605	32402.25	-0.3435	0.3656	0.0016
8	0.9	M	5	1.5	0.9	0.0000	0.0003	605	32402.25	602.5	32400.56	-0.3525	0.3622	0.0001
9	0.9	M	600	180.0	0.9	0.0000	0.0000	600	32400.00	300	8100.00	-1.7508	0.0400	0.0000

td8	1	RFT	700	210	Detection			Delay				Probability of Interruption		0.880928159
PC	0.95											Response		
Layer	Detection Probability	Location	Delay Time Mean	Delay Time STD	Probability of Detection	Probability of No Detection	Probability of First Detection	Cumulative Delay Time	Cumulative Variance	True Cumulative Delay Time	True Cumulative Variance	z-value	Response Force Arrival Probability	Specific Probability of Interruption
1	0.75	M	10	3.0	0.75	0.25	0.75	1189	40861.89	1184	40855.14	1.6605	0.9516	0.713698142
2	0.02	M	30	9.0	0.02	0.245	0.005	1179	40852.89	1164	40792.14	1.5925	0.9444	0.004721829
3	0.8	M	120	36.0	0.8	0.049	0.196	1149	40771.89	1089	39799.89	1.3430	0.9104	0.178430649
4	0.04	M	15	4.5	0.04	0.04704	0.00196	1029	39475.89	1021.5	39460.7025	1.1122	0.8670	0.001699266
5	0.8	E	214	64.2	0.8	0.009408	0.037632	1014	39455.64	800	35334	0.3548	0.6386	0.024033087
6	0.5	M	10	3.0	0.5	0.004704	0.004704	800	35334	795	35327.25	0.3371	0.6320	0.002972803
7	0.92	E	180	54.0	0.92	0.00037632	0.00432768	790	35325	610	32409	-0.3254	0.3724	0.001611836
8	0.9	M	10	3.0	0.9	3.7632E-05	0.00033869	610	32409	605	32402.25	-0.3435	0.3656	0.000123832
9	0.9	M	600	180.0	0.9	3.7632E-06	3.3869E-05	600	32400	300	8100	-1.7508	0.0400	1.35456E-06

td9	1	RFT	700	210	Detection			Delay				Probability of Interruption		0.880405708
PC	0.95											Response		
Layer	Detection Probability	Location	Delay Time Mean	Delay Time STD	Probability of Detection	Probability of No Detection	Probability of First Detection	Cumulative Delay Time	Cumulative Variance	True Cumulative Delay Time	True Cumulative Variance	z-value	Response Force Arrival Probability	Specific Probability of Interruption
1	0.75	M	10	3.0	0.75	0.25	0.75	1189	41397.39	1184	41390.64	1.6553	0.9511	0.713303841
2	0.02	M	30	9.0	0.02	0.245	0.005	1179	41388.39	1164	41327.64	1.5875	0.9438	0.004719012
3	0.8	M	120	36.0	0.8	0.049	0.196	1149	41307.39	1089	40335.39	1.3387	0.9097	0.178294903
4	0.04	M	15	4.5	0.04	0.04704	0.00196	1029	40011.39	1021.5	39996.2025	1.1086	0.8662	0.001697769
5	0.8	E	214	64.2	0.8	0.009408	0.037632	1014	39991.14	800	35869.5	0.3536	0.6382	0.024016308
6	0.5	M	10	3.0	0.5	0.004704	0.004704	800	35869.5	795	35862.75	0.3360	0.6315	0.002970798
7	0.92	E	180	54.0	0.92	0.00037632	0.00432768	790	35860.5	610	32944.5	-0.3242	0.3729	0.001613691
8	0.9	M	5	1.5	0.9	3.7632E-05	0.00033869	610	32944.5	607.5	32942.8125	-0.3333	0.3695	0.000125135
9	0.9	M	605	181.5	0.9	3.7632E-06	3.3869E-05	605	32942.25	302.5	8235.5625	-1.7376	0.0411	1.39352E-06

APPENDIX E

DATA VALUE GRAPH OF SENSITIVITY ANALYSIS WITH REGARDS TO DELAY TIME

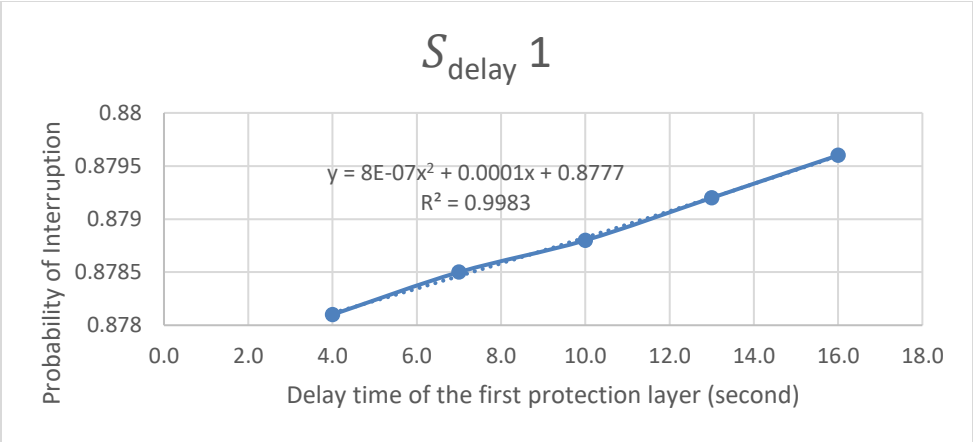

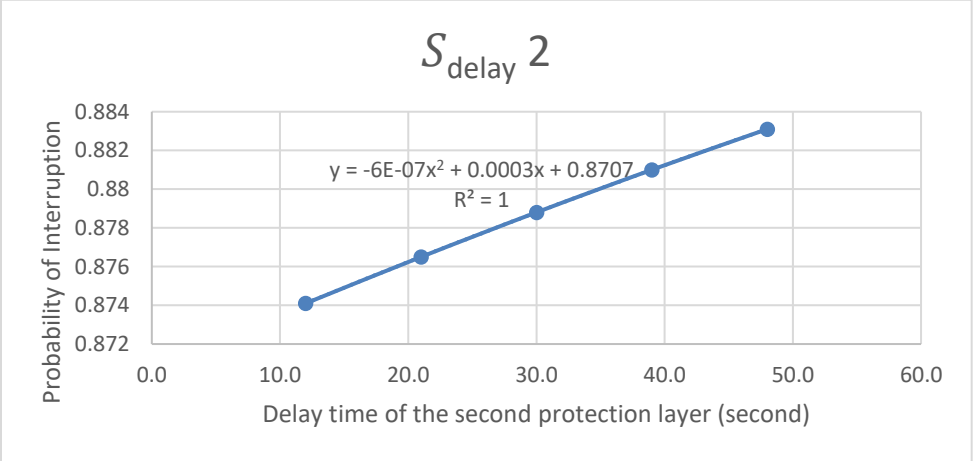

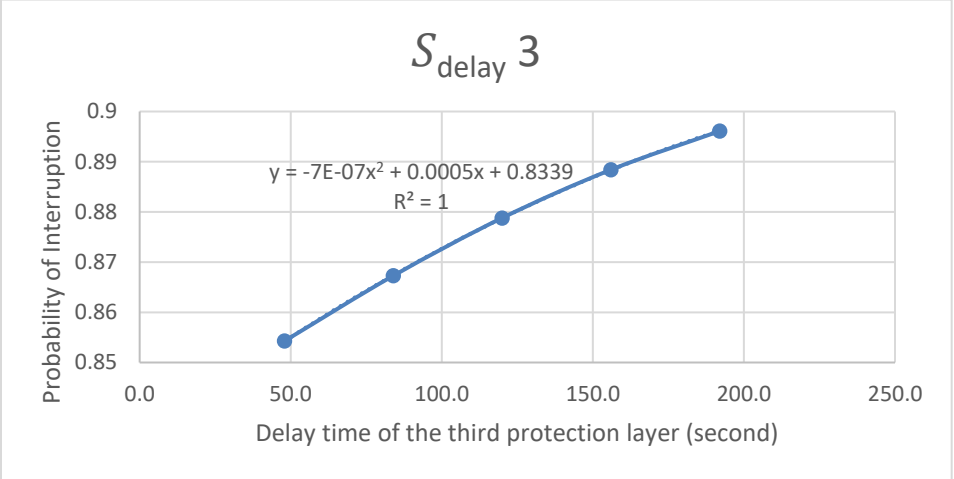

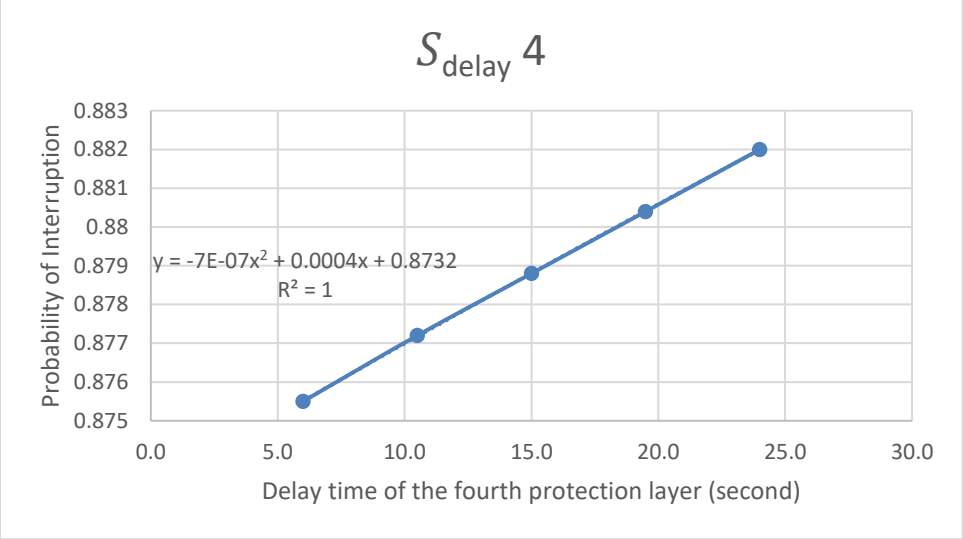
S_{delay} 4
Probability of Interruption
0.883
0.882
0.881
0.88
0.879
0.878
0.877
0.876
0.875
y = -7E-07x² + 0.0004x + 0.8732
R² = 1
0.0
5.0
10.0
15.0
20.0
25.0
30.0
Delay time of the fourth protection layer (second)

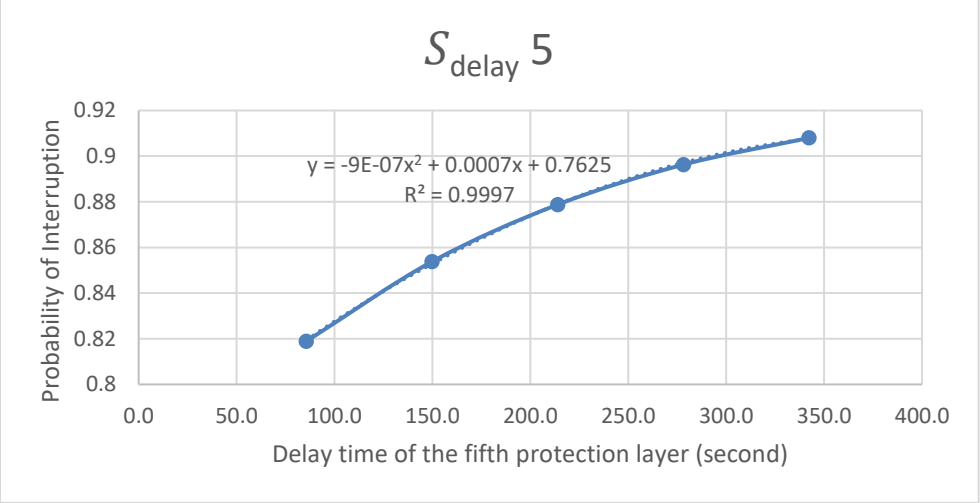
S_{delay} 5
Probability of Interruption
0.92
0.9
0.88
0.86
0.84
0.82
0.8
y = -9E-07x² + 0.0007x + 0.7625
R² = 0.9997
0.0
50.0
100.0
150.0
200.0
250.0
300.0
350.0
400.0
Delay time of the fifth protection layer (second)

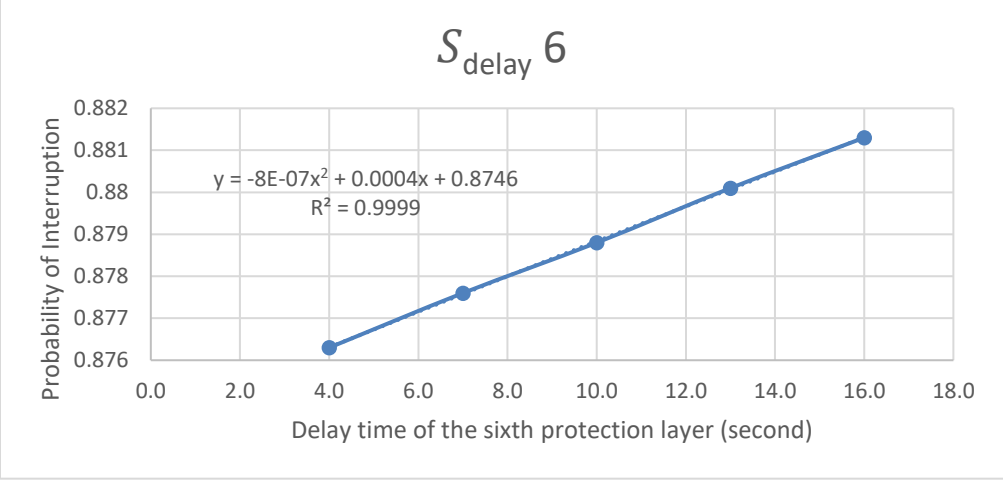
S_{delay} 6
Probability of Interruption
0.882
0.881
0.88
0.879
0.878
0.877
0.876
y = -8E-07x² + 0.0004x + 0.8746
R² = 0.9999
0.0
2.0
4.0
6.0
8.0
10.0
12.0
14.0
16.0
18.0
Delay time of the sixth protection layer (second)

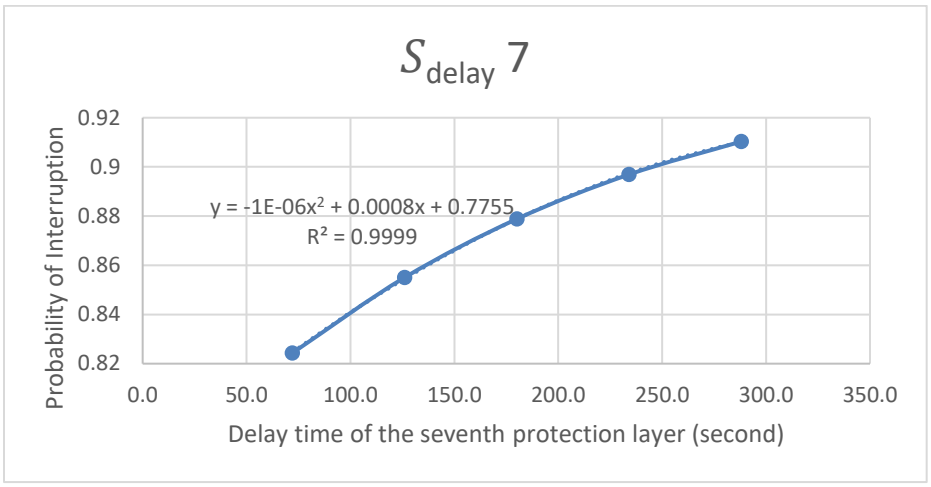
S_{delay} 7
Probability of Interruption
0.92
0.9
0.88
0.86
0.84
0.82
y = -1E-06x² + 0.0008x + 0.7755
R² = 0.9999
0.0
50.0
100.0
150.0
200.0
250.0
300.0
350.0
Delay time of the seventh protection layer (second)

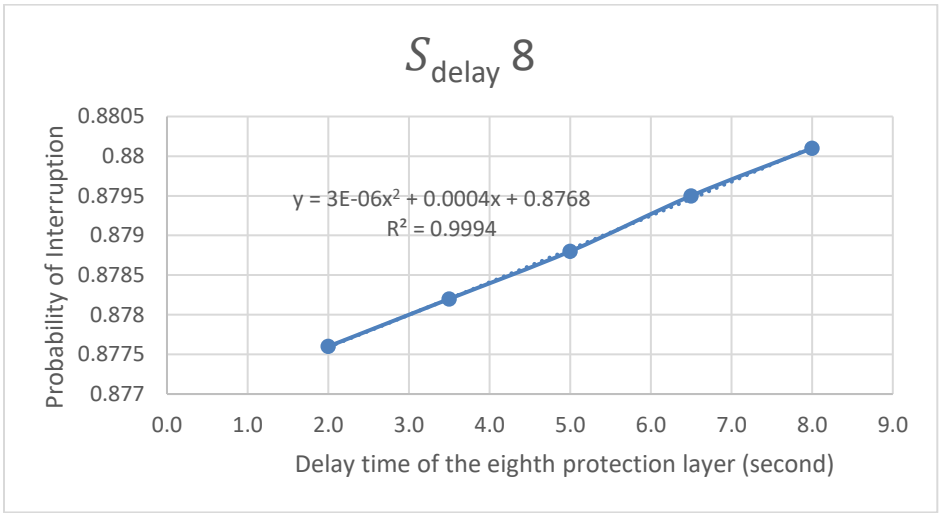
S_{delay} 8
Probability of Interruption
0.8805
0.88
0.8795
0.879
0.8785
0.878
0.8775
0.877
y = 3E-06x² + 0.0004x + 0.8768
R² = 0.9994
0.0
1.0
2.0
3.0
4.0
5.0
6.0
7.0
8.0
9.0
Delay time of the eighth protection layer (second)

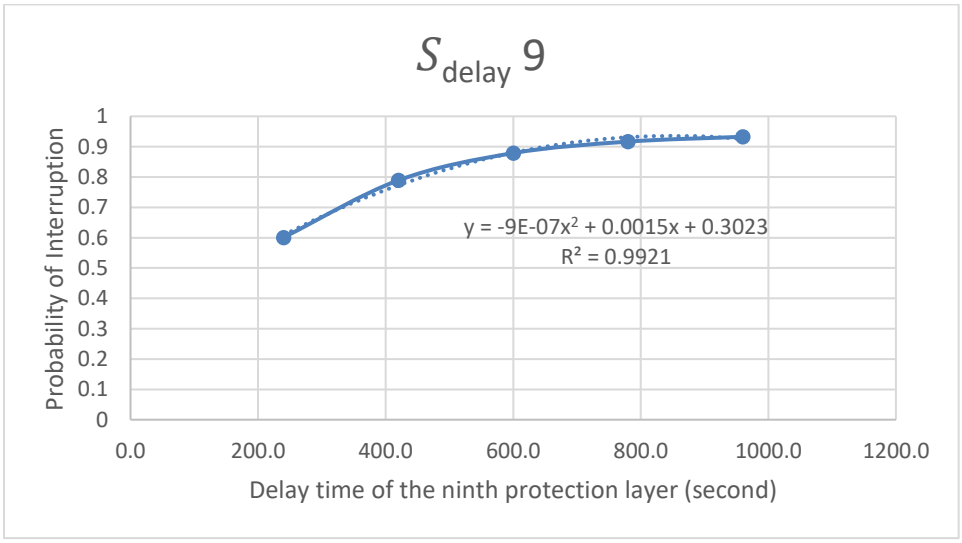
S_{delay} 9
Probability of Interruption
1
0.9
0.8
0.7
0.6
0.5
0.4
0.3
0.2
0.1
0
y = -9E-07x² + 0.0015x + 0.3023
R² = 0.9921
0.0
200.0
400.0
600.0
800.0
1000.0
1200.0
Delay time of the ninth protection layer (second)

APPENDIX F

ADVERSARY SEQUENCE DIAGRAM AND SINGLE PATH EASI CALCULATION TABLE OF THE COMPARISON FACILITY

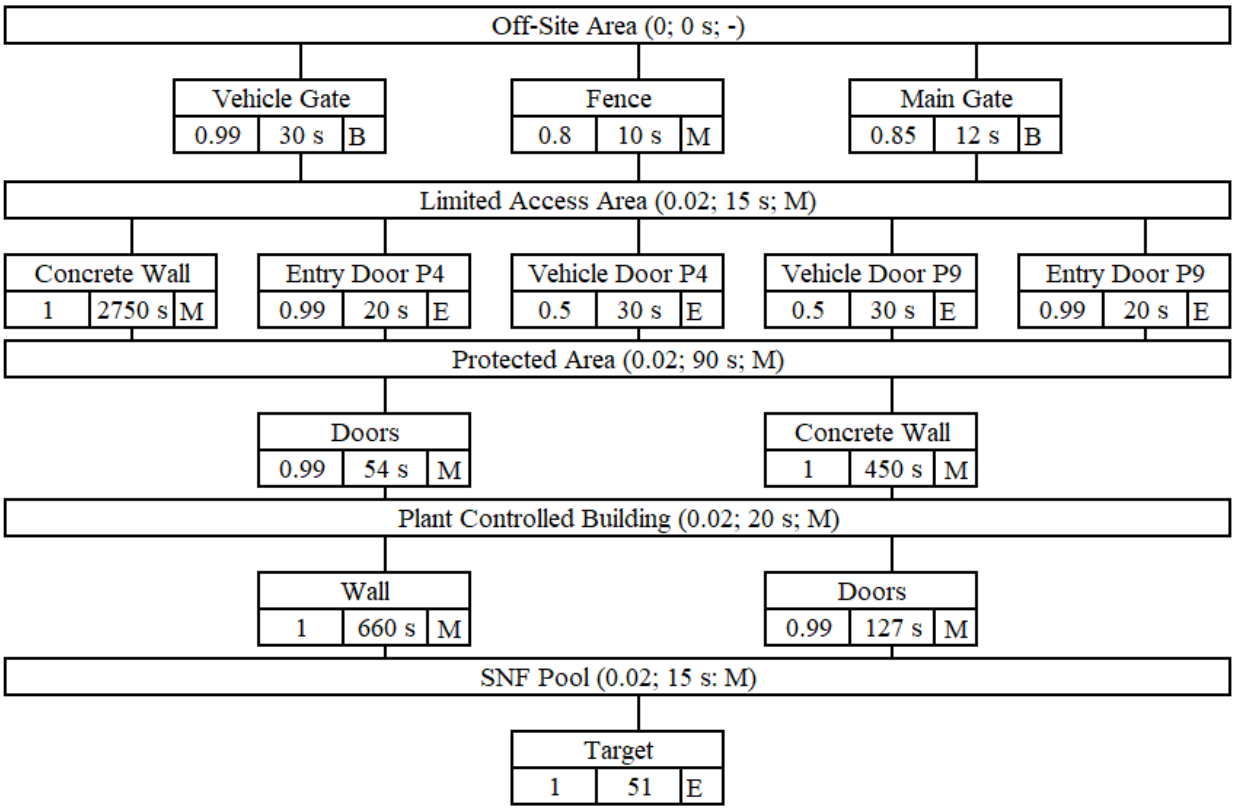

	1	RFT	270	40.24	Detection			Delay				Probability of Response		0.8942573
PC	0.97													
Layer	Detection Probability	Location	Delay Time Mean	Delay Time STD	Probability of Detection	Probability of No Detection	Probability of First Detection	Cumulative Delay Time	Cumulative Variance	True Cumulative Delay Time	True Cumulative Variance	z-value	Response Force Arrival Probability	Specific Probability of Interruption
1	0.8	M	10	3.0	0.8	0.2	0.8	487	3552.39	482	3545.64	2.9499	0.9984	0.7987284
2	0.02	M	90	27.0	0.02	0.196	0.004	477	3543.39	432	2996.64	2.3844	0.9914	0.0039658
3	0.5	E	30	9.0	0.5	0.098	0.098	387	2814.39	357	2733.39	1.3187	0.9064	0.0888236
4	0.02	M	90	27.0	0.02	0.09604	0.00196	357	2733.39	312	2186.64	0.6808	0.7520	0.0014739
5	0.99	M	54	16.2	0.99	0.0009604	0.09508	267	2004.39	240	1807.56	-0.5125	0.3042	0.0289192
6	0.02	M	20	6.0	0.02	0.0009412	1.92E-05	213	1741.95	203	1714.95	-1.1603	0.1230	2.362E-06
7	0.99	M	127	38.1	0.99	9.412E-06	0.000932	193	1705.95	129.5	617.2425	-2.9709	0.0015	1.383E-06
8	0.02	M	15	4.5	0.02	9.224E-06	1.88E-07	66	254.34	58.5	239.1525	-4.9061	0.0000	8.743E-14
9	1	E	51	15.3	1	0	9.22E-06	51	234.09	0	0	-6.7097	0.0000	8.992E-17

EASI calculation table of the MVP strategy of comparison facility

	1	RFT	270	40.24	Detection			Delay				Probability of Interruption		0.949171101
PC	0.97											Response		
Layer	Detection Probability	Location	Delay Time Mean	Delay Time STD	Probability of Detection	Probability of No Detection	Probability of First Detection	Cumulative Delay Time	Cumulative Variance	True Cumulative Delay Time	True Cumulative Variance	z-value	Response Force Arrival Probability	Specific Probability of Interruption
1	0.8	M	10	3.0	0.8	0.2	0.8	477	3507.39	472	3500.64	2.8231	0.9976	0.798097317
2	0.02	M	90	27.0	0.02	0.196	0.004	467	3498.39	422	2951.64	2.2482	0.9877	0.003950878
3	0.99	E	20	6.0	0.99	0.00196	0.19404	377	2769.39	357	2733.39	1.3187	0.9064	0.175870775
4	0.02	M	90	27.0	0.02	0.0019208	0.0000392	357	2733.39	312	2186.64	0.6808	0.7520	2.94785E-05
5	0.99	M	54	16.2	0.99	1.9208E-05	0.00190159	267	2004.39	240	1807.56	-0.5125	0.3042	0.000578384
6	0.02	M	20	6.0	0.02	1.8824E-05	3.8416E-07	213	1741.95	203	1714.95	-1.1603	0.1230	4.72359E-08
7	0.99	M	127	38.1	0.99	1.8824E-07	1.8636E-05	193	1705.95	129.5	617.2425	-2.9709	0.0015	2.76648E-08
8	0.02	M	15	4.5	0.02	1.8447E-07	3.7648E-09	66	254.34	58.5	239.1525	-4.9061	0.0000	1.74851E-15
9	1	E	51	15.3	1	0	1.8447E-07	51	234.09	0	0	-6.7097	0.0000	1.79834E-18

EASI calculation table of the rushing strategy of comparison facility